

Deforestation and Recovery of the Tropical Montane forests of East Africa

By

Sadadi Ojoatre (MSc)

Lancaster Environment Centre,
Faculty of Science & Technology, Lancaster University



**This thesis is submitted in fulfilment of the regulations for the degree of
Doctor of Philosophy**

July 2021

DECLARATION

I declare that this thesis has not been submitted in support of another degree at this or any other University. It is the result of my work. It is the outcome of my work and includes nothing that is the result of work done in collaboration except where specifically indicated. Many of the ideas in this thesis were the product of discussions with my supervisors Professor Mariana C. Rufino and Professor Jos Barlow (Lancaster Environment Centre, Lancaster University)



.....
Sadadi Ojoatre,
Lancaster University,
Lancaster, United Kingdom.
July 2021

STATEMENT OF AUTHORSHIP

This thesis was prepared as a thesis by papers. The chapters are presented in the format of papers intended for submission to peer-reviewed journals. Each chapter's reference list can be found in a combined reference list at the end of the thesis.

Chapter 1. Provides a general introduction and outlines the objectives of the thesis, structure of the thesis, and is not intended for publication.

Chapter 2. Mapping deforestation and recovery of tropical montane forests of East Africa. This chapter is intended for publication. S. Ojoatre, M. C. Rufino designed the research for this chapter, S. Ojoatre obtained the remote sensing data, processed, and analyzed the satellite images, and wrote the chapter. M. C. Rufino and J. Barlow provided the supervision and advice during and towards the development of the research questions, data analysis, structuring, and editing of the chapter.

Chapter 3. Determination of rate of forest aboveground biomass and species recovery in the tropical montane forest of East Africa. This chapter is also intended for publication. S. Ojoatre, J. Barlow, and M. C. Rufino designed the research for this chapter. S. Ojoatre conducted the sampling and field work, analyzed the results. S. Ojoatre wrote the chapter with supervisory support from J. Barlow and M. C. Rufino towards the structuring and editing of the chapter.

Chapter 4. Quantification of soil carbon and nitrogen stocks along forest recovery stages in the tropical montane forest of East Africa. This chapter is intended for publication. S. Ojoatre, J. Barlow, and M. C. Rufino designed the research for this chapter. S. Ojoatre conducted the sampling and field work, laboratory work and analyzed the results. S.

Ojoatre prepared the chapter with supervisory support from M. C. Rufino and J. Barlow.

Chapter 5. Comprises of the general discussion and conclusions of the thesis and is not intended for publication.



.....
Professor Mariana C. Rufino
Lancaster Environment Centre,
Lancaster University



.....
Professor Jos Barlow
Lancaster Environment Centre,
Lancaster University

ACKNOWLEDGMENT

I would like to thank the Almighty Allah Subhanahu Wa Ta'ala (SWT) for all He has done for me. I express my gratitude to the Centre for International Forestry Research (CIFOR) and Lancaster University who provided for me the funding and the opportunity to pursue this Ph.D. program. I am very grateful to Prof. Mariana Rufino and Prof. Jos Barlow who provided supervision for this Ph.D., for their continuous guidance, instrumental suggestions, constructive feedback, and comments till the completion of this Ph.D. research. Without their guidance, this research would hardly have come to fruition.

I would like to acknowledge the staff at CIFOR (Kenya) notably: Dr. Paulo Cerutti, Ruth, Douglas, Ivy, Laura, Nicole, Naomi, and Maurice for their unlimited support during the execution of the actual field work in the Mau Forest complex in Kenya. I would like to acknowledge Dr. Gabriel Yesuf who encouraged, motivated, and provided me with a shoulder to lean during the Ph.D. study demands. I would like to extend genuine thanks to the field staff of Kenya Forestry Services (KFS), Local community members, and my fieldwork team notably Mr. Stephen, Mr. Bitange, Mr. Mutai, Kenneth, Mwangi, Ruto, and Nicholas. I wish to thank all my Ph.D. colleagues at Lancaster; Ethan, Jacqueline, Camilla, Simoni, Jan, May, Rose, James, Ce, Juan, Christopher, Ekeoma, Victor Umar, Kasmaruddin, Ahmad, Ahmed, and Sule with whom we shared office and fruitful time in Lancaster throughout the study period.

I would like to acknowledge and extend my sincere gratitude to my great friends Alfred, Victor, Tonny, Ibrahim, Bernard, Lydia, and Aliga for their compassionate and brotherly support to me and my family back home in my absence. Your contact gave me strength, motivation, and courage to carry on with the rigorous study demands.

Finally, my everlasting gratitude goes to my Family that has stood with me throughout the Ph.D. study program, their encouragement, motivation, and sacrifice of all their interests. I am very thankful for their endurance, courage, and optimism during my long absence. I know they are eagerly looking up in the sky for my coming back home with success.

To all of you - my sincere, deep, heartfelt thank you!

ABSTRACT

Tropical montane forests are fragile ecosystems that provide a wide range of ecosystem services such as hydrological services, protection of biodiversity, and a contribution to climate change mitigation, yet they face degradation as well as losses due to deforestation. Deforestation poses a major threat yet whether these tropical montane forests recover from these changes is not well understood, especially for African montane forests. This study assessed rates of deforestation, and recovery using remote sensing of two important tropical montane forests of East Africa: the Mau Forest complex and the Mount Elgon forest. An in-depth study of aboveground biomass, species diversity and richness, and soil carbon and nitrogen stocks were conducted for the Mau forest complex. To conduct the detailed study, 47 forest plots were established to collect data subsequently used to calculate the rate of recovery of the aboveground biomass (AGB) and species recovery in 3 blocks of the Mau forest complex. From the same plots, soil samples were collected to assess the response of soil carbon (C) and nitrogen (N) stocks to 60 cm of soil depth from the different recovery stages.

This study found that 21.9% (88,493 ha) of the 404,660 ha of the Mau forest Complex was lost at an annual rate of $-0.82\% \text{ yr}^{-1}$ over the period between 1986-2017. However, 18.6% (75,438 ha) of the forest cover that was cleared during the same period and is currently undergoing recovery. In the Mt Elgon forest, 12.5% (27,201 ha) of 217,268 ha of the forest cover was lost to deforestation at an annual rate of $-1.03\% \text{ yr}^{-1}$ for the period between 1984 - 2017 and 27.2% (59,047 ha) of the forest cover that was lost is undergoing recovery. The analysis further revealed that for the Mau forest complex, agriculture (both smallholder and commercial) was the main driver of forest cover loss accounting for 81.5% (70,612 ha) of the deforestation, of which 13.2% was due to

large scale and 68.3% was related to the smallholder farming. For the Mt Elgon forest, agriculture was also the main driver of forest loss accounting for 63.2% (24,077 ha) of deforestation followed by the expansion of human settlements that contributed to 14.7% (5,597 ha) of forest loss. For the aboveground biomass (AGB), it was found that AGB recovered rapidly in the first 20 years at an annual rate of 6.42 Mg ha⁻¹, but the rate of recovery slowed to 4.67 Mg ha⁻¹ at 25 years and 4.46 Mg ha⁻¹, at 30 years of age. At 25 years, the mean AGB (198.32 ± 78.11 Mg ha⁻¹) was statistically indistinguishable from the mean AGB in the old growth secondary forest (282.86 ± 71.64 Mg ha⁻¹). Stem density, species diversity, and richness (i.e., Evenness index, Shannon's index, and Simpson's index) did not show any significant changes with the recovery stages of the secondary forest, although there existed a significant variation between the young secondary forests of age below 15 years from the old growth secondary forests. The study further found that, unlike the AGB and aboveground carbon (AGC), the soil C and N stocks were not significantly different across the recovery periods with mean soil C in the youngest forest 184.1 ± 41.0 Mg C ha⁻¹ and old growth secondary forest as 217.9 ± 51.8 Mg C ha⁻¹, the N stocks in the youngest forest was 16.4 ± 4.8 Mg N ha⁻¹ and 20.1 ± 3.9 Mg N ha⁻¹ for the old growth secondary forest.

The findings of the study indicate that these tropical montane forests of East Africa are under threat resulting from forest clearance and deforestation. The forest AGB recovers after 25 years while the tree species richness and diversity, soil C and N stocks do not change significantly with the recovery stages. The effects of disturbances i.e., forest fire, charcoal burning, grazing (livestock), elephant damage, and fuelwood collection on the soil C and N stocks within the different recovery stages were not significantly different between old growth secondary forests and the other

recovery stages. These findings contribute to the knowledge on the response of the tropical montane forest of East African to pressures of forest clearance and deforestation.

TABLE OF CONTENTS

DECLARATION.....	II
STATEMENT OF AUTHORSHIP	III
ACKNOWLEDGMENT	V
ABSTRACT	VII
TABLE OF CONTENTS	X
LIST OF FIGURES	XIII
LIST OF TABLES.....	XVIII
LIST OF EQUATIONS.....	XXI
LIST OF APPENDICES.....	XXII
LIST OF ACRONYMS	XXIV
1. GENERAL INTRODUCTION.....	1
1.1. Background.....	2
1.1.1. Tropical Montane Forests (TMFs).....	4
1.1.2. Disturbance and Recovery of the tropical montane forests (TMFs).....	5
1.1.3. Approaches for mapping forest disturbance, degradation, and recovery.....	10
1.1.4. Rate of recovery of the Tropical Montane forests (TMFs)	13
1.1.5. Belowground carbon responses to clearance and recovery of TMFs.	14
1.2. The Tropical montane forests of East Africa.....	14
1.2.1. The Mau forest complex	17
1.2.2. Mt Elgon forest.....	17
1.3. Aims of the study	21
1.3.1. Specific Objectives.....	21
1.4. Overall thesis structure	22
2. MAPPING DEFORESTATION AND RECOVERY OF TROPICAL MONTANE FORESTS OF EAST AFRICA	24
2.1. Introduction	27
2.2. Methodology	32
2.2.1. Study area	32
2.2.2. Data sources.....	33
2.2.3. Image analysis and classification	35
2.2.4. Forest cover change, deforestation, and forest disturbance	38
2.2.5. Rate of deforestation.....	39
2.3. Results.....	40
2.3.1. Land cover classification and forest cover change	40
2.3.2. Forest cover change from supervised classification	46
2.3.3. Forest cover change, deforestation, and recovery	46

2.3.4.	Rates of deforestation and recovery	49
2.4.	Discussion	52
2.4.1.	Mapping and classification of forest cover change	52
2.4.2.	Spatio-temporal forest cover change and drivers of deforestation and forest disturbance	54
2.4.3.	Rate of deforestation and recovery in the Montane forest of East Africa	56
2.5.	Conclusion	58
3.	DETERMINATION OF RATE OF ABOVEGROUND BIOMASS AND SPECIES RECOVERY IN THE TROPICAL MONTANE FOREST OF EAST AFRICA	59
3.1.	Introduction	62
3.2.	Materials and Methods.....	67
3.2.1.	Study area	67
3.2.2.	Data.....	68
3.2.3.	Aboveground biomass (AGB) estimation	71
3.2.4.	Species richness, diversity, and composition	72
3.2.5.	Statistical analysis	72
3.3.	Results.....	74
3.3.1.	Recovery rates of AGB, Species richness, and diversity.....	74
3.3.2.	Similarity to the old-growth forest: AGB, Species richness and diversity	77
3.3.3.	Similarity to the old-growth forest: Species Composition	79
3.4.	Discussion	82
3.4.1.	AGB Recovery rate.....	82
3.4.2.	Forest structural recovery	84
3.4.3.	Species richness and diversity.....	84
3.4.4.	Species dominance and Composition	85
3.4.5.	Study limitations and implications for policy planning and implementation	87
3.5.	Conclusion	89
4.	QUANTIFICATION OF SOIL CARBON AND NITROGEN STOCKS ALONG FOREST RECOVERY STAGES IN TROPICAL MONTANE FOREST OF EAST AFRICA	90
4.1.	Introduction.....	93
4.2.	Materials and methods.....	98
4.2.1.	Study area and experimental design.....	98
4.2.2.	Soil sampling and soil analysis	99
4.2.3.	Soil physical properties	101
4.2.4.	Soil chemical properties.....	101
4.2.5.	Statistical analysis	102
4.3.	Results.....	104
4.3.1.	Soil Characteristics	104

4.3.2.	Relationship between the soil properties.....	107
4.3.3.	Response of soil C and N stocks to recovery stages and Aboveground C ...	109
4.4.	Discussion	115
4.4.1.	Distribution of the soil properties	115
4.4.2.	Determination of soil organic carbon and nitrogen stocks	117
4.5.	Conclusion	122
5.	GENERAL DISCUSSION AND CONCLUSION	123
5.1.	Discussion and conclusion.....	124
5.2.	Summary of the research findings.....	124
5.2.1.	Recovery of the aboveground biomass, species diversity, and richness	124
5.2.2.	Effects of recovery on soil C and N stocks	126
5.2.3.	Limitations of the study and policy planning implications.....	129
5.2.1.	Relevance of the study and Future work.....	130
5.3.	Conclusion	132
	REFERENCES	134
	APPENDICES.....	189

LIST OF FIGURES

- Figure 1-1: Spectral response of vegetation, soil and water adopted from Chen et al., (2019). To classify forest, bands 1 (Blue), 2 (Green), 3 (Red), and 4 (Near-infrared) are used in a combination of 4 – 3 – 2 (false-color composite) for the standard Red, Green and Blue color guns. 13
- Figure 1-2: The global tropical forest region (A) and the East African Montane forest region (B). The five major Water towers of Kenya which are also classified as the Tropical Montane forests of East Africa: the Mau forest Complex (1), Mount Elgon forest (2), the Cherang'any Hills (3), the Aberdare ranges and Aberdare national park (4) and Mount Kenya forest and Mount Kenya National park (5); source: Patterson (2012). 16
- Figure 1-3: Fire outbreak in the Western Mau during the dry month (A) and Charcoal burning site in Western Mau (B) in the Mau forest complex. 19
- Figure 2-1: Location of the Mau forest complex and Elgon forest in East Africa. (a) Map showing the official boundaries of the Mt Elgon forests (Scott, 1998) and (b) Map showing the official boundaries of the Mau forest complex (KFS, 2009). 32
- Figure 2-2: Flow chart showing a summary of the methodology that was undertaken in the current study. The Landsat imagery data were acquired from the USGS database and processed i.e., mosaicked, and classified using the ENVI Software (1), available high-resolution imagery from Google earth engine for the study area were used to collect and identify the training and validation samples (2). The accuracy of the classified images was then assessed using the validation data, from the validated land cover/land use data, forest areas were extracted for each year under observation, assessed with

- the GFC data, change detection was carried to determine the deforestation and areas that are under-recovery (3). 36
- Figure 2-3: Examples from Mau forest complex of areas that show deforestation as a result of fire indicated by the red circle (A) and forest clearance and forest recovery as a result of encroachment (B). The high-resolution Google imagery is dated February 04, 2017. 38
- Figure 2-4: Land cover map from 1986 to 2017 for the Mau forest complex (A), and from 1984 to 2017 for the Mt Elgon forest (B) showing forest cover change within and outside the official boundaries of the two montane forests. 43
- Figure 2-5: Land use change transitions from forest to other land cover i.e., agriculture (large scale), agriculture (small-scale), rangeland, moorland, and bare land (open) in (A) the Mau forest complex and (B) Mt Elgon forest. Throughout the period, net forest gain, loss, and net change were calculated for the Mau forest complex and Mt Elgon forest (Fig. 6a and 6b). 44
- Figure 2-6: Changes in forest area for the various periods (1984/1986 - 2017) for the Mau forest complex (a) and Mt Elgon forest (b). Net change (in blue) is the difference between Gross gain and Gross loss. The bars represent the total change for each period while the values represent the annual change within the periods. A negative net result indicates overall forest conversion to other land covers. 45
- Figure 2-7: Forest cover change from 1986 to 2017 showing areas that remained forest throughout the time series analyzed, the forest that was disturbed and is currently undergoing recovery by 2017, and forest that has been permanently lost to deforestation in the Mau forest complex (A) and the Mt Elgon forest (B). 48

Figure 3-1: Location of the sample plots in the three forest blocks of the Mau forest complex distributed in the main recovery stages and the old growth secondary forest (A), the location of the three blocks with the whole of the Mau forest complex (B) and the Location of the Mau forest complex in Kenya (C). The plots are located on areas that were mapped (Chapter 2) as forest recovering and forest that existed throughout the time series.

67

Figure 3-2: Young secondary forest (sample plot No.2) of less than 10 years [A], Second secondary forest (plot No.21) of age up to 15 years after major clearance events [B], Secondary forest (plot No. 11) with age between 16 – 20 years [C], Secondary forest (plot No. 39) with the age of 21 – 25 years of age [D], 26 – 30 years of age [E] and the Old-growth (Mature) secondary forest class with over 33 years of age [F] in the Mau forest complex.

70

Figure 3-3: Relationship between the ecological metrics AGB and stand age in the blocks of Mau forest complex (a), grey dots are field observed plot AGB ($n = 36$). The model predicted AGB (blue curve) in relation to the stand age (years). The black horizontal dotted line represents the AGB at 20 years which separates the young and old-growth (mature) secondary forest. The figure also shows the relationships between the other ecological metrics i.e., stem density and stand age (b), species diversity indices with stand age i.e., Evenness (J) index (c), Shannon's diversity index (d), Simpson's diversity index (e), species richness (f) in the 3 Blocks of Mau Forest Complex. The grey dots and blue lines in all the figures from (b) – (f) also represent the respective field observation and the model predictions.

76

Figure 3-4 Mean variations in the secondary forest structure, species richness, and diversity of the age up to 30 years ($n = 36$) with the stage they become

statistically indistinguishable from old-growth (Mature) secondary forest (n = 11). (A) Variation in the mean AGB between the six forest classes based on the stand age in years, (B) Variation in stem density across the classes, (C) evenness diversity index, (D) Shannon's diversity index, (E) Simpson's diversity index and (F) Species richness across the six classes.

78

Figure 3-5 (i) Confidence Ellipses that suggests significance at < 0.05 and Overlaps between the different age groups, and (ii) Hull plots for the plots based on the Age groups. The old-growth plots, youngest (g10), (g15) show the greatest variance which can explain the significance of the age group in the adonis test (PERMANOVA)

81

Figure 4-1: Location of the 3 forest blocks of the Mau forest complex, the red dots show the 47 sample plots that are distributed within the old-growth (permanent forest since 1986) and the forest undergoing recovery (A), map of the Mau forest Complex from which the 3 blocks were selected and showing areas that were deforested since 1986 (B) and (C) shows the location of the Mau forest complex within Kenya

98

Figure 4-2: Photographs taken at the sampling sites showing evidence of clearance and disturbance: (a) Evidence of forest fire in plot 44 in Western Mau block, (b) a spot in plot 2 in Western Mau block where charcoal was recently prepared, (c) Part of forest where a charcoal kiln is being established (d) Signs of firewood collection and cutting of trees for fuelwood in South Western Mau block (e) Evidence of damage by elephants ; (f) Areas disturbed as a result of livestock grazing.

100

Figure 4-3: Soil C stocks estimation model coefficient with Age, Disturbance index (DI), soil pH, aboveground C, and the interaction effects between DI and soil pH as the model predictors for (A) overall model fitted with the best AIC for the whole soil profile, (B) shows the model effects of the

predictors at 0 - 10 cm depth, (C) for 10 - 30 cm and (D) for 30 - 60 cm.

The red dots and the confidence line indicate the negative effects while the blue dots and the lines indicate the positive effects.

113

Figure 4-4: Soil N stock estimation model coefficient and the interaction effect with

Age, Disturbance index (DI), soil pH and the interaction effects between

DI and soil pH as predictors (A) shows the overall model fitted with the

best AIC for the whole soil profile, (B) shows the model effect of the

predictors at 0 - 10 cm depth, (C) for 10 - 30 cm and (D) for 30 - 60 cm.

The red dots and the confidence line indicate the negative effects while

the blue dots and the lines indicate the positive effects

114

Figure 4-5: Variation of aboveground carbon (AGC) and soil organic carbon (SOC)

along the forest recovery periods in the Mau forest complex. Error bars

represent standard deviations.

119

LIST OF TABLES

Table 1-1: Environmental constraints/characteristics of the Tropical Montane forests of East Africa	4
Table 1-2: Major drivers/agents of forest clearance and deforestation	8
Table 2-1: Landsat data obtained from the USGS database for the Mau forest complex and Mt Elgon forest area. The selected images were those that were available for the study area with less than 10% cloud cover.	34
Table 2-2: Land cover classes and the scheme used in the study adopted from similar reported studies in the same current study area as well as the reported vegetation classification in Eastern Africa.	37
Table 2-3: Accuracy assessment for the supervised classification of the Mau forest complex (a) and the Mt Elgon forest (b)	40
Table 2-4: Estimates of forest cover loss using Supervised Classification (ML) compared to the GFC data for the Mau forest complex (a) and the Mt Elgon forest (b) for the period 2000 - 2017	46
Table 2-5: Forest cover change in the Mau forest Complex and Mt Elgon forest calculated from classified Landsat imagery from 1984 – 2017 using the supervised classification and change detection method.	49
Table 2-6: Observed forest cover loss in Mau forest complex (a) and Mt Elgon forest (b) within the official forest boundaries for the Mau Forest Complex and Mt Elgon forest.	50
Table 2-7: Observed forest cover gain (recovery) in the Mau forest complex and Mt Elgon forest within the official forest boundaries for the Mau Forest Complex and Mt Elgon forest.	50
Table 3-1: Forest classes based on the time when the forest was last degraded/cleared (estimated age) that were used to establish forest sample plots in the three blocks of the Mau forest Complex	69

Table 3-2 Comparison of model Akaike Information Criterion (AIC) between the null model and the Linear and GLS models for the various ecological response metrics	75
Table 3-3: Three most dominant species under various family recorded for each forest classes (recovery stages) in the 3 blocks of Mau forest Complex	80
Table 3-4: Estimated AGB recovery rates from previous studies across the tropical secondary forests compared to the current study	83
Table 4-1: Soil physical and chemical properties for plots sampled at different recovery periods of the Mau Forest Complex. The values indicate the mean, standard deviation (SD), and Coefficient of Variation (CV) of the data for the 6 recovery periods for Bulk Density (BD), Soil organic matter (SOM), Carbon concentration (C), Nitrogen concentration (N), C:N Ratio, Soil organic carbon (SOC), Total soil Nitrogen (TSN) and Aboveground Carbon (AGC).	106
Table 4-2: Correlation analysis for all the variables i.e. Bulk Density (BD), Soil Organic Matter (SOM), pH, Carbon concentration (C), Nitrogen concentration (N), C:N Ratio and Disturbance Index (DI). Note: Bold coefficients represent significance at ($p < 0.05$)	108
Table 4-3: Candidate models fitted to determine the relationship between the Total Soil Carbon (TSC) and Total Soil Nitrogen (TSN). The asterisk between covariates shows their interactive effects	109
Table 4-4: Mixed effect models for predicting the soil C stocks for 0 – 10, 10 -30, and 30 – 60 m soil profiles as well as the combined total soil carbon for 0 – 60 cm profile in the Mau forest complex. DI = Disturbance Index, AGC = Aboveground C derived from AGB. Average pH across the soil profile (0 – 60 cm) was used to determine the soil C stocks for the whole (Overall) profile. σ^2 = Residual Variance, ICC = Intra-class correlation coefficient, N = Number of groups (random), est. = Estimates	110

Table 4-5: Mixed effect models for predicting the soil N stocks for 0 – 10, 10 -30, and 30 – 60 m soil profiles as well as the combined total soil carbon for 0 – 60 cm profile in the Mau forest complex. DI = Disturbance Index, Average pH across the soil profile (0 – 60 cm) was used to determine the soil N stocks for the whole (overall) profile. σ^2 = Residual Variance, ICC = Intra-class correlation coefficient, N = Number of groups (random)

112

LIST OF EQUATIONS

Equation 2-1: Rate of deforestation	39
Equation 3-1: Allometric equation for estimating the AGB	71
Equation 3-2: Shannon's diversity Index (H')	72
Equation 3-3: Simpson's index (D)	72
Equation 3-4: Evenness index (E)	72
Equation 4-1: Estimation of soil bulk density (BD)	101
Equation 4-2: Estimation of the soil carbon stocks	102
Equation 4-3: Estimation of the soil nitrogen stocks	102

LIST OF APPENDICES

- Appendix 1: Training and validation samples based on visual interpretation from High-resolution Google imagery and Multispectral Landsat images. The figure shows the Land cover class identification and sample from the high-resolution imagery (a) and Landsat TM, ETM+ (5-4-3 spectral band combination), and Landsat 8 OLI (6-5-4 spectral band combination) (b) for each land cover class used for the classification scheme. 189
- Appendix 2: Areas that were forest in 1986, 2000, and cleared in 2017 on the Landsat 5, 7, and 8 imagery respectively displayed as a true color composite in RGB (321 spectral) band combination for Landsat 5, 7, and 432 spectral band combination for Landsat 8 in the 1st row (A), and the processed Imagery displayed in three standard RGB color guns as Band 1: Bare substrate (S) in red, Band 2: Live and Photosynthetic Vegetation (PV) in Green and dead /Non Photosynthetic Vegetation (NPV) in Blue in the 2nd row (B) 190
- Appendix 3: Areas that were forest in 1995 on the Landsat 5 imagery (A) displayed as a true color composite in RGB (321 spectral band combination) currently seen converted into agriculture in 2017 Landsat 8 imagery/high-resolution Google imagery (B) displayed in RGB (432 spectral band combination). 191
- Appendix 4: Spatial Autocorrelation plots for the residuals of the models for determining the recovery rates in the Mau forest complex. 192
- Appendix 5: Stress plot for the NMDS for the species ordination (A) and the Ellipses plot for the MDS analysis (B). 193
- Appendix 6: Summary of the inventory data showing the forest structure and species and families in the sampled plots in Mau forest complex 194

Appendix 7: Summary of forest structure and composition i.e. Diameter at Breast height (DBH), tree height (H), Stem Density, Basal area (BA), aboveground biomass (AGB), and aboveground Carbon (AGC); Forest species richness and diversity indices i.e. Shannon's diversity index (H), Evenness (J) and the Simpson's Diversity Index (D) for the 47 plots in the three blocks of the Mau forest complex distributed in the 6 different recovery stages.	196
Appendix 8: Identified and recorded species and the percentage composition in the 3 Blocks of Mau forest complex	197
Appendix 9: Soil physical and chemical properties for plots sampled at different recovery periods of the Mau Forest Complex. The values indicate the mean, standard deviation (SD) of the data for the 6 recovery periods for Bulk Density (BD), Soil organic matter (SOM), Carbon concentration (C), Nitrogen concentration (N), C:N Ratio, Soil organic carbon (SOC), Total soil Nitrogen (TSN) and Aboveground Carbon (AGC) at plot level with combined soil profile (0-60 cm).	200
Appendix 10: Model diagnostic plots for the selected Total Soil Carbon (TSC) prediction (Soil C stocks).	201
Appendix 11: Model diagnostic plots for the selected model for Total Soil Nitrogen (TSN) prediction (Soil N stocks).	202

LIST OF ACRONYMS

AGB	Aboveground Biomass
AGC	Aboveground Carbon
AIC	Akaike Information Criterion
BD	Bulk Density
BGC	Belowground Carbon
BIC	Bayesian Information Criterion
CBD	Convention on Biological Diversity
DI	Disturbance Index
DBH	Diameter at Breast Height
ESA	European Space Agency
ETM+	Enhanced Thematic Mapper
EVI	Enhanced Vegetation Index
FAO	Food and Agricultural Organization of the United Nations
GEE	Google Earth Engine
GFC	Global Forest Change
GoK	Government of Kenya
GIS	Geographical Information System
ICC	Intra-class Correlation Coefficient
IPCC	Intergovernmental Panel on Climate Change
IUCN	International Union for Conservation of Nature
KFS	Kenya Forest Service
KWTA	Kenya Water Towers Agency
LAI	Leaf Area Index
LOI	Loss-on-Ignition

LULC	Land Use Land Cover
MLC	Maximum Likelihood Classification
NDVI	Normalized Difference Vegetation Index
NFA	National Forest Authority
OLI	Operational Land Imager
PCA	Principal component analysis
REDD+	Reduced Emission from deforestation and forest degradation
RMSE	Root Mean Square Error
SOM	Soil Organic Matter
SOC	Soil Organic Carbon
TM	Thematic Mapper
TMF	Tropical Montane forests
TSN	Total Soil Nitrogen
UNEP	United Nations Environment Programme
UNFCCC	United Nations Framework Convention on Climate Change
USGS	United States Geological Surveys
UWA	Uganda Wildlife Authority
VCT	Vegetation Change Tracker
WWF	Worldwide Fund for Nature
µm	Micrometer

1. GENERAL INTRODUCTION



An aerial view of the section of Mau Forest in Southwestern Mau Forest showing the forest and the neighbouring largescale farms [photo by Patrick Sheperd/CIFOR] (a), Mara River inside Mau Forest complex (b) and forest stand in a Mature Forest plot in Southwestern Mau Forest (c). Photos b and C were taken during the field work in March 2019.

1.1. Background

Forests account for 31% of the total land cover and provide vital ecosystem functions that sustain the biodiversity and minimize the effects of climate change (FAO, 2020; Potapov et al., 2021). The forests sequester and store large amounts of carbon in woody vegetation and soils which remains balanced depending on the stability and undisturbed ecosystem functioning (Houghton, Byers, and Nassikas, 2015; Pugh et al., 2019). Of the global forest cover, tropical forests cover 45% i.e. both tropical lowland with 87% and tropical montane forests 13% of the forest area (FAO, 2020; Salinas et al., 2021).

Tropical montane forests (TMFs) are characterized by numerous endangered species and are reported to be one of the major reservoirs of carbon (Cuni-Sanchez et al., 2021). Yet these forests face severe alteration in structure and composition as a result of disturbance and are undergoing recovery (Ding, Zang, Lu, and Huang, 2017; Edwards, Massam, Haugaasen, and Gilroy, 2017). Forest disturbance is a broad term that refers to discrete events that change the physical structure and composition of the forest ecosystem. The events may encompass changes in forest canopy cover leading to gaps that may vary spatially depending on the cause that may be both natural and anthropogenic. The changes in the canopy may be due to the removal or clearance of trees within the forest as a result of the disturbance events (Sasaki and Putz, 2009). Different criteria are used to determine whether an existing landscape is classified or defined as a forest for example according to the United Nations Framework Convention on Climate Change (UNFCCC), a forest comprises of an area between 0.05 – 1 ha characterized with between 10 – 30 (%) canopy cover and between 2 – 5 m height of trees (Asner, 2013; Sasaki and Putz, 2009). However, according to the Food and Agriculture Organization of the United Nations (FAO), a forest may be

defined by 40% canopy cover with trees that are 5 meters tall. Over a period of time, forest clearance may alter the structure and composition of the forest ecosystems (Johnstone et al., 2016; Mohandass, Campbell, Hughes, Mammides, and Davidar, 2017), yet it remains within the definition of forest hence collectively referred to as disturbance (Shapiro et al., 2021). Globally, the TMFs face clearance due to both natural processes for example drought and anthropogenic processes such as deforestation, forest fires, logging, and other forms of degradation (Gallegos et al., 2016; Suescún et al., 2017; Vásquez-Morales et al., 2017)

Across sub-Saharan Africa, the TMFs have experienced severe deforestation, logging, forest fires, and encroachment due to agriculture expansion (DeVries, Verbesselt, Kooistra, and Herold, 2015; Vollstädt et al., 2017) causing changes in forest composition and functioning (Bussmann, 2001; Jung et al., 2017). In order to sustainably manage these forest ecosystems, the understanding of the rate of clearance, deforestation, and rate of forest recovery is essential. Also, the understanding of the relationship between soil physical and chemical properties plays important role in the recovery process especially species recovery, abundance, and coexistence (Long et al., 2018).

In East Africa, the Mau forest complex and Mt Elgon forest are one of the major TMFs that have faced intense processes of forest disturbance (Brandt et al., 2018). Yet, the forest provides critical ecosystem services such as the provisioning of water to urban and rural populations (Jiang, Bamutaze, and Pilesjö, 2014; Kanui, Kibwage, and Murangiri, 2016). The forest benefits the local communities with essential household products (Langat, Maranga, Aboud, and Cheboiwo, 2016).

1.1.1. Tropical Montane Forests (TMFs)

Tropical Montane Forest (TMF) are rainforests that are found in areas with varying elevation and are reported to be the world's high biodiversity hotspots (Richter, 2010; Salinas et al., 2021). In East Africa, the TMFs are found in areas with minimum elevation of 800 m and are characterised with Afroalpine vegetation from over 1,000 m elevation (White, 1983). The TMFs ecosystems harbour various and unique species both flora and Fauna, for example in East Africa, the TMFs are characterised with natural vegetation types ranging from savanna to cloud forests and alpine vegetation, they provide habitat for approximately 3,000 species of plants and animal (Hemp and Hemp, 2018; Wang and Gamon, 2019)

The TMFs of East Africa grow under specific environmental constraints notably elevation, rainfall, and human interaction (Table 1-1)

Table 1-1: Environmental constraints/characteristics of the Tropical Montane forests of East Africa

Constraint/Characteristics	Range	Reference
Elevation	> 800 m	White (1983) White (1983)
Temperature	10 °C – 30 °C	
Rainfall	1,000 mm which varies with Inter – Tropical Convergency Zones (ITCZ)	White (1983)
Vegetation	At lower elevation, the dominant vegetation is forest and higher altitude, they are characterised with Alpine vegetation composed of heath and moorlands	White (1983)

The tropical montane forests of East Africa have historically been subjected to forest cover loss. In the recent decades, the governments have made efforts to conserve these forests, yet they still face disturbance from the local communities. Prior to the

1980's, the land had been allocated to the local settlements as a result of colonial government policies.

The tropical montane forests of East Africa offer various benefits to the local community especially, provision of fuelwood, timber, poles etc. At national level, they offer income in terms of tourism and indirectly providing economic resilience to the countries through value addition (Crafford and Strohmaier, 2012). Globally, the TMFs offer ecological benefits especially their contribution to the regulation of climate by sequestering and storing the carbon (Hofer and Zingari, 2014).

1.1.2. Disturbance and Recovery of the tropical montane forests (TMFs)

Bawa and Hadley (1991) defined disturbance in terrestrial forest ecosystems as 'a relatively discrete event causing a change in the physical structure of the environment'. Disturbance shapes the forest's systems, by influencing the composition, structure, and functional process (Dale et al., 2001). The disturbance is a widespread phenomenon in tropical montane forests (Crausbay and Martin, 2016; Panayotov et al., 2017), this is attributed to both natural (fire, landslides, high energy windstorms, and natural die out) and human activities that have changed the dynamics in the recent years (Frelich, 2002; Holl, 2012). Whereas clearance as a result of wind has been identified in most temperate forests (Holeksa et al., 2016; Peterson, et al., 2016; Nagel et al., 2017), meanwhile drought and climate conditions from wet and humid to dry conditions (Pederson et al., 2014).

The term forest disturbance is related to forest degradation which refers to the reduction of the capacity of a forest to provide goods and services (Simula, 2009), meanwhile Schoene et al., (2007) defined forest degradation as "changes within the forest which negatively affect the structure or function of the stand or site, and thereby

lower the capacity to supply products and/or services". Forest degradation is a direct result of disturbance that varies with extent as well as severity (Schoene et al., 2007).

Several studies such as Seidl et al., (2017) have provided a synthesis of climate change effects on disturbance agents, with a view of how they influence forest disturbance. The agents mainly focus on the natural drivers of forest disturbance especially, wind, fire, insects, and pathogens among others. Most of the effects were evaluated under three different pathways i.e., direct, indirect, and interaction-related effects of climate change on forest disturbance. However, the study of Seidl et al., (2017) was undertaken at a global scale as compared to the study in East Africa and specifically the Mau forest complex and Mt Elgon forest that face disturbance from anthropogenic pressures though little is known about the extent to which this has affected the forest cover. While Seidl et al., (2014) also noted that forest disturbance due to climate change has an impact on the capacity of forests to sequester and sink carbon, the main drivers of disturbance cited in the study of Seidl et al., (2014) were forest fires, wind, and bark beetles. The effects of disturbance do not only affect carbon stocks but wider ecosystem services and in the Mau forest complex and Mt Elgon forest, little is known about the effects of natural disturbance on carbon and ecosystem services and the overall response of the ecosystem. Thorn et al., (2017) also investigated the effects of natural disturbance due to windstorms, bark beetle and consequently assessed the salvage logging effects on biodiversity and found out that, the disturbance resulting from salvage logging provides a strategy to keep the forest ecosystem natural. Salvage logging allows logging of trees within forest area that has been damaged by natural disturbances and maximizes economic return as well as pest control that would have been lost as a result of the disturbance (Mehr, Brandl, Kneib, and Müller, 2012; Noss and Lindenmayer, 2006). In areas where salvage

logging was not undertaken, natural succession took place. In the case of the Mau forest complex and Mt Elgon forest, it is believed that the main drivers of forest disturbance or clearance are anthropogenic in nature especially change in land use where the forest is cut for agricultural expansion, logging and charcoal burning as reported by Were et al., (2013). These activities are however detrimental to the forest cover rather than a strategy to manage the forest while maximizing the economic returns as reported by Thorn et al., (2017). It should therefore be noted that the study of Thorn et al., (2017) was conducted in a temperate forest meanwhile the current study area is in a tropical montane forest that has a different physiological characteristic. Meanwhile, Rutten et al., (2015) carried out a study of the forest structure and composition in both selectively logged and non selectively logged forests to assess the effects of selective logging approach in Mt Kilimanjaro forest, a montane forest in East Africa. The findings of the study revealed that, the selectively logged forest had more stem diversity compared to those that were not selectively logged. Meanwhile, Gourlet-Fleury et al., (2013) revealed that selective logging and thinning increased AGB and recovery of central African tropical lowland rain forests, however, the current study was carried out in a tropical montane forest as opposed to a lowland rain forest in central Africa.

According to Crafford et al. (2012) large revenues are generated from illegal deforestation from Kenya's montane forests and this is seen as an incentive to deforestation. Interventions to reduce and reverse the impacts of degradation and clearance of montane forests for example afforestation and reforestation are vital to improving the provision of ecosystem services such as provision of hydrological services (Trabucco, Zomer, Bossio, van Straaten, and Verchot, 2008). Petursson et al., (2013) conducted an institutional analysis of the deforestation process within the

protected areas of Mt Elgon forest and reported that despite the establishment of protected areas in the Mount Elgon forest, deforestation has persisted. The main driver of the persistent deforestation in the Mt Elgon forest was illegal logging (Petursson et al., 2013). Petursson et al., (2013) further revealed that deforestation possesses ecological effects as well as social conflicts and demonstrated that the deforestation in the protected areas was driven by institutional and political factors. Froliking et al., (2009) also identified major processes that are collectively referred to as forest disturbance in a forest ecosystem as indicated in Tab. 1-2.

Table 1-2: Major drivers/agents of forest clearance and deforestation

Agent/Type	Description	Cause
Logging	Clear cut, selective cut, reduced impact; Logging for poles, timber, and fuel wood (firewood)	Anthropogenic
Charcoal burning	Cutting of trees for making charcoal	Anthropogenic
Land conversion	Permanent (land remains non-forest use), temporary (land cultivated for few years, regeneration, or regrowth) focusing on agriculture both large scale and smallholder.	Anthropogenic
Urban and Road construction	Urban expansion and infrastructure development like roads	Anthropogenic
Fires	Most fires are associated with anthropogenic activities.	Natural/ Anthropogenic
Firwood Collection	Locals collecting and cutting down trees for fire and fuelwood for domestic use	Anthropogenic
Grazing (Livestock and Elephants)	Livestock grazing by the local community as well as Elephant damage resulting from grazing of the Elephants and wildlife	Natural/ Anthropogenic

Much as forest clearances resulting from natural and anthropogenic agents have been researched across various regions, spatial and temporal dynamics vary with different forest biomes (Froliking et al., 2009). In Africa, studies on forest clearance were undertaken in the Democratic Republic of Congo and Tanzania (Ahrends et al., 2021; Shapiro et al., 2021) with limited information regarding the assessment of forest clearance in the TMFs. Potapov et al., (2012) also quantified forest cover loss in the

Democratic Republic of Congo and discovered that between the years 2000 – 2010, total gross forest cover loss increased by 13.8% with a forest loss rate of 0.4% in protected areas. Meanwhile, similar studies conducted in Mt Elgon, where the role of protected areas and changing contexts (management and policies) were evaluated and the findings revealed that protected areas continued to lose forest cover (Sassen et al., 2013). It should be noted that these studies did not consider annual change analysis to provide information on the annual rate of forest cover change resulting from clearance and how they recover over time.

The time taken by a forest to recover following a clearance differs by region. Cole et al., (2014) evaluated the recovery and resilience of tropical forests following a clearance and discovered that most forests in Central America and Africa recover faster compared to those from South America and Asia following exposure to natural large infrequent clearances as opposed to post-climate and human impacts. The study of Cole et al., (2014) also revealed that site-specific higher frequencies of clearance elevates recovery rates which shows the resilience in an exposed forest to past deforestation. However, the study by Cole et al., (2014) focused on the influence of climate (rainfall /precipitation) as the main natural driver of clearance and burning, forest clearing for agriculture as the main anthropogenic agents of the forest clearance. It should further be noted that the study of Cole et al., (2014) was conducted at a continental scale and used a standardized rate of forest clearance events as compared the current study in the Mau forest complex and Mt Elgon forest which are at ecosystem scale which requires a clear investigation of past clearance and recovery rates at a local scale.

Rosa et al., (2015) assessed the relationship between the agents of land cover change associated with the forms of land cover degradation, the study focused on three landscape metrics to model forest transitions (i.e., forest to deforested, regeneration to deforested, and deforested to regeneration) in Amazonia. The study revealed that the landscape in the Amazonia had shown a strong decrease in forest cover which suggested and demonstrated the relevance of using land cover change models that could be relevant to understand the forest cover change in the Mau forest complex and Mt Elgon forest that are believed to have changed over time.

Forest clearance and deforestation in Eastern Africa dates to the 1990s and varies from different localities within the region depending on the demands of the communities as well as government policies. According to Mitchell (2010), practical management of forests requires the understanding of the past dynamics leading to forest cover clearance. Various studies have cited agricultural expansion as the main driver of tropical forests clearance as the forest land are seen as the main source of new agricultural lands. Due to the growing population, there has been an increase in the demand for the agricultural products as well extraction from the forests products for subsistence purposes (Choksi, 2019; Gibbs et al., 2010)

1.1.3. Approaches for mapping forest disturbance, degradation, and recovery

Approximately 70% of the earth is covered with vegetation which forms the most vital component of the ecosystem (Jensen, 2007). Remote sensing tools have widely been used for assessing and quantifying forest cover change i.e., clearance, and detection of loss due to deforestation, and they provide an affordable assessment of forest cover change (Mitchell, Rosenqvist and Mora, 2017; Cohen et al., 2020; De Marzo et al.,

2021). The availability of satellite data at global level particularly Landsat data has come with new developing trends in vegetation monitoring at local and regional scales (Cohen and Goward, 2004).

To manage the forest ecosystem sustainably and effectively, there is a need for information on the trends and conditions of the forest. Given the change of land cover and forest, in particular, there is a need for consistent information on the forest change and this can be offered by the remote sensing tools (Achard et al., 2002). Several studies have used remote sensing particularly Landsat data for assessing and quantifying forest cover loss (Cohen et al., 2010; Goward et al., 2008; Hansen et al., 2010; Pratihast et al., 2014). However, according to Froking et al., (2009), space-borne remote sensing approaches still have challenges for mapping forest clearance in areas with high land-use dynamics requiring frequent observation at least annually to capture high temporal clearances and cover loss events. Landsat data has been frequently used in annual and biennial temporal resolutions to map and monitor forest cover change (Cohen et al., 2010; Gu et al., 2016; Hermosilla et al., 2015). Cohen et al., (2010) detected trends in forest recovery and clearing using annual Landsat time series and they conducted validation using the TimeSync algorithm, and compared the results with LandTrendr (Kennedy, Yang, and Cohen, 2010). The TimeSync according to Cohen et al., (2010) in addition to change detection algorithm calibration and map validation also allows comparative exploration of the behavior of the spectral indices, masking of forest versus non-forest, and quantification of change transitions. Meanwhile (Huang et al., 2010) used a vegetation change tracker (VCT) algorithm for reconstructing recent history of forest distribution from available Landsat data. The VCT method is based on the spectral and temporal properties of the forest, stand

clearance, and post-clearance recovery process. These methods accordingly offer acceptable results about trends of forest degradation and recovery.

Previous research has demonstrated that available Landsat data can provide near real-time monitoring of forest disturbance or forest change (Devries et al., 2013). To date, many applications have been developed to map forest disturbance and degradation, assess the recovery, and monitor overall change to forest cover. These approaches range from image to image change detection and time series analysis (Hirschmugl et al., 2017). However, most of the recent studies reported have mapped and detected forest clearance and cover changes from using remote sensing at global scale (Hansen et al., 2013). There still exist gap in information on degradation at national and local scales (Hirschmugl et al., 2017). The reported approaches use the available multispectral Landsat data and detect the forest cover change from the spectral signatures. Fig. 1-1 indicates the spectral response of the three main features i.e. green vegetation (which includes forests, grass, and crops), soil, and water (Chen, Guerschman, Cheng, and Guo, 2019). The features are either directly classified using the traditional classification algorithms (for example Maximum Likelihood) or indirectly detected from the indices like NDVI, EVI LAI among others. The direct detection of forest cover resulting from clearance may require use of fine resolution imagery (i.e., Landsat with 30 x 30 m resolution) which can detect changes in forest cover (Hansen, et al., 2008).

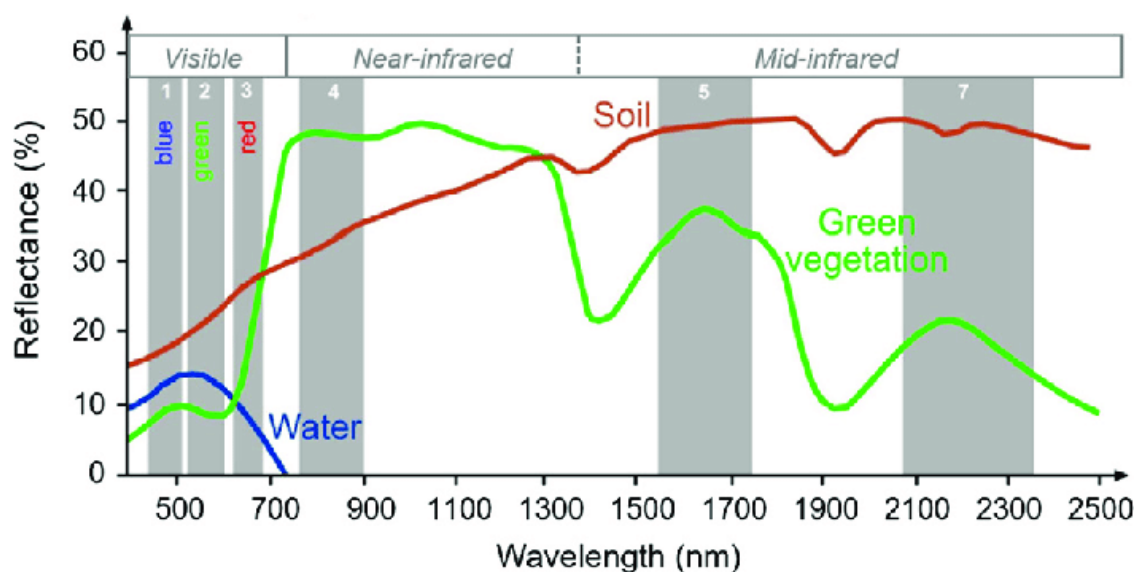


Figure 1-1: Spectral response of vegetation, soil and water adopted from Chen et al., (2019). To classify forest, bands 1 (Blue), 2 (Green), 3 (Red), and 4 (Near-infrared) are used in a combination of 4 – 3 – 2 (false-color composite) for the standard Red, Green and Blue color guns.

Baldyga et al., (2007) assessed land-use change in the Mau forest complex and concluded that there is a significant change in land use across a range of spatial scales. However, the study of Baldyga et al., (2007) used bi-temporal images to determine the land-use change in River Njoro watershed. The assessment involved analysis of bi-temporal satellite data. Past research studies undertaken in the Mau forest complex and Mt Elgon forest focus on land use and land cover change over two different periods usually between decadal time spans. Yet, there is a need for annual information on the trends of forest change for sustainable management.

1.1.4. Rate of recovery of the Tropical Montane forests (TMFs)

Tropical montane forests are reported to be regenerating and rapidly expanding with much debate on how they replicate old-growth (mature) intact forests (Goosem et al., 2016). In this current study, forest recovery refers to the re-establishment of forest structure and composition following clearance for instance redevelopment of forest biomass and canopy structure. The rate of recovery of the components depends on the magnitude and severity of the stand and structural replacement of the events for

example clearance, logging, fire, windstorms (Frolking et al., 2009). The recovery process can be measured from the structure and composition i.e. the return of biomass, stem density, basal area as well as species richness and diversity after the degradation process (Hector et al., 2011; Lin et al., 2015). The processes of recovery may also follow different trajectories depending on nature of degradation i.e., in cases of fire, forest clearances are usually followed by a limited pioneer species that may be influenced by small seed dispersals. The rate of recovery can also depend on the pre-clearance situation, the processes of seedling establishment and nutrient cycling, and the inherent productivity of the land (Johnstone and Chapin, 2006).

1.1.5. Belowground carbon responses to clearance and recovery of TMFs.

Forest soils have played the role of a sink of carbon with association to changes in forest land management (Kucuker, Guney, Oral, Coptu, and Onay, 2015). Forest clearance has been reported to have significantly decreased soil C and N concentrations (Guan, Tang, Fan, Zhao, and Peng, 2015). Conversion of the land cover has a great influence on the soil C and N concentrations (Thomas, Hao, and Willms, 2017). Understanding belowground or soil C response to recovery and clearance in forest areas is essential for understanding the best approaches that can be used in the restoration process and policy formulation in order to maximise the C sink and storage.

1.2. The Tropical montane forests of East Africa

The East African montane forests approximately cover a total area of 65,500 Km² (25,300 square miles), from Mt Kinyeti in the Imatong mountains of Southern Sudan, extending towards south to Mt Moroto in the north eastern Uganda and Mt Elgon that

lies on the Uganda – Kenya border (WWF, 2021). In Kenya, the montane ecoregion follows the mountains east and west of the eastern rift valley (Fig. 1-2) with the associated volcanoes for example the Aberdare range, Mt Kenya, the Mau complex, Mt Kulal, Nyiru, and the Nguruman escarpments of Kenya. The region stretches to Mt Kilimanjaro, Meru, Ngorongoro, Mbalu highlands, and Mt Hanang in northern Tanzania (WWF, 2007).

The Mau forest Complex and Mt Elgon forest that have been selected in this study are faced with long history of Management and use. In 1930s the Mau forest was considered as crown land under the colonial government and then made a National Reserve in 1945 and officially gazetted in 1954 as a Forest Reserve under the Forest Act (Klopp and Sang, 2011; KFS, 2022). Similarly, the history of Mount Elgon forest can be traced to the 1900 colonial East Africa where Mt Elgon was broadly referred to as a protected area which was classified as a game reserve and forest reserve where the former focused on wildlife and the later focused on the forest resources (Petursson, Vedeld and Sassen, 2013).

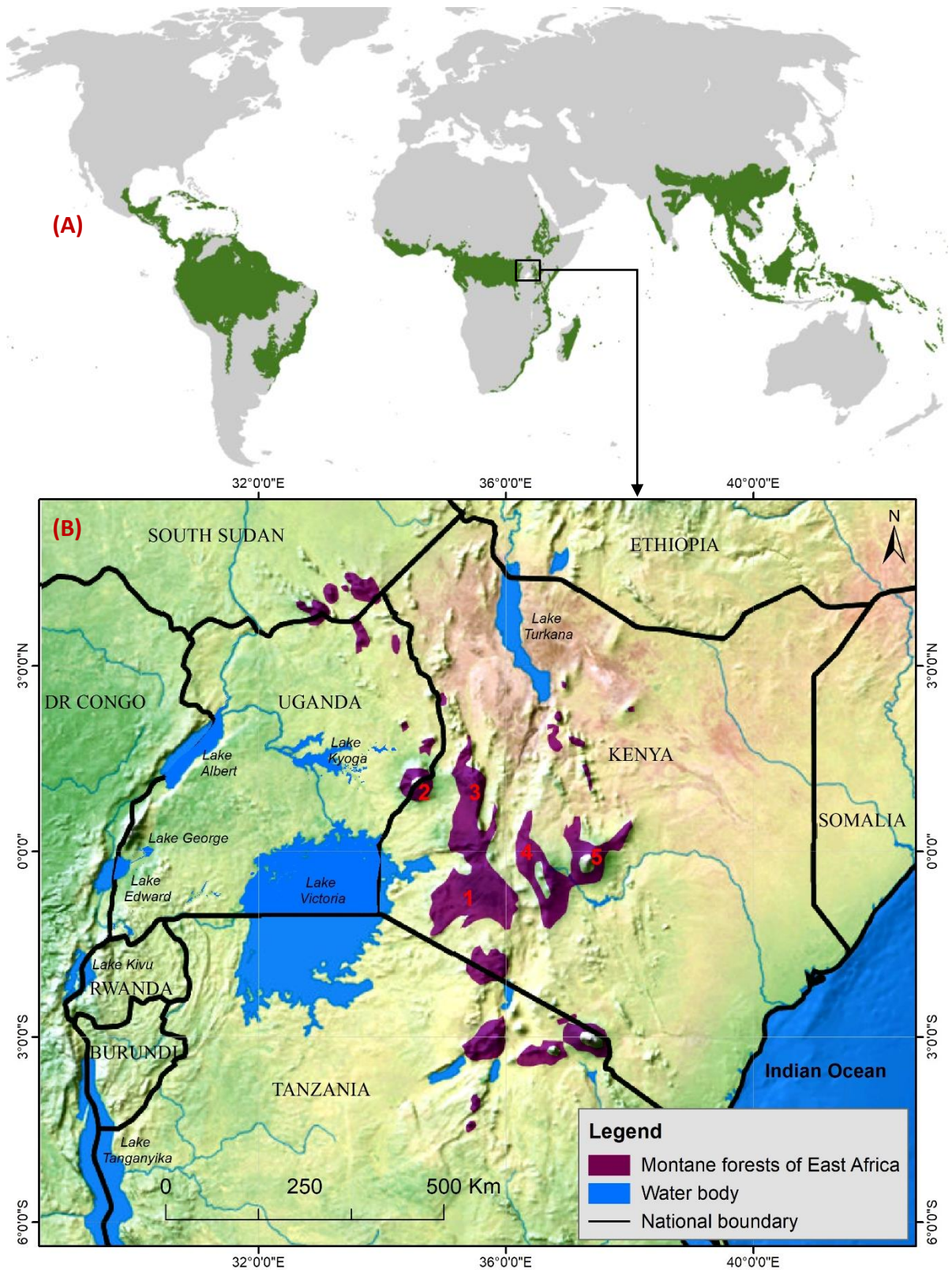


Figure 1-2: The global tropical forest region (A) and the East African Montane forest region (B). The five major Water towers of Kenya which are also classified as the Tropical Montane forests of East Africa: the Mau forest Complex (1), Mount Elgon forest (2), the Cherang'any Hills (3), the Aberdare ranges and Aberdare national park (4) and Mount Kenya forest and Mount Kenya National park (5); source: Patterson (2012).

1.2.1. The Mau forest complex

The Mau forest complex is located in the rift valley region of Kenya and it is the largest water tower (major water catchments areas) of Kenya which stores water during the rainy season and releases it in the dry season (Nabutola, 2010a). The forest is also the largest closed-canopy montane forest in Kenya. The Mau forest ecosystem comprises several forest blocks namely from Narok, Masai Mau, Eastern and Western Mau, Southern to South West Mau as well as Transmara regions with the major catchment area for 12 rivers draining into lake Baringo, Nakuru, Turkana, Natron, and the trans-boundary Lake Victoria shared by Kenya, Uganda, and Tanzania (Olang and Kundu, 2011; Chrisphine, Maryanne and Mark, 2015; Boitt, 2016). Olang and Kundu (2011) also reported that the Mau forest complex region receives an annual rainfall of 1300 mm without the consideration of the climate extremes; the North-South movement of Inter - tropical Convergence Zones (ITCZ) that is modified by the relief features influences the climate. The Mau forest complex region is characterised with cold to hot and humid weather conditions. The lower part of the region is characterised with arid and semi-arid. The mean annual rainfall averages of 750 mm are recorded from December to March (KFS, 2021; WWF, 2021). The forest provides habitat to key biodiversity endemic species such as African olive (*Olea europaea subsp. cuspidata*), *Dombeya torrida* (tree species) and shrubs (KFS, 2021) and for birds species such as *Hieraaetus ayresii*, *Stephanoaetus coronatus*, *Sheppardia polioptera* among others in Kenya (BirdLife International, 2021).

1.2.2. Mt Elgon forest

Mt Elgon forest is located approximately 100 Km northeast of Lake Victoria (Penny Scott, 1998) and it is a protected area that covers approximately 2045 Km² (Mukadasi, Kaboggoza, and Nabalegwa, 2007). It is a volcanic mountain with five major peaks

located in Eastern Uganda and Western Kenya at approximately 01°07'06"N and 34°31'30"E. The five major peaks include; Wagagai with 4,321 meters (m) above sea level, Mubiyi (4,211 m), Masaba (4,161 m) all these are predominantly located in Uganda meanwhile Koitobos (4,222 m) is in Kenya and Sudek which stands at (4,302 m) is located on the Kenya/Uganda border (Wielochowski and West Col Productions., 1989). Uganda Wildlife Authority currently manages Mt Elgon forest and the national park since the merging of the Uganda National Parks (UNP) with the Game department.

The montane forests of East Africa have been widely reported to be facing the pressure of clearance and degradation due to agricultural expansion and demand for fuel wood due to the rising population (Sassen et al., 2013; DeVries et al., 2015). They experience severe selective tree logging hence changes in the species composition (Bussmann, 2001). Both Mt Elgon forest and the Mau forest complex face intense anthropogenic pressures and degradation (Buyinza and Nabalegwa, 2008; Mugagga et al., 2012). According to (GoK, 2012; KFS, 2017), the degradation is mainly induced by the communities that live adjacent to the forests. The reported anthropogenic pressures include deforestation to convert the land use from forestry to other land uses like subsistence farming, charcoal burning, encroachment for settlement (Chrisphine et al., 2015; Jacobs et al., 2017), and poor land management have undermined the ability of these landscapes to provide critical ecosystem services like support to the hydrological cycle (Jiang et al., 2014; Kanui et al., 2016). The TMFs of East Africa have faced degradation i.e., fires, charcoal burning (Fig. 1-3)



Figure 1-3: Fire outbreak in the Western Mau during the dry month (A) and Charcoal burning site in Western Mau (B) in the Mau forest complex.

Several land cover change studies have been undertaken in the Mau forest Complex and Mt Elgon forests (Bailis et al., 2015; Baldyga et al., 2007; Olang and Kundu, 2011), but the influence and trends of the different drivers of forest cover change as well as the rate of forest loss are not well documented. Measures aimed at halting deforestation and restoring tree cover have been instituted in the past decade by stakeholders in the region (Kanui et al., 2016; Sassen et al., 2013). However, the information on the effectiveness of these measures in achieving sustainable forest and water management is lacking (Kwata, 2015).

Sun et al., (2005) discovered that a reduction of forest Leaf Area Index (LAI) would increase streamflow in forested watersheds; this would consequently increase the ground water table in wetlands. MIKE SHE model was used to simulate the effects of land use and climate change on watershed hydrology (Lu, 2006), the results revealed that forest removal would cause water table levels to rise, however, the results in a wetland were not significant. It should therefore be noted that the study of Lu (2006) was conducted in the United States, although the montane forests of East Africa (the Mau forest complex and Mt Elgon forest) are water catchment to several streams and Lakes in East Africa (Joseck et al., 2016; Nabutola, 2010)

D'Almeida et al., (2007) has found out that deforestation in Amazonia shows a contrasting effect on the hydrological regimes. The condition and terrain of tropical montane forests have made them unique ecologically and hydrologically due to the terrain/altitude compared to low-lying tropical forests (Bruijnzeel, Scatena, Hamilton, Bubb, and Das, 2010). In addition, studies carried out to assess the relationship between forest cover change and hydrological regimes indicate that forest cover loss increases runoff and consequently supply of water (Boitt, 2016; Guzha, Rufino, Okoth, Jacobs, and Nóbrega, 2018; Luo et al., 2018; Zhang et al., 2016).

The montane forests directly provide woody biomass in form of fuel wood, timber as well as poles which contributes positively to the national economy (Crafford, Rita, et al., 2012; WWF, 2005). The rift valley region of Kenya has undergone a massive land cover change in the past decades hence ecological changes due to agricultural activities particularly smallholder farming (Baldyga et al., 2007; Luke Omondi Olang, Kundu, Bauer, and Fürst, 2011).

The Mt Elgon forest, shared by Uganda and Kenya, is also an important water catchment, with rivers draining into Lake Turkana and Lake Victoria. The Mt. Elgon conservation area covers areas under Uganda Wildlife Authority and Kenya Forest Service and the Kenyan Wildlife Service (Roussel and Daval, 2012). The Water Towers of Kenya and most notably Mau forest complex positively influence the economic resilience of Kenya as a country (Crafford, et al., 2012). The forest sector in Kenya provides various products that directly support the livelihood of the local communities such as the Ogiek who have settled around the Mau forest Complex (Langat et al., 2016) and the Sabaots ethnic community in Mt Kenya (Ongugo, Njuguna, Obonyo, and Sigu, 2001).

1.3. Aims of the study

To assess the rate of clearance and recovery of the TMFs in East Africa, this research project aims to quantify the trends and rate of forest loss due to deforestation in the Mau forest complex and Mt Elgon forest, determine the rate of natural recovery of the forest i.e. structure and composition notably aboveground biomass, species diversity, and richness; assess the changes and response of soil physical and chemical properties i.e. soil C and N, soil organic matter (SOM), bulk density (BD).

In order to achieve the aims, remote sensing tools and techniques were used to quantify the rate of forest clearance and current trends of deforestation and forest recovery from the time since the forest was last cleared. In addition, the study also assessed the changes in soil physical and chemical properties in different recovery regimes in the montane forest of east Africa. To minimize the false classification, the current study used satellite imagery collected during the dry months in the Mau forest complex. The main goal of this study is to quantify the stage of forest degradation and clearance in in two montane forests of East Africa (Mt Elgon forest and Mau forest complex) and determine the rate of forest recovery in the Mau forest complex.

1.3.1. Specific Objectives

1. To assess the trend, rate of deforestation, and forest clearance in the Mau forest complex and Mt Elgon forest.
2. To determine the rate of forest recovery (biomass and species) in the tropical montane forest of east Africa.
3. To determine changes in C stocks, soil physical and chemical properties in different recovery regimes in the Tropical Montane forest of East Africa.

1.4. Overall thesis structure

The thesis will be organized into five (5) chapters. The current chapter (1) contains the general introduction and background to the study; aims and objectives as well as the research questions.

Chapter 2: Focuses on the assessment of the rate of deforestation and forest degradation in the tropical montane forests of East Africa (the Mau forest complex and Mt Elgon forest) the specific objectives/research questions include:

- To identify the areas where deforestation and forest clearing has occurred
- To determine when the first and last deforestation took place
- To assess and determine the annual rate of deforestation and recovery in the montane forests of east Africa.

Chapter 3: Focuses on the determination of the rate of forest recovery in the tropical montane forest of East Africa. In this chapter, the study assessed how forest structure and composition recover after clearance and deforestation. The forest structural and compositional parameters measured include stand height (H), diameter at breast height (DBH), stand density, basal area (BA), aboveground biomass (AGB), species richness, and diversity across different recovery stages (stand age).

Chapter 4: Focuses on the determination of the changes in soil physical and chemical properties in different recovery stages and quantifying soil C and N stocks. The soil properties include soil bulk density (BD), soil organic matter (SOM), soil pH, soil C and N concentration (N), soil C:N ratio, and disturbance index (DI).

Chapter 5: Synthesizes and discusses the whole thesis and indicates how the key findings and objectives of the research study were achieved. It also indicates how the

findings of the research can be integrated into existing policies to improve forest monitoring and management as well as the conclusions.

2. MAPPING DEFORESTATION AND RECOVERY OF TROPICAL MONTANE FORESTS OF EAST AFRICA



Evidence of cutting down of trees for fuelwood, (a) and (b) Southwestern Mau Forest, collection of firewood and charcoal burning (C) in Transmara block in Mau Forest complex – Photographs taken during the field work in the Mau forest Complex in March 2019.

Abstract

Deforestation poses a major threat to the tropical montane forest ecosystems of East Africa. Tropical montane forests provide key and unique ecological and socio-economic benefits to the local communities and host diverse flora and fauna. There is evidence of ongoing deforestation and forest clearance in these montane forests although estimates diverge among different sources suggesting rates of 0.4-3% yr⁻¹. Quantifying deforestation rates and identifying areas that are affected by deforestation is critical to design conservation and sustainable forest management policies. This study quantified the rate of deforestation and forest recovery over the last three decades based on the available remote sensing data for the Mau Forest Complex and Mount Elgon forests in Kenya and Uganda using remote sensing imagery from the Landsat time series. This study presents trends in areas of forest loss, rates of deforestation, and forest recovery providing quantitative evidence that can be used for effective monitoring and management of these forests. With the analysis, classification accuracies of 86.2% and 90.5% and Kappa Coefficients of 0.81 and 0.88 were obtained for the Mau Forest Complex and the Mt Elgon forests, respectively. This study shows that 21.9% (88,493 ha) of the 404,660 ha of Mau forest was lost at an annual rate of -0.82% yr⁻¹ over the period between 1986 - 2017, 18.6% (75,438 ha) of the forest cover that was disturbed during the same period and is currently undergoing recovery. In the Mt Elgon forest, 12.5% (27,201 ha) of 217,268 ha of the forest cover was lost to deforestation at an annual rate of -1.03 % yr⁻¹ for the period between 1984 - 2017 and 27.2% (59,047 ha) of the forest cover disturbed is undergoing recovery. The analysis further revealed that for the Mau forest Complex, smallholder and large-scale agriculture were the main driver of forest cover loss accounting for 81.5% (70,612 ha) of the deforestation, of which 13.2% was as a result of large scale

agriculture and 68.3% was related to the smallholder agriculture. For the Mt Elgon forest, agriculture was also the main driver accounting for 63.2% (24,077 ha) of deforestation followed by the expansion of human settlements that contributed to 14.7% (5,597 ha) of forest loss. This study provides new ecosystem wide estimates of the rate of deforestation for the Mau forest complex and Mt Elgon forest ecosystems. These rates are higher than previously estimated and this study identified areas where recent deforestation occurred, which provides a quantitative basis for forest restoration programs and to design conservation policies.

2.1. Introduction

Deforestation poses a global challenge to humanity due to its contribution towards greenhouse gas (GHG) emissions to the atmosphere and the impact that forest loss has on the hydrological cycle globally. Forests regulate water flows in catchments by playing an important role in the interception of rainfall, reducing runoff, attracting rainfall through their high evapotranspiration rates, and contributing to condensation (Sheil, 2018; Sheil and Murdiyarso, 2009). Forests also contribute to cloud formation by releasing biogenic volatile compounds into the atmosphere, which accelerate condensation (Ellison et al., 2017), contrarily deforestation increases the surface temperature which contributes to increased evaporation and reduces evapotranspiration (Lawrence and Vandecar, 2015). Since 1990, an estimated total of 420 million hectares of forests have been lost globally because of conversion to other land uses most notably agriculture and human settlements. Between 2015 and 2020, the global rate of deforestation was estimated at 10 million ha yr⁻¹ down from 16 million ha yr⁻¹ in the 1990s (FAO and UNEP, 2020). Between 2001 and 2019, forest clearing resulted in global gross GHG emission of 8.1 ± 2.5 GtCO₂e yr⁻¹, yet tropical forests contribute most (5.3 ± 2.4 GtCO₂e yr⁻¹) to the removal of atmospheric carbon dioxide (CO₂) emissions (Harris et al., 2021).

Despite the importance of tropical forests, their cover has dropped from 1,966 million ha in 1990 to 1,770 million ha in 2015 (FAO, 2015; Keenan et al., 2015; MacDicken, 2015). Large areas of tropical forests have been deforested between 2000-2012 of which 20% were in Africa (Kim, Sexton, and Townshend, 2015; Mitchard, 2018). The tropical forests in sub-Saharan Africa are facing a rapid loss as a result of deforestation and degradation at an estimated annual conversion rate of approximately 0.4 to 0.5% yr⁻¹ (Mayaux et al., 2005; FAO, 2015). The reported rapid loss of the forest land may

also be associated with the increasing demand for land for agriculture and human settlements which means that forests are the main target for conversion (Kissinger et al., 2012; Curtis et al., 2018). The rates at which forests are lost have been reported for global and continental scales, for example, by the Global Forest Change (GFC) platform and Global Forest Watch (Hansen et al., 2013). The GFC data shows forest gain and loss from 2001 and these forest cover change estimates provide the global perspective of the forest cover change with accuracy that differs largely by region. The usefulness of global datasets at a local scale has not been closely examined for East Africa in particular the Mau forest Complex and Mt Elgon forest (Hamunyela et al., 2020), although evidence elsewhere suggests that GFC underestimates rates at a local scale (Milodowski, Mitchard, and Williams, 2017) and in Tanzania (Ahrends, et al., 2021). The GFC dataset (Hansen et al., 2013) provides estimates of the scale and magnitude of forest cover change as a gain or loss, and although these estimates are valuable there is a need to distinguish permanent losses due to deforestation and to identify areas under-recovery over time especially through forest clearing events i.e. fragmentation, logging, shifting cultivation or fires (Curtis et al., 2018; Grantham, Costa, Elsen, Laurance, and Watson, 2020). Reliable estimates for the rates of deforestation for Africa are lacking at both national or regional levels (Achard et al., 2014). Understanding the magnitude and spatial distribution of deforestation hotspots is crucial to effectively monitor, sustainably manage, and protect tropical forest ecosystems (Hansen et al., 2008).

In East Africa, the annual rates of deforestation at the national level are debated and estimated at 0.05% yr⁻¹ (Kenya) for the period 1990 - 2010 and 0.4-3% yr⁻¹ (Uganda) in 2016 (Mwangi, Cerutti, Doumenge, and Nasi, 2018). These rates are contentious and differences in estimates arise due to differences in forest types, measurements,

definitions of forest cover, and reporting methods (MacDicken, 2015). This study aims to contribute reliable estimates of forest change for East African montane forests, focusing on two important forests of Kenya and Uganda because of their ecological and socio-economic value to the whole region (Cavanagh, 2017; KEFRI, 2018; WWF, 2007). The East African montane forests are found in moderate to high altitudes comprising of several separate mountain areas above 2,000 meters spanning from South Sudan through Uganda and Kenya to Northern Tanzania along the Rift valley (EAC, UNEP, and GRID-Arendal, 2016) as indicated in Figure 1-2.

In Kenya and Uganda, the montane forests are referred to as the “Water towers of East Africa” because they play significant roles in the regulation of the water cycle (Nabutola, 2010). These “water towers” include the Mau Forest Complex, Mount Kenya, the Cherangani hills, Aberdare Range, and the Mt Elgon forest that borders both Uganda and Kenya (Kenya Water Towers Agency, 2015). These montane forests and especially the Mau forest complex and Mt Elgon forest face high risks of deforestation and forest clearance resulting from human encroachment (Brandt et al., 2018; Sassen et. al., 2013; Mugagga et. al., 2012). Previous studies on these montane forests focused on the land-use change dynamics in a section or specific blocks of the Mau forest complex and the Mt Elgon forests with a focus on land cover and land-use change (e.g. Baldyga et al., 2007; Were et al., 2013). Although some studies such as Ayuyo and Sweta (2014); Kimutai and Watanabe (2016); Swart (2016) assessed land use and land cover change and the underlying drivers for the Mau forest complex, their findings do not report rates of deforestation, forest clearing and the rates of forest recovery. This study presents the latest estimates of deforestation and compares these two important forests in their dynamics of change, the underlying drivers of forest change, and the extent of forest recovery. Quantifying the rates of deforestation and

understanding its underlying causes is a critical element for designing and developing policies aimed at tackling forest cover loss for example by government or international agencies to support the implementation of the programs such as REDD+ (Entenmann et al. 2014).

Different remote sensing tools and approaches are used to detect, monitor, and map forest loss due to deforestation and other forms of forest clearance. For example, Breaks For Additive Season and Trend (BFAST) which uses Landsat time-series data (DeVries et al., 2015), TimeSync (Cohen, Yang and Kennedy, 2010), spectral forest recovery trajectories (Frazier, Coops and Wulder, 2015), and supervised image classification (Margono et al., 2012). The progress achieved with developing methodologies has been supported by the availability of Landsat data at no cost from United States Geological Surveys (USGS) database that makes it feasible to assess trends in forest cover change over time (Griffiths et al., 2014; Mitchell, Rosenqvist and Mora, 2017). This study assesses trends of forest cover change leading to forest loss using the freely available satellite data of the use of Landsat time-series data for mapping deforestation and recovery (gain) after the resulting forest clearance. In this study, deforestation is defined according to Hirata et al., (2012) as “direct human-caused conversion of forested land to non-forested land” and therefore detected as a loss. In this study, Landsat imagery from 1984 was classified to determine forest cover change i.e., determine the rate of deforestation (loss) and forest recovery (gain) in Mau forest complex and Mt Elgon forest.

The specific research objectives were;

- (i) to identify the areas where deforestation has occurred
- (ii) to detect when the first and last deforestation took place

- (iii) to quantify the annual rate of deforestation and recovery for montane forests.

To address the specific objectives, the study used the archived and freely available Landsat data collected between December – March every time series from 1984/1985 to 2017 to analyze forest cover change. Images with no cloud cover or up to 10% cloud cover were selected from the Landsat data archives and supervised classification with Maximum Likelihood (ML) algorithm was used to classify and determine the forest cover change.

2.2. Materials and Methods

2.2.1. Study area

The study areas were the Mau Forest Complex (01°2'21.60" S, 36° and 0°14'33.04" N, 35°13'40.92E) in Kenya and Mt Elgon forest (01°07'06"N and 34°31'30"E) located in western Kenya and eastern Uganda (Fig. 1). The Mau forest ecosystem comprises several forest blocks namely: Narok, Masaya Mau, Eastern, and Western Mau, Southern to Southwestern Mau, and Transmara regions (Chrisphine et al., 2015). This forest is the major catchment area for 12 rivers (Chrisphine et. al., 2015; Olang and Kundu, 2011) draining into Lake Baringo, Nakuru, Turkana, Natron, and the Trans-boundary Lake Victoria shared by Kenya, Uganda, and Tanzania.

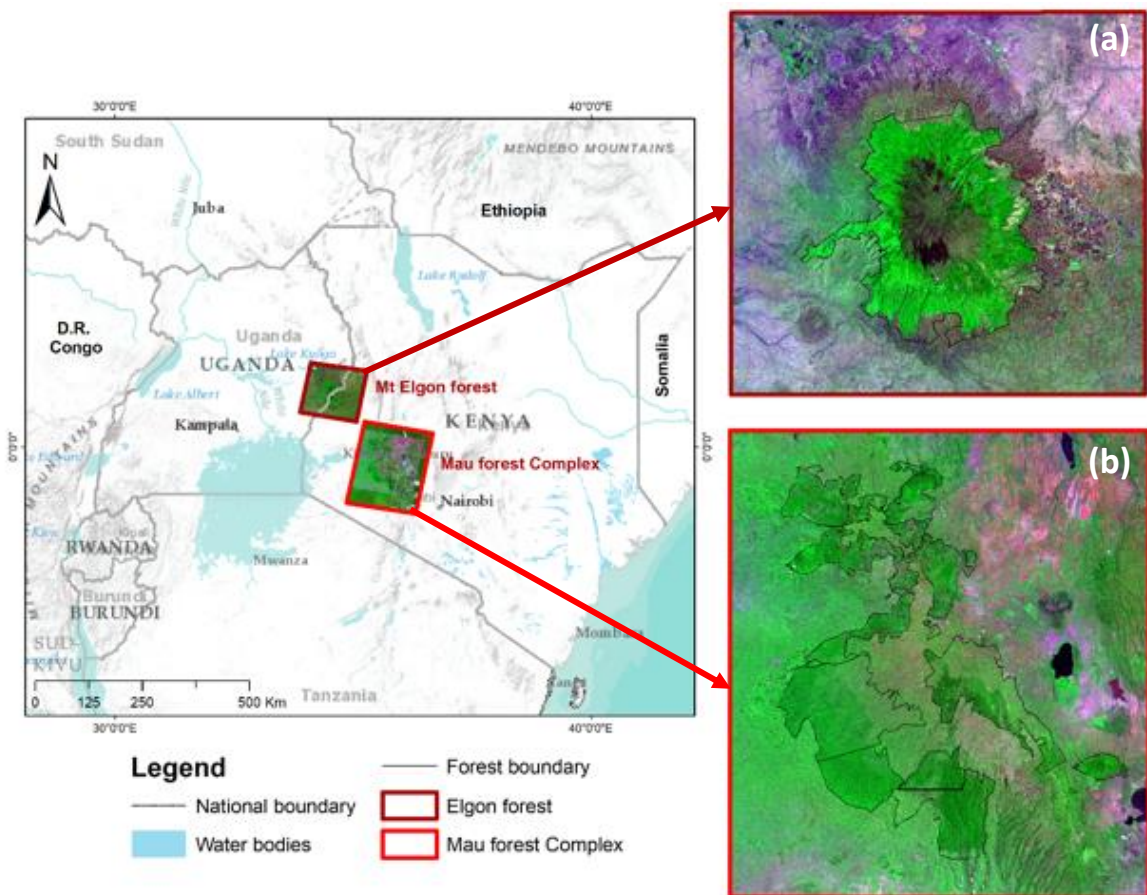


Figure 2-1: Location of the Mau forest complex and Elgon forest in East Africa. (a) Map showing the official boundaries of the Mt Elgon forests (Scott, 1998) and (b) Map showing the official boundaries of the Mau forest complex (KFS, 2009).

2.2.2. Data sources

This study used Landsat satellite imagery acquired from the USGS archives for the study area including Path/Raw 170/59 (for Mt Elgon forest) and 169/60 – 61 for the Mau forest complex as indicated in Tab. 2-1. Available data from Landsat 4 and 5 Thematic Mapper [TM], Landsat 7 Enhanced Thematic Mapper Plus [ETM+], and Landsat 8 OLI were collected during dry months (from December to March) for both the Mau forest Complex and Mt Elgon forest ecosystems. Forest boundaries created in 2009 for the Mau forest Complex were obtained from the Kenya Forest Service (KFS) and for the Mt Elgon forest from the National Forestry Authority (NFA) for the part of Mt Elgon forest located in Uganda. The Mt Elgon forest boundary was demarcated in 1968 for the Kenyan side and in 1992 for the Uganda side (Scott, 1998). The Landsat data were processed and classified using GIS and remote sensing (image analysis) software mainly; ArcGIS and ENVI using the steps indicated in Fig. 2-2.

Table 2-1: Landsat data obtained from the USGS database for the Mau forest complex and Mt Elgon forest area. The selected images were those that were available for the study area with less than 10% cloud cover. Additionally, the images were selected for the period between December – March, every year which reflects the dry season in the study area to avoid the influence of vegetation phenology to be classified as forest.

Path/Raw	Date of Acquisition	Sensor	Number of Images	Study Area
169/60-61	09/01/1985	L5 TM	2	Mau forest complex
169/60-61	28/01/1986	L5 TM	2	Mau forest complex
169/60-61	01/03/1989	L4 TM	2	Mau forest complex
169/60-61	21/01/1995	L5 TM	2	Mau forest complex
169/60-61	12/02/2000	L7 ETM+	2	Mau forest complex
169/60-61	14/02/2001	L7 ETM+	2	Mau forest complex
169/60-61	01/02/2002	L7 ETM+	2	Mau forest complex
169/60-61	04/02/2003	L7 ETM+	2	Mau forest complex
169/60-61	30/01/2010	L5 TM	2	Mau forest complex
169/60-61	26/02/2014	L8 OLI	2	Mau forest complex
169/60-61	17/03/2015	L8 OLI	2	Mau forest complex
169/60-61	16/02/2016	L8 OLI	2	Mau forest complex
169/60-61	17/01/2017	L8 OLI	2	Mau forest complex
169/60-61	05/02/2018	L8 OLI	2	Mau forest complex
170/59	31/12/1984	L5 TM	1	Mt Elgon forest
170/59	08/03/1986	L5 TM	1	Mt Elgon forest
170/59	27/03/1987	L5 TM	1	Mt Elgon forest
170/59	18/02/1988	L4 TM	1	Mt Elgon forest
170/59	12/01/1995	L5 TM	1	Mt Elgon forest
170/59	06/03/2000	L7 ETM+	1	Mt Elgon forest
170/59	05/02/2001	L7 ETM+	1	Mt Elgon forest
170/59	07/01/2002	L7 ETM+	1	Mt Elgon forest
170/59	10/01/2003	L7 ETM+	1	Mt Elgon forest
170/59	21/01/2010	L5 TM	1	Mt Elgon forest
170/59	05/03/2014	L8 OLI	1	Mt Elgon forest
170/59	03/01/2015	L8 OLI	1	Mt Elgon forest
170/59	23/02/2016	L8 OLI	1	Mt Elgon forest
170/59	09/02/2017	L8 OLI	1	Mt Elgon forest
170/59	12/02/2018	L8 OLI	1	Mt Elgon forest

This study also used the Global Forest Change (GFC) dataset from 2000 to 2017 (version 1.5), which was obtained from the google earth engine database (<http://earthenginepartners.appspot.com/science-2013-global-forest>) resulting from the analysis of time series Landsat data (Hansen et al., 2013). The 30-meter resolution data were obtained in 10 x 10° granules. For the Mau forest complex and Mt Elgon forest, 0° – 10°N, 30° – 40°E and 0° – 10°S, 30° – 40°E granules were downloaded from the University of Maryland (UMD) database with all the data layers such as ‘treecover2000’, ‘loss’, ‘gain’, ‘loss year’, ‘datamask’, ‘first’ (circa year 2000) or ‘last’

(circa year 2014). In this study, the 'lossyear' layer was used to compare with the forest loss from supervised classification results for the period 2000 – 2017.

GFC quantifies the trend in forest cover change (gain and loss) from the year 2000, which has been reported to present limitations at the local scale (Sannier et. al., 2016; Hamunyela et al., 2020) compared to the supervised classification approach to determine forest cover change since 1986 (Mau forest Complex) and 1984 (Mt Elgon forest).

2.2.3. Image analysis and classification

Supervised classification with the Maximum Likelihood algorithm (ML) was undertaken to assess forest cover change. The ML classifier considers the centers of the clusters (class), shape size, and the orientation of the clusters by calculating the statistical distance based on the mean values and covariance matrix of the clusters (Bakx, Janssen, Schetselaar, Tempfli, and Tolpekin, 2012). The acquired Landsat imagery shown in Tab. 2-1 were processed, classified, analyzed and the results were compared with the forest cover change from GFC data for the corresponding period. The supervised classification approach used in the current study requires reference data for training and validation. Available high-resolution Google imagery dated February 04, 2017, was used to obtain the reference data for training and validation of the classified Landsat data following (Fortier, Rogan, Woodcock, and Runfola, 2011; Rutkowska, Dubalska, Bajger-Nowak, Konieczka, and Namieśnik, 2014; Zhu, Woodcock, and Olofsson, 2012). Classification accuracy was assessed using the error matrix (confusion Matrix) with the high resolution (50 cm) Google images used as the reference data following (Olofsson et al., 2014; Strahler et al., 2006; Vogelmann et al., 2017).

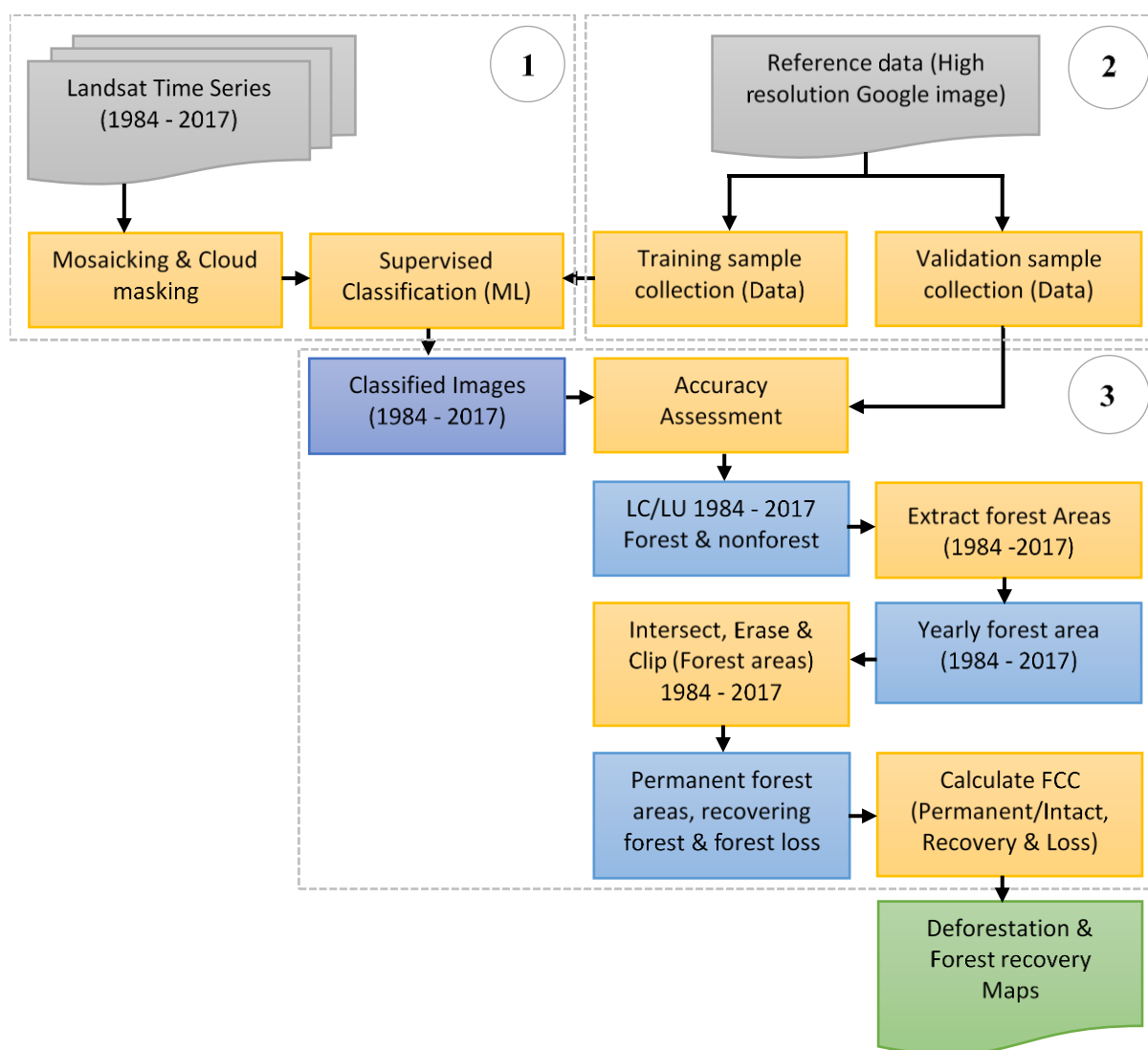


Figure 2-2: Flow chart showing a summary of the methodology that was undertaken in the current study. The Landsat imagery data were acquired from the USGS database and processed i.e., mosaicked, and classified using the ENVI Software (1), available high-resolution imagery from Google earth engine for the study area were used to collect and identify the training and validation samples (2). The accuracy of the classified images was then assessed using the validation data, from the validated land cover/land use data, forest areas were extracted for each year under observation, assessed with the GFC data, change detection was carried to determine the deforestation and areas that are under-recovery (3).

To map forest cover change, seven (7) land cover classes (with the corresponding land use) were defined namely: forest, agriculture (large scale), agriculture (small scale), rangelands, settlement/urban, and moorland as described in Tab. 2-2. The land use and land cover classes were defined based on criteria and classification schemes obtained from previous studies carried out in the current study area and the region

(FAO, 2014; Houghton et al., 2012; Mugagga et al., 2015; Ongong'a and Sweta, 2014; Sassen et al., 2013) and the vegetation map of the Eastern Africa region (VECEA Team, 2020).

Table 2-2: Land cover classes and the scheme used in the study adopted from similar reported studies in the same current study area as well as the reported vegetation classification in Eastern Africa.

Land cover/land use Class	Description (FAO/National Classification and Vegetation map for Africa)
Forest (F)	Trees with closed canopy visible on high-resolution imagery. With height >2 m, canopy cover of >30%.
Agriculture large-scale (LA)	Large scale commercial agriculture including tea estates of >2 ha, large scale irrigated and mechanized agriculture.
Agriculture smallholder (SA)	Smallholder agriculture (Small-scale) mainly rainfed with fields of <2 ha for subsistence farming purposes.
Rangeland (R)	This involves open land cultivated with pasture and grasslands.
Settlements/urban (SU)	Bare land, developed with high density especially urban areas, infrastructure, and markets with limited farmlands.
Moorland (M)	Extensive low-growing vegetation characterized with heath in high altitude >1500 meters above sea level commonly referred to as Afro-alpine vegetation
Water (W)	This includes lakes, rivers, or open water (both natural and man-made).

In order to correctly match the classes or features observed on the high resolution (50 cm) Google imagery with the same features on the 30 m resolution Landsat Imagery, a visual interpretation of the high-resolution Google imagery and the Landsat multispectral image (appendix 1) side by side was undertaken to obtain 500 training and validation samples used for the supervised classification of the multispectral Landsat images. The visual Image analysis allows spontaneous recognition of features on both set images and then draw a logical inference which then can be used to implement the digital image classification by selecting classification samples based on the clear understanding of the classes (Bakx et al., 2012).

2.2.4. Forest cover change, deforestation, and forest disturbance

Forest cover changes were quantified from the classified satellite images selected with at least <10% cloud cover during the dry months of the study area (December to March) every year from 1986 to 2017 for the Mau forest complex and 1984 to 2017 for the Mt Elgon forest shown in Tab. 2-1. To quantify forest cover change over time, the multispectral images and the high-resolution imagery of the study area were visually interpreted and areas showing deforestation (loss) and forest recovery (gain) were identified as shown in Fig. 2-3, before supervised classification was undertaken.

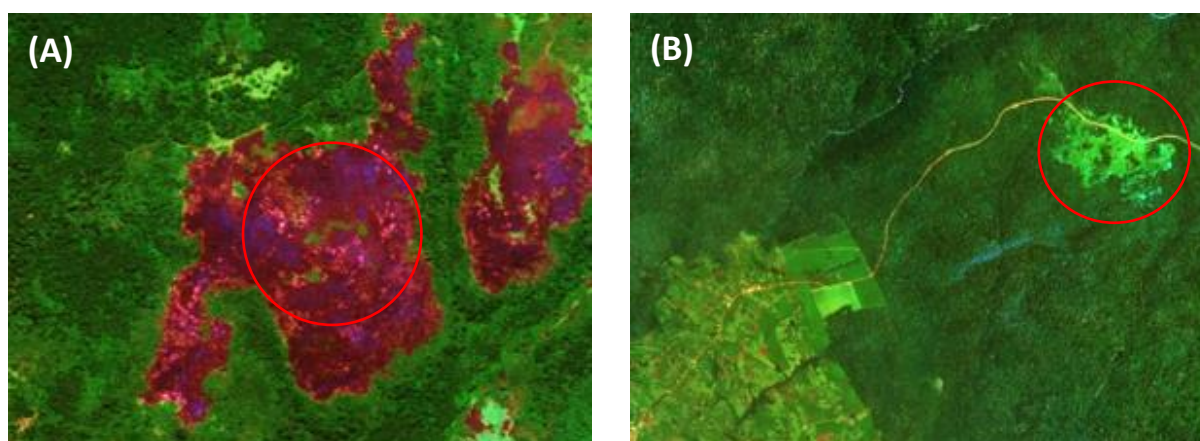


Figure 2-3: Examples from Mau forest complex of areas that show deforestation as a result of fire indicated by the red circle (A) and forest clearance and forest recovery as a result of encroachment (B). The high-resolution Google imagery is dated February 04, 2017.

From the classified imagery, forest area for each year was extracted and used to calculate; firstly, forest areas that were lost to deforestation and did not recover, secondly forest areas that were deforested and were undergoing recovery, and thirdly, forest areas that stayed forest since the beginning of the time series. To quantify the areas that were permanent forest, recovering and lost (deforested), the current forest boundaries for the Mau forest complex and Mt Elgon forest (Government of Kenya, 2017) were used to clip and estimate area changes within the forest boundary for both forests.

2.2.5. Rate of deforestation

The rate of deforestation was calculated from the yearly detected change in forest cover. This study adopts the method by Puyravaud (2003), who proposed the use of the mean annual rate of change of forest cover over time. The method has been widely used to quantify the rate of deforestation and land cover change across the tropics (e.g. Grinand et al., 2013; Schulz et al., 2010; Reimer et al., 2015). The rate of deforestation (Eqn. 1) is based on the change analysis and the method accounts for variations in date for the image acquisitions.

Equation 2-1: Rate of deforestation

$$r = (1/(T_2 - T_1)) \times \ln(A_2/A_1)$$

where: r = the deforestation rate per year (% yr⁻¹)

T_1 = Year for the beginning of the time step (initial year)

T_2 = Year for the end of the time step (final year)

A_1 = Forest area at the beginning of the time step (initial year)

A_2 = Forest area at the end of the time step (final year)

Classified images for the Mau Forest Complex and Mt Elgon forest were used to determine the change in land cover from forest to the other land cover/land use types (gross loss) and other land covers to forest (gross gain), the net change was calculated by subtracting the gross loss from the gross gain for the timespans based on the available imagery. To determine the transition of change from forest to other land covers/land use types, a matrix table for the classified land cover/use types was generated and the change areas were obtained. To determine the rate of deforestation, the current official forest boundaries for both Mt Elgon forest and the Mau forest complex were used to carry out change detection to identify areas that were deforested.

2.3. Results

2.3.1. Land cover classification and forest cover change

Land cover and forest cover change in the Mau forest complex are presented for the period 1986 - 2017 and the Mt Elgon forest for the period 1984 - 2017 (Fig. 4). Seven land cover classes were identified namely forest, agriculture (large scale), smallholder agriculture, rangelands, open/bare land, moorland, and water. Overall classification accuracy of 86.2% with Kappa coefficient of 0.81 was attained for the Mau forest complex and 90.5% (Kappa coefficient of 0.87) for the Mt Elgon forest as indicated in Tab. 2-3 (a) and (b). In the Mau forest complex, rangelands were classified with the lowest producer accuracy (P) of 44.51% and the settlements/urban were classified with a lower user accuracy (U) of 30.64%. For the Mt Elgon forest, agriculture (A) had the lowest producer accuracy of 67.16% and the open/bare land class had the lowest user accuracy of 60.77%.

Table 2-3: Accuracy assessment for the supervised classification of the Mau forest complex (a) and the Mt Elgon forest (b)

(a) The Mau forest complex										
Overall Accuracy = 86.2%, Kappa Coefficient = 0.81										
Class	Confusion Matrix							Total	P (%)	U (%)
	F	AL	SA	R	B	W				
F	89.96	0.52	0.21	0.00	0.00	0.00	21.23	89.96	99.45	
AL	0.12	88.19	0.93	0.00	0.80	0.00	6.16	88.19	93.42	
SA	9.83	4.19	91.51	36.01	0.08	0.00	42.91	91.51	82.87	
R	0.00	0.24	4.03	44.51	0.00	0.00	7.48	44.51	78.86	
B	0.09	6.86	3.32	19.48	99.12	0.07	6.27	99.12	30.64	
W	0.00	0.00	0.00	0.00	0.00	99.93	15.96	99.93	100.0	

F = Forest, AL = Agriculture (Largescale), SA = Agriculture (Smallholder), R = Rangeland, B = Bare land (Open Land) and W = Water, P = Producer accuracy and U = User accuracy

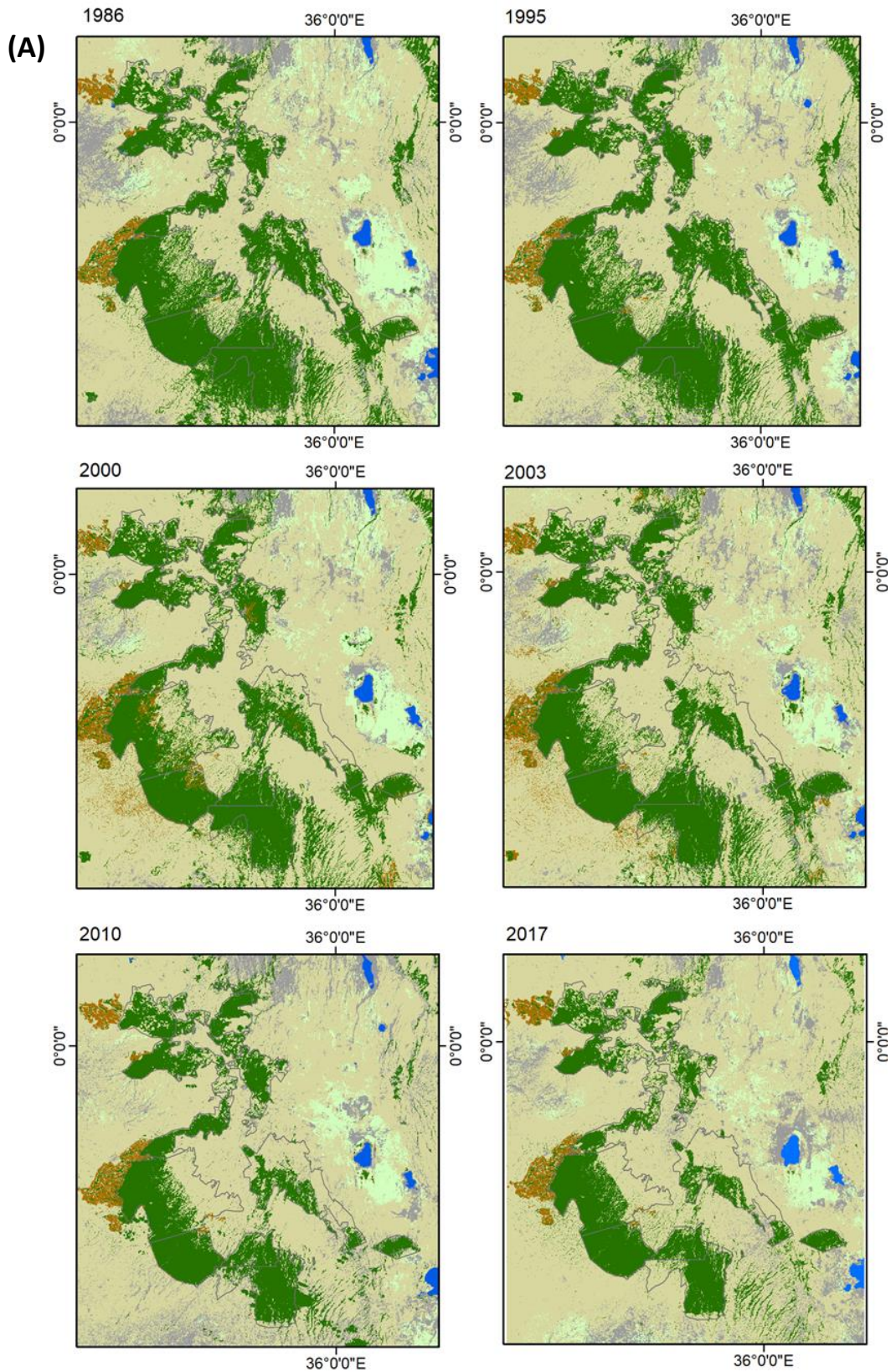
(a) Mt Elgon forest

Overall Accuracy = 90.50%, Kappa Coefficient = 0.87

Class	Confusion Matrix						Total	P (%)	U (%)
	F	A	R	M	B	W			
F	100	0.00	0.00	0.00	0.00	0.00	19.45	100.0	100.0
A	0.00	67.16	0.55	0.00	1.54	0.00	18.88	67.16	98.92
R	0.00	22.66	99.45	0.00	3.82	0.00	31.44	99.45	79.45
M	0.00	0.88	0.00	100	0.00	0.00	20.29	100.0	98.80
B	0.00	9.30	0.00	0.00	94.64	0.00	6.59	94.64	60.77
W	0.00	0.00	0.00	0.00	0.00	100	3.35	100.0	100.0

F = Forest, A = Agriculture, R=Rangeland, M = Moorland B = Bare land (Open Land) and W=Water P= Producer accuracy and U = User accuracy

The analysis shows that in the Mau forest complex, forest areas that existed outside the current forest boundary of 2009 were converted to mainly agriculture both small and large scale. For the Mt Elgon forest, agriculture was also the main land cover/use to which forest area was lost.



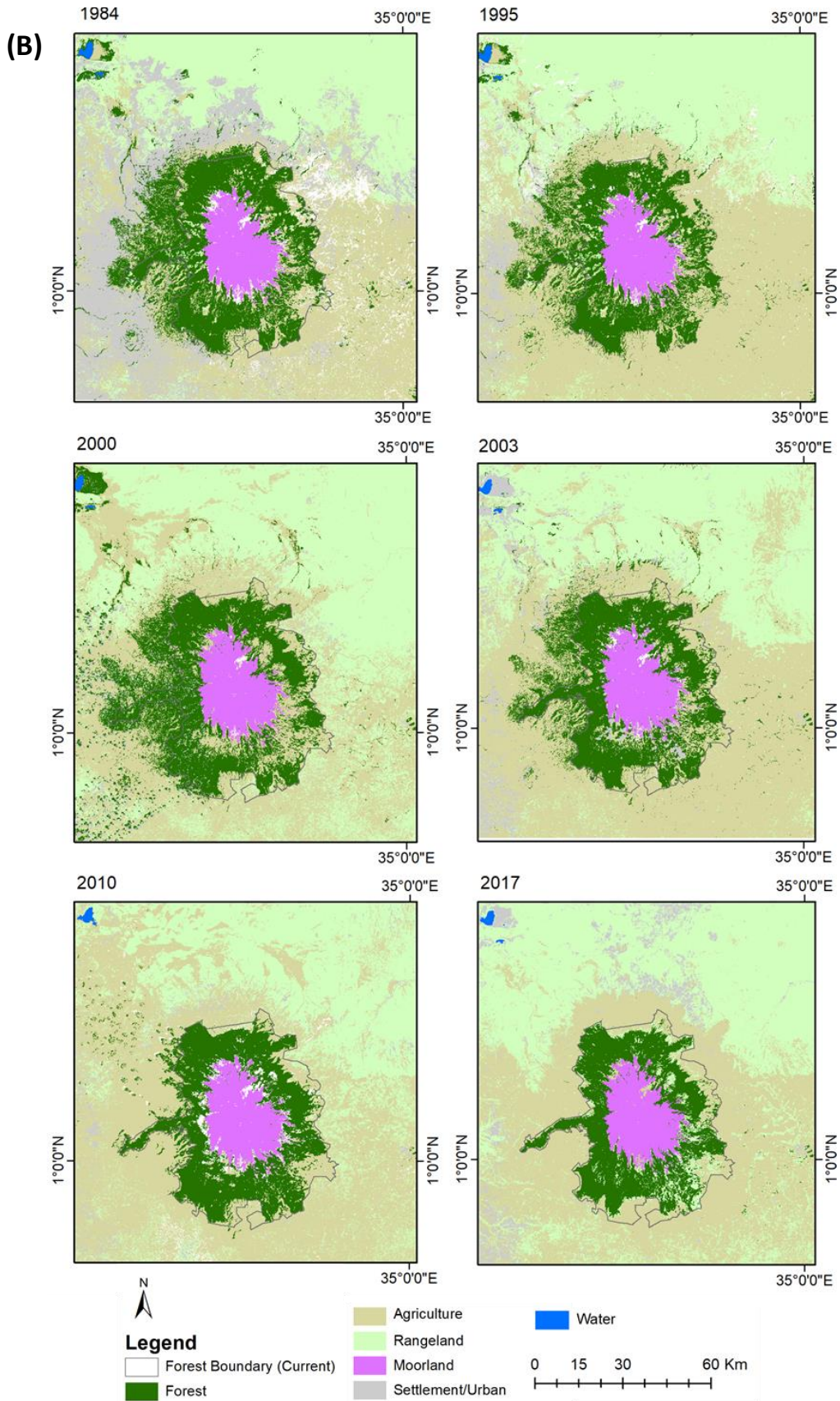


Figure 2-4: Land cover map from 1986 to 2017 for the Mau forest complex (A), and from 1984 to 2017 for the Mt Elgon forest (B) showing forest cover change within and outside the official boundaries of the two montane forests.

The results show that 81.5% (70,612 ha) of forest cover was lost mainly to agriculture between 1986 to 2017, of which 13.2% (11,440 ha) was attributed to large scale agriculture and 68.3% (59,172 ha) was attributed to smallholder agriculture in the Mau forest complex (Fig. 2-5a). For the Mt Elgon forest, agriculture was also the main land cover to which forest was lost accounting for 63.2% (24,077 ha) followed by settlement at 14.7% (5,597 ha) as indicated in (Fig. 2-5b).

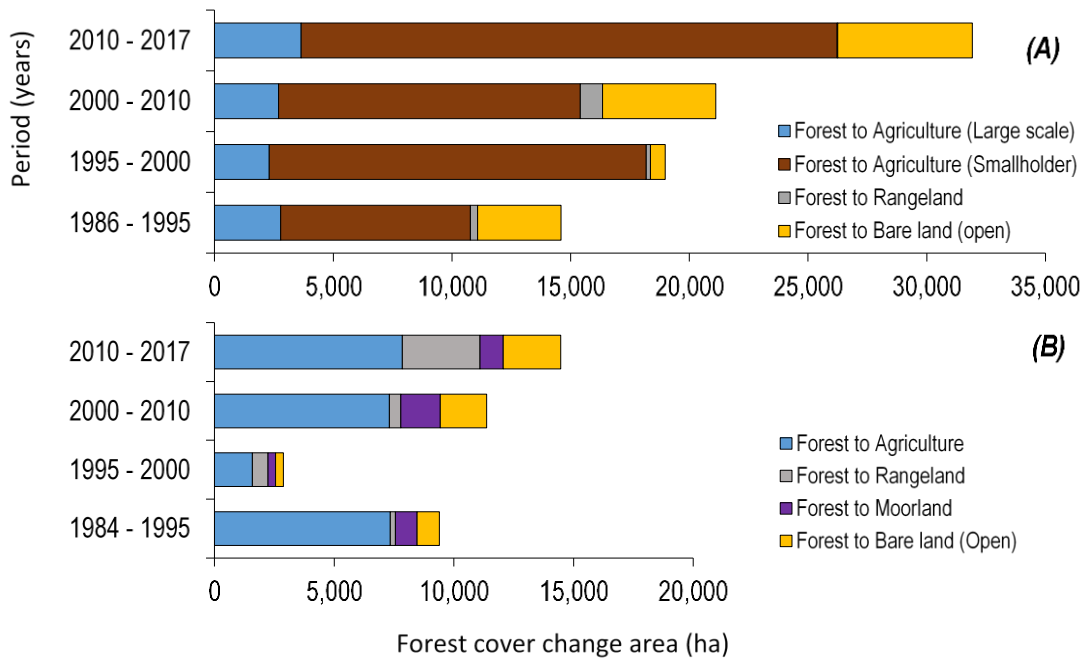


Figure 2-5: Land use change transitions from forest to other land cover i.e., agriculture (large scale), agriculture (small-scale), rangeland, moorland, and bare land (open) in (A) the Mau forest complex and (B) Mt Elgon forest. Throughout the period, net forest gain, loss, and net change were calculated for the Mau forest complex and Mt Elgon forest (Fig. 6a and 6b).

From the gross changes (loss and gain), net forest cover change was established for all the years based on the available imagery for the Mau forest complex as shown in Fig. 2-6(A) and for the Mt Elgon forest as indicated in Fig. 2-6(B)

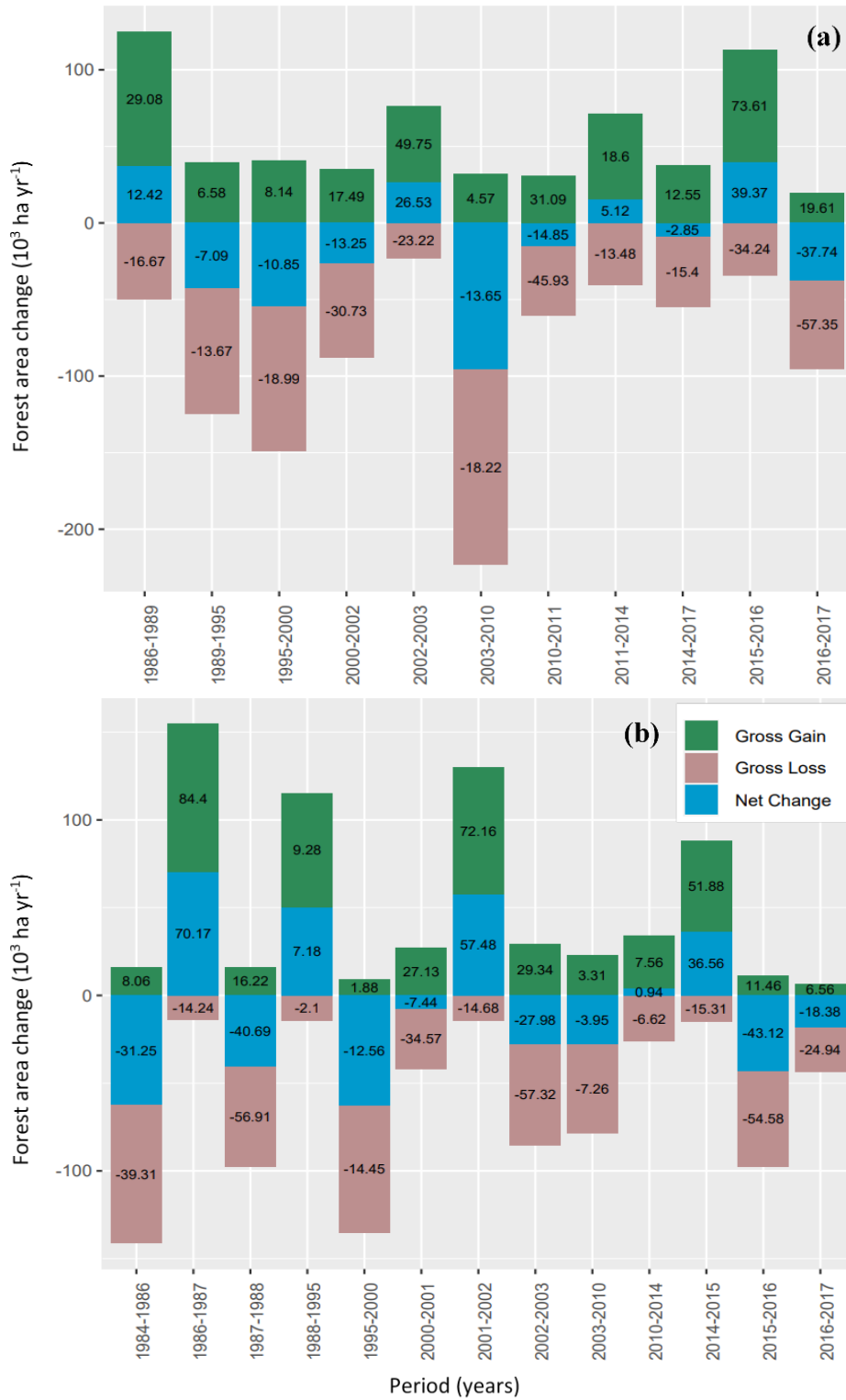


Figure 2-6: Changes in forest area for the various periods (1984/1986 - 2017) for the Mau forest complex (a) and Mt Elgon forest (b). Net change (in blue) is the difference between Gross gain and Gross loss. The bars represent the total change for each period while the values represent the annual change within the periods. A negative net result indicates overall forest conversion to other land covers.

2.3.2. Forest cover change from supervised classification

The forest cover loss in the Mau forest complex was assessed for the period 1986 to 2017 and in Mt Elgon forest for the period 1984 to 2017 for the available Landsat imagery that were classified using the supervised classification (maximum likelihood classifier) approach. The forest area (gains and losses) obtained from the supervised classification were compared to the corresponding estimates from GFC for the period 2000 – 2017. The results indicate that in the period 2000 - 2017, GFC detected a forest cover loss of 17.0 % (68,848 ha) out of the 404,660 ha in the Mau forest complex and 5.3% (11,501 ha) of the 217,268 ha of forest loss in the Mt Elgon forest. The analysis conducted in this study with supervised classification from the same period (2000 - 2017) estimated similar overall figures for the Mau forest complex with 16.8% (68,155 ha) and larger forest loss with 7.6% (16,496 ha) for the Mt Elgon forest as presented in Tab. 2-4.

Table 2-4: Estimates of forest cover loss using Supervised Classification (ML) compared to the GFC data for the Mau forest complex (a) and the Mt Elgon forest (b) for the period 2000 - 2017

Period (2000 - 2017)	Mau Forest Complex				Mt Elgon Forest			
	ML		GFC		ML		GFC	
	Area (ha)	%	Area (ha)	%	Area (ha)	%	Area (ha)	%
Deforestation	68,155	16.8	68,848	17.0	16,496	7.6	11,501	5.3
Remained forest	282,779	69.9	276,446	68.3	120,497	55.5	166,356	76.6
Non-forest	53,668	13.3	59,308	14.7	80,275	37.0	39,411	18.1
Total	404,602	100	404,602	100	217,268	100	217,268	100

2.3.3. Forest cover change, deforestation, and recovery

Forest cover changes from 1986 to 2017 for the Mau forest complex and the Mt Elgon forest from 1984 to 2017 within their respective official forest boundaries are shown in Fig. 7. The hotspots, forest blocks, and areas that are more pronouncedly affected by deforestation were the Southwestern Mau, Eastern Mau, Londiani (Western Mau), and Maasai Mau. For the Mt Elgon forest, deforestation was more pronounced in the Kapchorwa area of Uganda and the Southern part of the Mt Elgon forest on the Kenyan

side of the forest. The result also revealed the specific areas in the two montane forests where forest cover was lost to other land cover types (deforestation) within the study period and areas that were undergoing forest recovery.

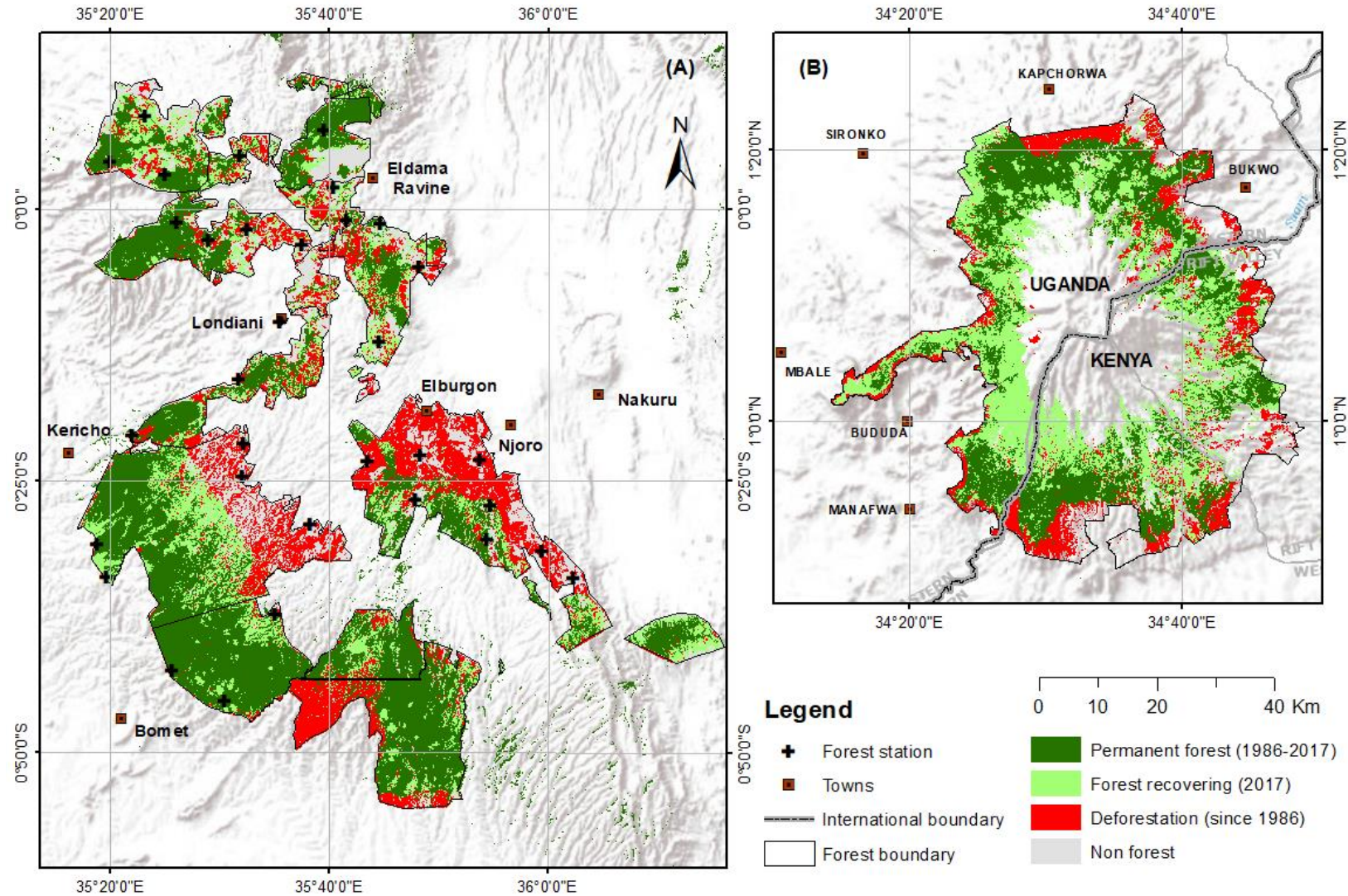


Figure 2-7: Forest cover change from 1986 to 2017 showing areas that remained forest throughout the time series analyzed, the forest that was disturbed and is currently undergoing recovery by 2017, and forest that has been permanently lost to deforestation in the Mau forest complex (A) and the Mt Elgon forest (B).

The analysis shows that during the 1986-2017 period, 42.6% (172,250 ha) of the Mau forest complex remained forest, 21.9% (88,493 ha) of the forest area was lost to deforestation and 18.6% (75,438 ha) was disturbed and is currently at different stages of recovery as shown in Tab. 2-5. For the Mt Elgon forest, 24.1% (52,369 ha) of the forest remained forest between 1984 to 2017, and 12.08% (26,250 ha) of the forest area was deforested and 27.6% (59,998 ha) was disturbed and is currently undergoing recovery as indicated in Tab. 2-5.

Table 2-5: Forest cover change in the Mau forest Complex and Mt Elgon forest calculated from classified Landsat imagery from 1984 – 2017 using the supervised classification and change detection method.

Forest cover	Mau forest complex		Mt Elgon forest	
	Area (ha)	(%)	Area (ha)	(%)
Permanent forest (1984 - 2017)	172,250	42.6	52,369	24.1
Deforested area (2017)	88,493	21.9	27,201	12.5
Forest under recovery (2017)	75,438	18.6	59,047	27.2
Non-forest	68,479	16.9	78,651	36.2
Total	404,660	100	217,268	100

2.3.4. Rates of deforestation and recovery

The multi-temporal assessment of the rate of deforestation covers 31 years (the Mau forest complex) and 33 years for Mt Elgon forest as shown in Tab. 2-6 (a) and (b) respectively. The results indicate that an estimated 88,493 ha of the Mau forest complex was lost to deforestation at an annual rate of -0.86% for the period 1986 – 2017 and an estimated 27,201 ha for the Mt Elgon forest at a rate of -1.03% during the same period. The recovery rates for the Mau forest complex and the Mt Elgon forest were estimated at an average of 2,434 ha yr⁻¹ and 1,789 ha yr⁻¹, respectively presented in Tab. 2-7.

Table 2-6: Observed forest cover loss in Mau forest complex (a) and Mt Elgon forest (b) within the official forest boundaries for the Mau Forest Complex and Mt Elgon forest.

Mau forest complex (a)

Time [T ₁]	Time [T ₂]	Period (T ₂ - T ₁)	Area (ha) [A ₁]	Area (ha) [A ₂]	Def _[Period] (ha)	Deforestation rate yr ⁻¹ [%]
1986	1989	3	336,181.3	334,563.3	1,618.0	-0.2
1989	1995	6	334,308.3	330,095.2	4,213.0	-0.2
1995	2003	8	330,095.2	285,342.4	44,752.8	-1.8
2003	2010	7	285,342.4	257,817.4	27,525.0	-1.5
2010	2014	4	257,817.4	253,223.4	4,594.0	-0.5
2014	2017	3	253,223.4	247,688.0	5,535.4	-0.7
Average						-0.8

Mt Elgon forest (b)

1984	1988	4	138,350.0	118,904.4	19,445.6	-3.8
1988	1995	7	118,904.4	116,699.6	2,204.8	-0.3
1995	2003	8	116,699.6	121,138.5	-4,438.9	0.5
2003	2010	7	121,138.5	121,732.9	-594.4	0.1
2010	2014	4	121,732.9	116,552.9	5,180.0	-1.1
2014	2017	3	116,552.9	111,149.0	5,403.9	-1.6
Average						-1.0

Table 2-7: Observed forest cover gain (recovery) in the Mau forest complex and Mt Elgon forest within the official forest boundaries for the Mau Forest Complex and Mt Elgon forest.

Station	Time [T ₁]	Time [T ₂]	Period (T ₂ - T ₁)	Area recovered/ Gain (ha)
Mau forest Complex	1986	1989	3	7,710.2
	1989	1995	6	3,803.7
	1995	2003	8	18,573.1
	2003	2010	7	10,565.1
	2010	2014	4	15,562.9
	2014	2017	3	19,222.9
Mt Elgon forest	1984	1988	4	8,239.4
	1988	1995	7	6,353.9
	1995	2003	8	19,850.4
	2003	2010	7	9,075.8
	2010	2014	4	6,825.2
	2014	2017	3	8,702.4

Deforestation rates were higher for the Mau forest Complex between 1995 and 2003 where 44,753 ha were lost and in the period between 2003 and 2010 when 27,525 ha of the forest cover were lost as shown Tab. 2-6a. For the Mt Elgon forest, deforestation

was high between 1984 - 1988 when 19,446 hectares of the forest were lost as shown in Tab. 2-6b.

2.4. Discussion

2.4.1. Mapping and classification of forest cover change

This study produced a new set of maps that show the extent of intact forest and degraded forest following clearance since 1984 for the two montane forests in East Africa. The study estimated the forest area that stayed as forest from the beginning of the time series from 1986 (Mau forest complex) and 1984 (Mt Elgon forest) until 2017, identified areas that were lost due to deforestation and those that are undergoing recovery. Supervised image classification with maximum likelihood (ML) algorithm was used and attained a classification accuracy of 86.20% (Kappa coefficient of 0.81) for the Mau forest complex and 90.50% (Kappa coefficient of 0.88) was obtained for the Mt Elgon forest. Deforestation was determined using the change detection method between the various time series (Margono et al., 2012). The classification accuracy in this study for the Mau forest complex is comparable with a related classification that was undertaken by Were et al., (2013) who reported a classification accuracy of 80% in the Eastern Mau forest reserve, a section of the Mau forest complex for the years 1985, 2000 and 2011. However, the results from Were et al., (2013) were only for a small section of the Mau forest complex. In this study, the training and validation samples for the maximum likelihood classification were obtained from the available high-resolution Google images for the two study areas, an approach that conforms with the best practices described by Olofsson et al., (2014). Several factors contribute to the accuracy of the classification, especially the reliability associated with the use of the high-resolution Google image with a variation in the dates of acquisition with the classified Landsat imagery. The differences in the date of acquisition may introduce possible errors into the class definition and allocation due to changes that occur after the acquisition of the Landsat imagery and before the acquisition of the Google

Imagery. Using ML for land cover mapping and carrying out change detection provides a challenge in class identification and definition given the images were collected during the dry months of the study area to be able to segregate forest cover from other land cover types. For example, small-scale agricultural land where harvesting has taken place could be assigned to the settlement and vice versa. ML assigns classes based on likelihood, and this likelihood and the classes assigned are used to assess the forest cover change at each time step. However, these challenges were minimized by using the forest masks to focus the changes within the areas that had been forest at the beginning of the time series.

The study further shows that the forest cover loss detected from the supervised classification were less than the loss detected by Hansen et al., (2013) by 0.2% for the period 2000 – 2017 in the Mau forest Complex and in Mt Elgon forest the supervised classification results were relatively higher than the loss detected by Hansen et al., (2013) by 2.3%. Hansen et al., (2013) results indicate gross forest loss of 17.0 % (68,848 ha) for the Mau forest complex and 5.3% (11,501) for the Mt Elgon forest. These estimates from Hansen et. al., (2013) for the period (2000 – 2017) are comparable to the results from the classification in this current study which revealed 16.8% (68,155 ha) and 7.6% (16,496 ha) forest cover loss for the Mau forest complex and Mt Elgon forest respectively for the same period. The variations could be associated with differences in method, scales, and thresholds used as well as the processes involved. For example, ML is operator-based with a focus on the changes in the spectral value in different periods, while Hansen et al., (2013) uses the canopy cover percentage and determines change using the bagged decision tree in Google Earth Engine (GEE) with images collected during the growing season (Arjasakusuma, Kamal, Hafizt, and Forestriko, 2018).

2.4.2. Spatio-temporal forest cover change and drivers of deforestation and forest disturbance

A comprehensive assessment of the forest cover changes due to deforestation and the following forest recovery for the two largest montane forests of East Africa covering together 621,928 ha (404,660 ha for the Mau forest complex and 217,268 ha for Mt Elgon forest) was undertaken. Over the period from 1984 – 2017, this study showed that 21.9% (88,493 ha) and 12.5% (27,201 ha) of the Mau forest and Mt Elgon forest respectively was lost to deforestation and 18.6 % (75,438 ha) for the Mau forest complex and 27.2% (59,047 ha) of Mt Elgon forest are currently undergoing different stages of recovery as indicated in (Fig. 2-7). Despite the losses, the two Montane forests have been regarded as the largest closed-canopy forest in East Africa that play significant roles in carbon sequestration, regulation of rainfall, nutrient cycling, soil formation, and support to biodiversity (Gichuhi, 2013; Omoding et al., 2020; Otieno, 2016; Plumptre et al., 2019). The Mau forest Complex and Mt Elgon forest are very important ecosystems and water catchments to the East African region (Muhweezi et. al., 2007; Hesslerová and Pokorný, 2011; Chrisphine et. al., 2015). Due to various factors ranging from natural to anthropogenic disturbances, these Montane forests have faced large-scale deforestation and disturbance (Landmann and Dubovyk, 2014; Mutugi and Kiiru, 2015). In the Mau forest complex, the findings of the current study demonstrate that deforestation has been attributed largely to agriculture with the largest losses in forest cover resulting from the conversion of forest to small-scale agriculture 59,172 ha (68.3%). While in Mt Elgon forest, agriculture was also the main driver of forest cover loss accounting for 63.2% (24,077 ha). Previous studies also reported agriculture as the main driver of the land cover changes in the Mt Elgon and Mau regions indicating 4,500 ha of Mt Elgon forest that has been converted (Petursson et.al., 2013), and in the Mau forest complex region at a total of 145,850 ha (1,458.5

km²) as reported by Swart, (2016). Temporally, the current study discovered that forest cover has been largely lost to agriculture in the two study areas. This agrees with the findings of Were et al., (2013) for the Eastern Mau forest and Lake Nakuru basin sections of the Mau forest complex, which revealed that there was an increase in cropland expansion and built-up area by an annual rate of 6% and 16% and a decrease in the forest cover as a consequence for the period from 1973 to 2011. Kissinger et al. (2012) associated forest cover loss with increasing demand for land to expand agriculture at a global level, this study confirms these claims and demonstrates that most of the forest cover was lost to agriculture for both the study areas. Curtis et al., (2018) reported deforestation rates in Africa being driven by shifting agriculture i.e. small to medium-scale forest and shrubland conversion for agriculture that is later abandoned and followed by subsequent forest regrowth. However, this study determined that smallholder agriculture contributed to 68.31% of forest loss and large scale agriculture to 13.2%, and most of this area remains under agriculture, making it the main driver of forest cover loss as suggested by (Albertazzi, Bini, Lindon, and Trivellini, 2018; Hosonuma et al., 2012). The higher rate of loss of forest cover to agriculture may also be associated with the influence of the politics in the allocation and resettlement of communities (Mbugua, 2011). Although, the political drivers to change may be classified as indirect drivers of forest cover change. The current study further showed that deforestation in the Mau forest complex and Mt Elgon forest occurs in small patches of less than 1 ha, which may be associated with the activities of farming communities adjacent to the forest as reported by the empirical studies by (Brandt et al., 2018; Sassen et. al., 2013). The finding of this study demonstrates that most of the areas deforested were mainly at the edges of agricultural lands both smallholder and large scale tea farms.

2.4.3. Rate of deforestation and recovery in the Montane forest of East Africa

Deforestation has been reported to be pervasive in sub-Saharan Africa especially in the Democratic Republic of Congo (DRC) rainforests and the Miombo woodlands due to smallholder agriculture and increasingly commodity crop cultivation (Song et al., 2018), however, the rates are largely for lowland tropical rainforests. This study quantified the rate of deforestation and recovery for the two east African montane ecosystems which revealed 88,493 ha reduction in the forest cover from 336,181.3 ha at an annual rate of $-0.82\% \text{ yr}^{-1}$ for the Mau Forest Complex. While in the Mt Elgon forest, forest cover reduced by 27,201 ha from 138,350 ha in 1984 to 111,149 ha by 2017 at an annual rate of $-1.03\% \text{ yr}^{-1}$ as indicated in Tab. 2-6. The estimated rates in this study are lower than the estimated national rates of 0.54% for African natural forest (FAO, 2015b), although this can be due to differences in methods used, errors arising from the use of rudimentary methods (without remote sensing tools) that have been used in FRAs to adjust estimates of forest area based on the results of these national surveys to a common reporting year (Keenan et al., 2015). Comparing the rates of deforestation from this study with other reported rates can be challenging because of differences in datasets used, scale, and boundaries of the study areas. Most studies for the Mau forest complex do not quantify forest cover changes for the whole forest but in selected specific blocks out of the 22 blocks. For example, Were et al., (2013) estimated changes for the Lake Nakuru basin, Kinyanjui et al., (2013) calculated changes for the Southwestern and Transmara blocks of the Mau forest complex, and Swart, (2016) assessed the land cover change in the region that includes the Mau forest complex. These previous studies focused on the land-use change and the main

drivers within specific blocks, whereas the current study covers the quantification of the rate of forest cover change and recovery across all the blocks of the Mau forest complex.

This study shows that the rate of deforestation in the Mau forest complex is also higher than the nationally reported annual rates by the Food and Agriculture Organization of the United Nations (FAO) for Kenya and Uganda at the national level since there are no site-specific reported rates of deforestation for the period 1990 to 2010 at 0.32% per year for Kenya and the findings for the Mt Elgon forest are below the national reported annual rate of 0.4 - 3% per year for Uganda for the period 1990 to 2010 (FAO, 2013). In comparison with the regional studies that have assessed rates of deforestation, the annual rates for the Mau forest complex and Mt Elgon determined in this study were slightly higher about the findings of Brink et al., (2014) that indicated an increase in the annual rate of deforestation from 0.2% in the period from 1990 - 2000 to 0.4% from 2000 - 2010. However, the resolution of satellite data that was used in determining forest cover change and rate of deforestation in this current study is much higher (30 x 30m) than that used for the previously reported rates. For example, the study by Brink et al., (2014) used 20 x 20 km resolution to determine the rate of deforestation across Eastern Africa, and therefore, this study established the rate of deforestation and recovery at the landscape level for specific forest ecosystems (the Mau forest complex and Mt Elgon forest) in Kenya and Uganda.

2.5. Conclusion

Deforestation has been a major problem facing the Mau forest Complex and Mt Elgon forests in Kenya and Uganda, yet the annual rate of deforestation over time has not been previously quantified. This study provides a detailed multi-temporal and extensive spatial analysis of these two important forests hence providing an annual rate of forest loss to deforestation and the rate of forest clearance. The results provide a basis and spatial-temporal status of the forest for the development of effective monitoring of the two forest ecosystems from the areas that are currently deforested and those that are undergoing recovery. The study findings also provide the relevant scientific evidence on the trends of forest cover loss due to deforestation and forest cover clearance in the Mau forest complex and Mt Elgon forest and add to the limited information regarding the changes in montane forest ecosystems. The use of MLC approach alongside the GFC data for assessing the rate of deforestation and forest disturbance in the Mau forest complex and Elgon forest benchmarks the wider use and application of these data datasets for assessing deforestation and forest clearance in the East African forests.

3. DETERMINATION OF RATE OF ABOVEGROUND BIOMASS AND SPECIES RECOVERY IN THE TROPICAL MONTANE FOREST OF EAST AFRICA



Forest fires observed in Londiani - Western Mau Forest complex (a) and previous fires inside the areas that are undergoing recovery (b) and (c). Photographs taken from the Mau forest Complex during the field work in March 2019.

Abstract

Tropical Montane forests are fragile ecosystems that provide a wide range of ecosystem services that range from provision of hydrological services, protection of the biodiversity and contribution to climate change mitigation. Yet these TMFs face degradation and clearance, and their recovery is not well understood. The current study assessed the rate of AGB and species recovery following clearance. The current study established 47 forest inventory plots to determine the rate of AGB and species recovery in 3 blocks of the Mau forest complex in the rift valley region of Kenya. The current study showed that AGB recovered rapidly in the first 20 years at an annual rate of 6.42 Mg ha^{-1} , but the rate of recovery slowed to 4.67 Mg ha^{-1} at 25 years and 4.46 Mg ha^{-1} , at 30 years of age. The current study further revealed that at 25 years, the mean AGB of $198.32 \pm 78.11 \text{ Mg ha}^{-1}$ was statistically indistinguishable from the mean AGB in the old growth secondary forest which was $282.86 \pm 71.64 \text{ Mg ha}^{-1}$. Stem density did not show any significant difference across the recovery stages with $321.25 \pm 101.34 \text{ tree ha}^{-1}$ in the youngest secondary forest and $445 \pm 187.58 \text{ tree ha}^{-1}$ in the old growth secondary forests. Also, species diversity and richness indices did not show any significant changes with the recovery of the secondary forest for example; the Evenness (J) index in the youngest secondary forest was 0.66 ± 0.18 and in the old growth secondary forest was 0.75 ± 0.13 , Shannon's (H) index was 1.25 ± 0.45 and 1.63 ± 0.51 for the youngest and old growth secondary forests respectively, the Simpson's (D) index was 0.47 ± 0.19 and 0.36 ± 0.16 for the youngest and old growth secondary forests respectively. Although there existed a significant variation between the young secondary forests of age below 15 years from the older and old growth secondary forests in terms of AGB, the findings of this study suggest that the Montane tropical forests of East Africa require 25 years to recover AGB that is indistinguishable from the estimated AGB of the old growth secondary forest. The insignificant results for the

species diversity and richness indices suggest that species recovery in the tropical montane forest of East Africa is slow and requires a longer time to recover following forest clearance.

3.1. Introduction

Tropical montane forests (TMFs) cover 23% of global forest areas (Price et al., 2011) and provide essential ecosystem services that include the provision of water, carbon sequestration, and biodiversity conservation (Beta, 2019; Brienen et al., 2015; Martínez et al., 2009; Soh et al., 2019; Spracklen and Righelato, 2014). TMFs are also faced with deforestation and forest disturbance (Crausbay and Martin, 2016), which have been on the rise due to the underlying increase in human populations (Carr, et.al., 2005) and development. Direct investments resulting from economic inequalities and flex-crops have also been reported to significantly impact forest cover and biodiversity loss (Ceddia, 2020) and inference by (Lambin, Geist, and Lepers, 2003) indicate that the major driver of deforestation and forest disturbance in tropical region is 81% by economic factors rather than the increasing population. However, the expansion of subsistence farming mainly shifting cultivation is associated with a growing population especially in Africa. With projections indicating a continuous increase in population (Gerland et al., 2014) and particularly higher population in East Africa at a rate of 2.82% compared to the world rate of 1.19% (Hamunyela et al., 2020), the demand for land to expand agriculture in the tropical regions can be expected to place further pressure on the forests (Bussmann, 2002; Brandt et al., 2017; Mwangi et.al., 2018). Shifting cultivation is reported to be the highest driver of tree cover loss in Africa by 92% with map-based estimates and $93 \pm 3\%$ sample-based estimates from 10 x 10 grid cells (Curtis et al., 2018). Due to these threats to the tropical forests, their abilities to sequester carbon and support biodiversity are waning (Hubau et al., 2020).

Despite these pressures, or as part of the shifting agriculture fallow phase, some TMFs are in the process of recovery from the cleared forest. Understanding the rate of forest

recovery is important to understand the role of these recovering secondary forests in mitigating climate change and conserving biodiversity. This can inform the success of programs like REDD+ (Deklerck et al., 2019; Huang, 2015), through the provision of robust estimates of carbon sequestration (Chazdon et al., 2016), and is vital for countries to evaluate progress towards global commitments under the United Nations Framework Convention on Climate Change (UNFCCC) and The Convention on Biological Diversity (CBD). Substantial progress has been made on understanding the recovery rate of lowland forests in some parts of the world (e.g. Poorter et al., 2016; Gourlet-Fleury, et al., 2013; Loo et. al., 2017; Bauters et al., 2019; Deklerck et al., 2019), with results showing that these forests recover much of their original biomass within 20 years (Poorter et al., 2016), yet they are much slower in terms of composition, while the subtropical forest requires a longer period of not less than 50 years to obtain structural recovery following disturbance (Lin et al., 2015). But in human-modified forests, there exist convergence in the structure after 20 years following abandonment (Loo, Song, and Chao, 2017). The recovery rates across the lowland forests vary by the different climatic conditions between the regions (Becknell et.al., 2012; Lewis et al., 2013). The forest recovery rates could also be influenced by the presence of remnant trees and the previous crops cultivated before abandonment for example the biomass recovery rates in the forest of West Africa (N'Guessan et al., 2019).

For tropical montane forests, post-disturbance aboveground biomass and forest structure also vary by altitude (Acharya, Chettri, and Vijayan, 2011; Imani et al., 2017). Specific tree species require over 100 years to attain the diameter at breast height (DBH) of 20 - 25 cm in Afromontane dry forests (Mokria et. al., 2015). In cases of disturbance associated with fires, there is an increase in the small stems in the early stages after the fires resulting from regeneration pattern but there are no significant

differences in larger trees from burnt and unburnt stands (Oliveras et al., 2018). Selectively logged forests have shown higher overall stem density than non-logged forests in Kilimanjaro forest which indicates recovery of the montane forests (Rutten, Ensslin, Hemp, and Fischer, 2015b). While tree species in areas that have experienced clearance have shown higher species richness than old-growth secondary forest and more severely degraded areas (Sassen and Sheil, 2013). Most of the forest structure and composition recovery especially aboveground biomass accumulation studies in Africa are undertaken in plantation forests which have limited ecological value as well as the basis for informing rates of recovery in the natural forests (Bonner et. al., 2013). The mean total biomass C densities in indigenous forests have shown significantly higher biomass densities than those in the plantation forests (Omoró et. al., 2013). The default rate of annual net biomass change used as reference levels exists for tropical and neotropical subregions (Requena et al., 2019), although for East Africa, these reference levels are based on data collected from a tropical low land forest (Otuoma et al., 2016). However, African mountain forests are predicted to have higher annual aboveground carbon recovery rates which are higher than the IPCC (Intergovernmental Panel on Climate Change) default rates (Cook-Patton et al., 2020). In East Africa and the Mau forest complex, in particular, the disturbed forests have shown the potential to regenerate and attain ecological recovery (Kinyanjui et. al., 2013) but this is not clearly stated in terms of the stage and age. It has been noted that long-term conservation and management policies that provide and ensure protection from the surrounding land use contribute to the successful recovery of forests (Mensah, Egeru, Assogbadjo, and Glèlè Kakaï, 2020).

In the face of the previous studies that have demonstrated the response of tropical montane forest to degradation and clearance, there are limited studies on TMF rates

of recovery in east African forests and particularly in the Mau forest complex, with existing understanding coming from a few sites in lowland tropical forests or plantations for example (Otuoma et al., 2016). Secondly, it is not known when the recovering montane forests reach the equivalence with old-growth forests. Thirdly, recovery can be measured in different ways, and it is not clear how the recovery rates vary from different forest ages and old-growth equivalence across different ecological metrics, from those linked to Carbon (C) accumulation (biomass) to diversity and composition. In addition, the need to understand the transitions that result in the understanding of the recovery of forest structure and composition e.g. aboveground biomass (AGB) following disturbance is critical (IUCN, 2015) to effectively restore the natural forest by the management authorities to ensure restoration efforts are successful (Deklerck et al., 2019).

This current study addresses three key knowledge gaps by assessing the aboveground biomass (AGB), forest structure, species richness, diversity, and composition in 47 secondary (recovering) and old-growth (forests that existed before the beginning of the time series) forest plots distributed along a chronosequence of time since the clearance in the Mau forest complex, a tropical montane forest in East Africa. The key research questions were;

- (i) Is there a significant change in ecological condition over time, and if so?
- (ii) what is the shape of the response (linear or non-linear) and the rate of change at different time points?
- (iii) At what age do secondary forests become statistically indistinguishable from old-growth forests in terms of biomass, diversity, and species composition?

The findings from the analysis were used to discuss and understand the rate of forest recovery in the montane forest of east Africa. This chapter is based on the estimated and mapped forest cover area that was lost to deforestation and currently undergoing recovery as indicated in the Chapter 2 of this thesis. The time since last clearance and deforestation was used to determine the age classes used for assessing the recovery of AGB, forest structure and species composition in the three blocks of the Mau forest complex (i.e. Western Mau, Southwestern Mau and Transmara blocks).

3.2. Materials and Methods

3.2.1. Study area

The study was conducted in three forest blocks of the Mau forest complex i.e. the Western Mau, Southwestern Mau, and Transmara, located between $0^{\circ} 11' 28.2228''\text{S}$, $35^{\circ} 40' 21.0828''\text{E}$ and $0^{\circ} 48' 13.086''\text{S}$ $35^{\circ} 17' 7.548''\text{E}$ (Fig. 3-1) in the rift valley region of Kenya. The study area is classified as tropical Afromontane rainforest with an altitude ranging between 1800 – 2800 m above sea level (Kinyanjui, et. al., 2013; Paulo et. al., 2015). The soils of the study area are composed of Quaternary volcanic deposits with topsoil comprised mainly of clay loam and silt clay loam (Tarus, Kirui, and Obwoyere, 2019)

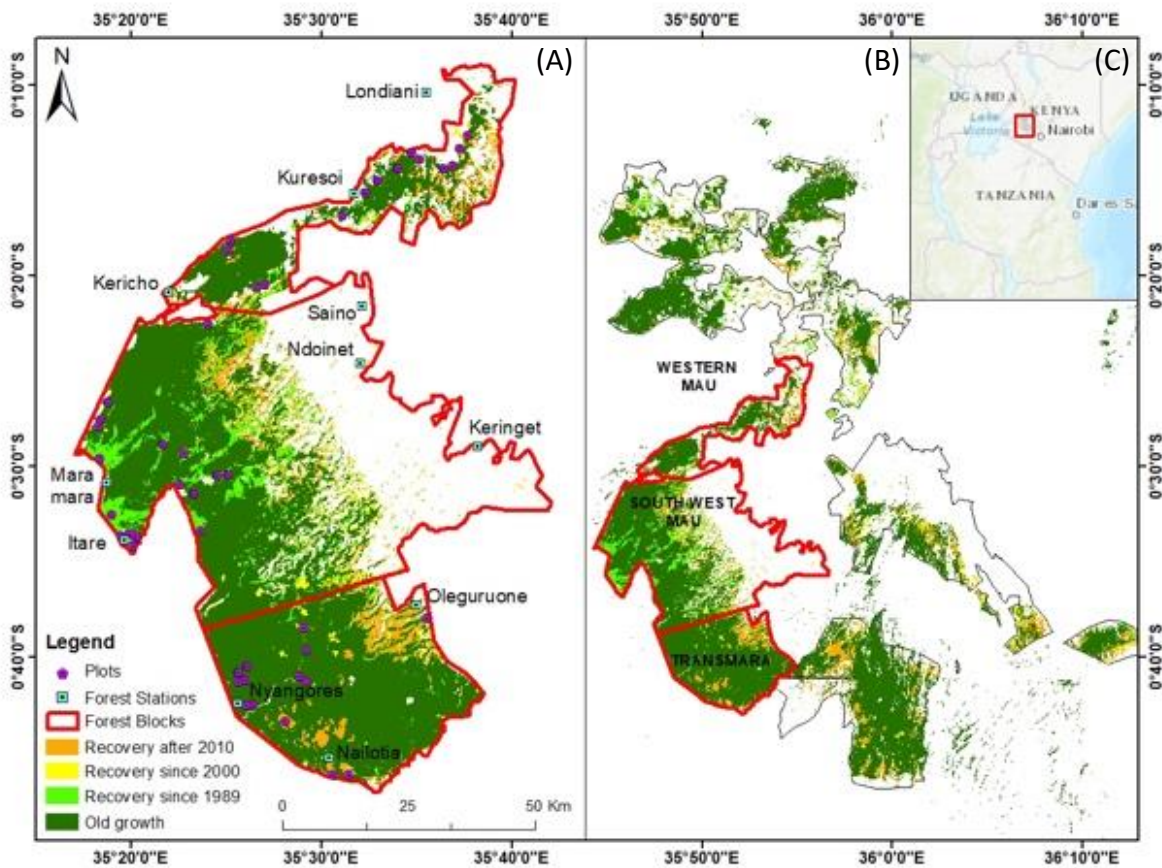


Figure 3-1: Location of the sample plots in the three forest blocks of the Mau forest complex distributed in the main recovery stages and the old growth secondary forest (A), the location of the three blocks with the whole of the Mau forest complex (B) and the Location of the Mau forest complex in Kenya (C). The plots are located on areas that were mapped (Chapter 2) as forest recovering and forest that existed throughout the time series.

3.2.2. Data

Forest area of different ages from Chapter 2 of this study were used to select and survey a total of 47 sample plots of 0.1 ha (20 m x 50 m). The sample plots were established and surveyed between March – June 2019 in the Mau forest complex following the RAINFOR protocol for inventories in the tropical forests (Marthews et al., 2014). The plot dimension was selected to allow for local forest composition and structure variations (Lucas et al., 2002). In each established plot, Diameter at Breast Height (DBH) was measured at 1.3 m of bole height for all live trees with a diameter greater or equal to 10 cm using diameter tape. Tree height was measured using Suunto Clinometer for all the live trees in the plot with DBH \geq 10 cm. In addition, tree species were also identified and recorded with the help and technical support of the Forest experts from the Kenya Forest Services (KFS) and the local community who identified the tree species with the local and scientific names as well as their traditional uses..

Forest cover change maps from 1986 to 2017 that were produced through supervised classification of the 30 x 30-meter resolution Landsat imagery from the Chapter two of this study were used identify the areas for the plots. The maps were used to determine the last time degradation/clearance (defined here as complete clearance of the stand) happened from which the forest stand age was estimated.

Table 3-1: Forest classes based on the time when the forest was last degraded/cleared (estimated age) that were used to establish forest sample plots in the three blocks of the Mau forest Complex

Class	Age	Description
1	<10 years	Forest area that was severely cleared or lost and only show recovery since 2010, mostly referred as Youngest Secondary Forest (YSF)
2	10 - 15	Forest area that was cleared but were stable for the recent 15 years
3	15 - 20	Forest area that experienced clearance or loss but recovery started after year 2000
4	20 - 25	Forest area that started to recovery from 1995 without being cleared or lost again until 2017
5	25 - 30	Forest area that started to recover since 1990 and 1995 as shown on the time series.
6	Old growth (>30 years)	Forest area that has stayed as forest since the beginning of the time series (1986) and their exact age is unknown

The forest cover that did not experience disturbance after 1986 was considered as an old growth secondary forest (mature) class with unknown age as it has existed since the beginning of the time series and used as reference old growth to determine the rate of recovery. Six forest classes were created (Table 3-1), of which the five classes (n = 36) were of the known age of up to 30 years and the sixth class (n = 11) of the forest with the age of greater 33 years with their observed biophysical characteristics as shown in Fig. 3-2.

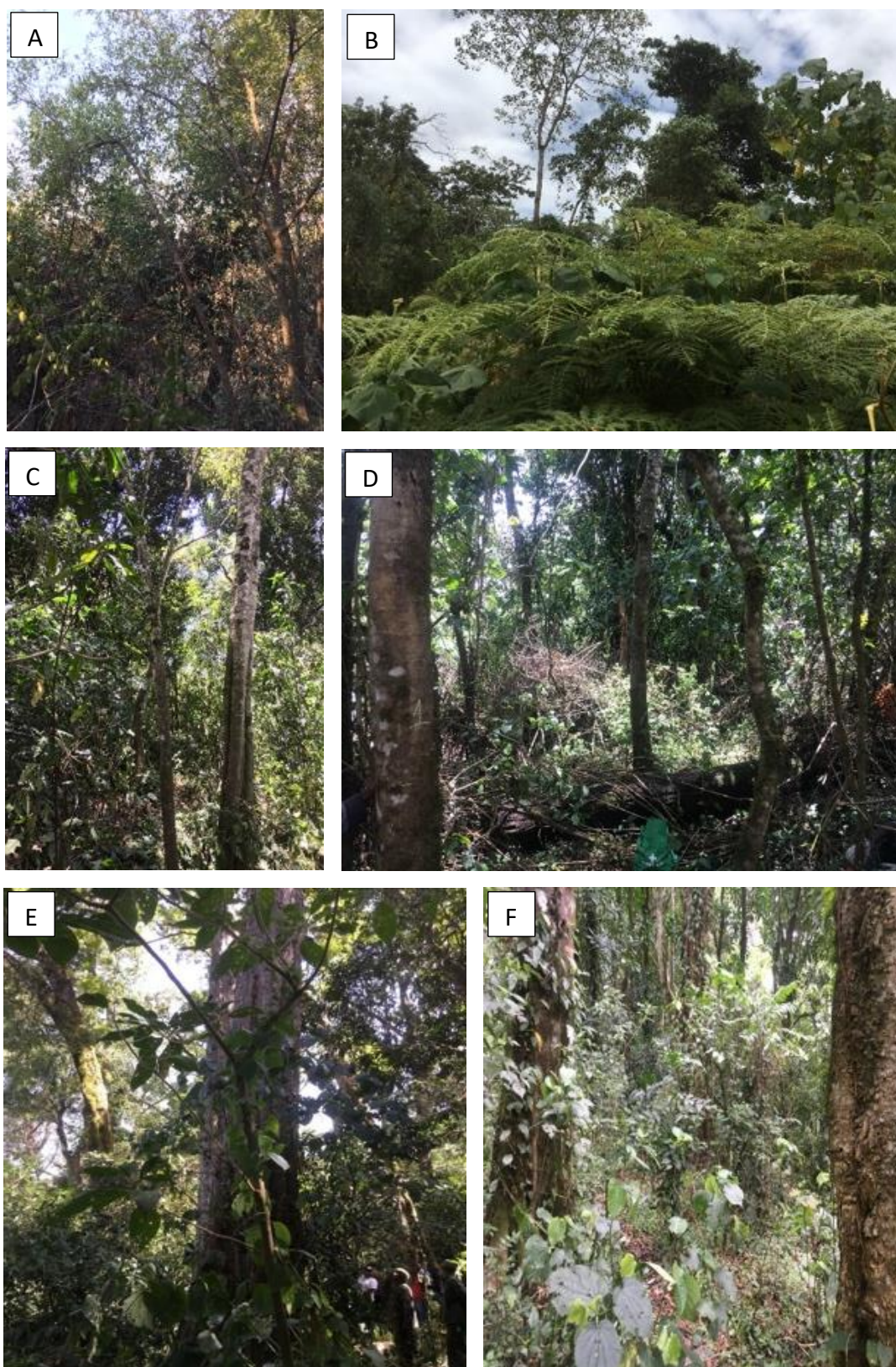


Figure 3-2: Young secondary forest (sample plot No.2) of less than 10 years [A], Second secondary forest (plot No.21) of age up to 15 years after major clearance events [B], Secondary forest (plot No. 11) with age between 16 – 20 years [C], Secondary forest (plot No. 39) with the age of 21 – 25 years of age [D], 26 – 30 years of age [E] and the Old-growth (Mature) secondary forest class with over 33 years of age [F] in the Mau forest complex.

3.2.3. Aboveground biomass (AGB) estimation

Aboveground biomass was determined for the individual trees using pantropical allometric equation (equation 1) developed by (Chave et al., 2005) and improved in (Chave et al., 2014). The pantropical allometric equation was adopted since it has been widely used in Eastern Africa as the site and species - specific models for all the tree species in the study area (Mokria et al., 2015; Imani et al., 2017). Although the site and species-specific allometric equations are noteworthy in the quantification of forest aboveground biomass (Kebede and Soromessa, 2018), the pan-tropical model has shown performance when tested with tree aboveground biomass compared to the local allometric models and applicability to different tree species (Chave et al., 2014).

Equation 3-1: Allometric equation for estimating the AGB

$$AGB_{est} = 0.0673 \times (\rho D^2 H)^{0.976}$$

Where;

- AGB*: Represents the estimated Aboveground Biomass (kg),
- D*: Refers to the Diameter at Breast Height (DBH) measured at 1.30 m for every tree with DBH of >10 cm measured in (cm),
- H*: is the height of all the trees measured in the plot with the DBH of >10 cm measured in (m)
- ρ*: Represents the wood-specific gravity (wood density) of the trees measured in (g).

The wood density data used for determining the AGB was obtained from the regional wood density database for eastern Africa and the global wood database (Jerome Chave et al., 2009; World Agroforestry Centre, 2016). In cases where wood density for specific tree species was not available, the wood density at the family or genus levels were used following (Chave et al., 2006; Poorter et al., 2016).

3.2.4. Species richness, diversity, and composition

Tree species diversity was determined using Shannon's species diversity index following (Githae et. al., 2008; Shannon, 1948), Simpson's index (Simpson, 1949), richness index (Menhinick, 1964), and the evenness metrics (Pielou, 1966; Cao and Zhang, 1997; Majumdar, Shankar, and Datta, 2014; Wang *et al.*, 2018). The species richness and diversity were assessed using the four diversity indices i.e., Shannon's diversity index (H'), Simpson's index (D), and Evenness (E) were determined using equations 3-2 to 3-4.

Equation 3-2: Shannon's diversity Index (H')

$$\text{Shannon's diversity Index } (H') = \sum p_i * \ln(p_i)$$

Equation 3-3: Simpson's index (D)

$$\text{Simpson's index } (D) = 1/\sum p_i^2$$

Equation 3-4: Evenness index (E)

$$\text{Evenness index } (E) = H/H_{max}$$

The species composition analysis was undertaken using the non-metric multidimensional scaling (NMDS) tool. The distance matrix (matrix of dissimilarities) was established using the square root transformation to remove the influence of the most dominant species (Bauer and Albrecht, 2020; Bray and Curtis, 1957).

3.2.5. Statistical analysis

To address question 1, the study used both linear and nonlinear mixed effect models to determine the rate of recovery of the AGB and species richness and diversity for the different forest classes identified (Bates et. al., 2015; Pinheiro et. al., 2015; R core

Team, 2018). For this analysis, the current study only analyzed forest areas that were known to be secondary based on the known age from the satellite imagery (n = 36 plots), excluding the old-growth forests with an unknown or non-existing time since abandonment (i.e., before the beginning of the time series). The current study selected between linear and nonlinear Generalized Least Squares (GLS) models based on the model AIC. Forest stand age was log-transformed to account for the nonlinear increase in AGB with stand age (Requena Suarez et al., 2019). The models with lower Akaike Information Criterion (AICs) were selected for the different forest structure and composition variables as shown in Tab. 3-1.

To address question 2, this current study used a two-way analysis of variance (ANOVA) to determine the variation in the forest structure i.e. basal area, stem density, AGB in the different forest classes, species diversity indices, and composition using the plot-level data. Additional Turkey's post hoc tests were undertaken to determine the statistically significant differences between the multiple comparisons within the forest classes.

To address question 3, the current study carried out the permutational multivariate analysis of variance (PERMANOVA) using distance matrices (Warton, Wright, and Wang, 2012), and displayed the results visually using NMDS plots.

3.3. Results

3.3.1. Recovery rates of AGB, Species richness, and diversity

All the six response metrics had strong and significant relationships with secondary forest age after the last recorded clearance. AGB, basal area, stem density, and species richness were all best explained by a non-linear GLS model, in which the rate of recovery declines with age as indicated in Tab. 3-1 and Fig. 3-3. For example, AGB recovered rapidly in the first 20 years at an annual rate of 6.42 Mg/ha, but the annual rate of recovery slowed to 4.67 Mg/ha at 35 years and 4.46 Mg/ha at 30 years of age.

Both diversity indices (Shannon's and Simpson's) had a linear relationship with forest age, where Shannon's index was increasing, and Simpson's index was decreasing as shown in Fig. 3-3 (d) and Fig. 3-3 (e) respectively. All model residuals were tested for spatial autocorrelation, and none was detected as presented in appendix 4.

Table 3-2 Comparison of model Akaike Information Criterion (AIC) between the null model and the Linear and GLS models for the various ecological response metrics

Response Metric	AGB (Mg/ha)	BA (m/ha)	Stem Density (trees/ha)	Evenness (J)	Shannon's (H)	Simpson's (D)	Species Richness
AIC – Null Model	440.39	279.33	483.71	-34.82	45.19	-26.32	172.10
AIC – Linear Model	416.00	251.53	483.15	-38.36	38.04	-34.42	168.21
AIC – GLS Model	401.75	246.42	465.17	-27.37	44.79	-23.64	167.73
Delta AIC LM/GLS	14.25	5.11	17.98	-10.99	6.75	-10.78	0.48
Delta AIC Best Model and Null Model	38.65	32.91	18.53	-7.45	7.15	8.10	4.37

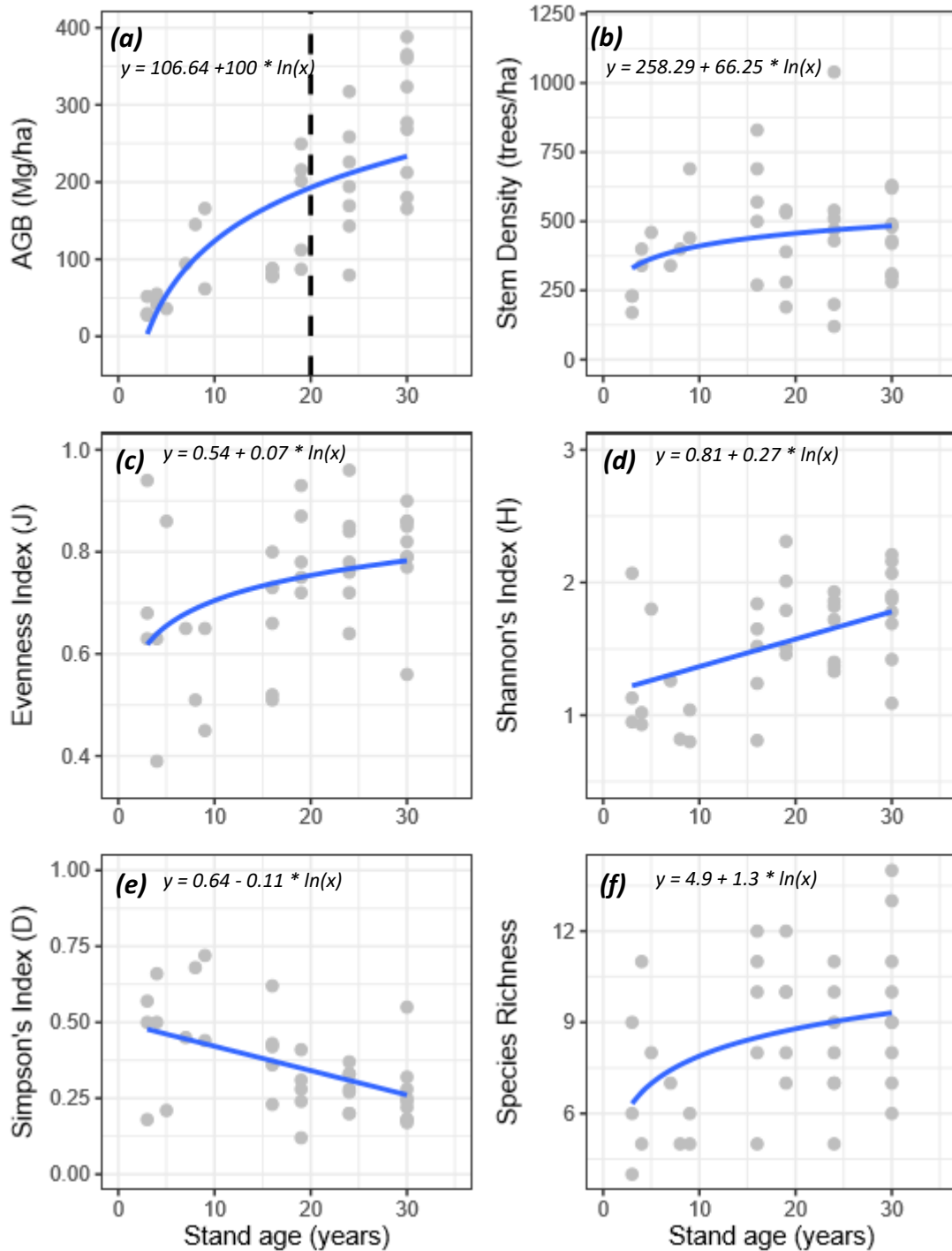


Figure 3-3: Relationship between the ecological metrics AGB and stand age in the blocks of Mau forest complex (a), grey dots are field observed plot AGB ($n = 36$). The model predicted AGB (blue curve) in relation to the stand age (years). The black horizontal dotted line represents the AGB at 20 years which separates the young and old-growth (mature) secondary forest. The figure also shows the relationships between the other ecological metrics i.e., stem density and stand age (b), species diversity indices with stand age i.e., Evenness (J) index (c), Shannon's diversity index (d), Simpson's diversity index (e), species richness (f) in the 3 Blocks of Mau Forest Complex. The grey dots and blue lines in all the figures from (b) – (f) also represent the respective field observation and the model predictions.

3.3.2. Similarity to the old-growth forest: AGB, Species richness and diversity

The different metrics of ecological condition had different patterns in terms of their statistical similarity to the old-growth forest plots in this current study. At 25 years the mean AGB (198.32 ± 78.11 Mg/ha) was statistically indistinguishable from the mean AGB in the old growth secondary forest as indicated in Fig. 3-4 (A). None of the other metrics showed statistical differences between the old growth forest plots and the secondary forest age classes.

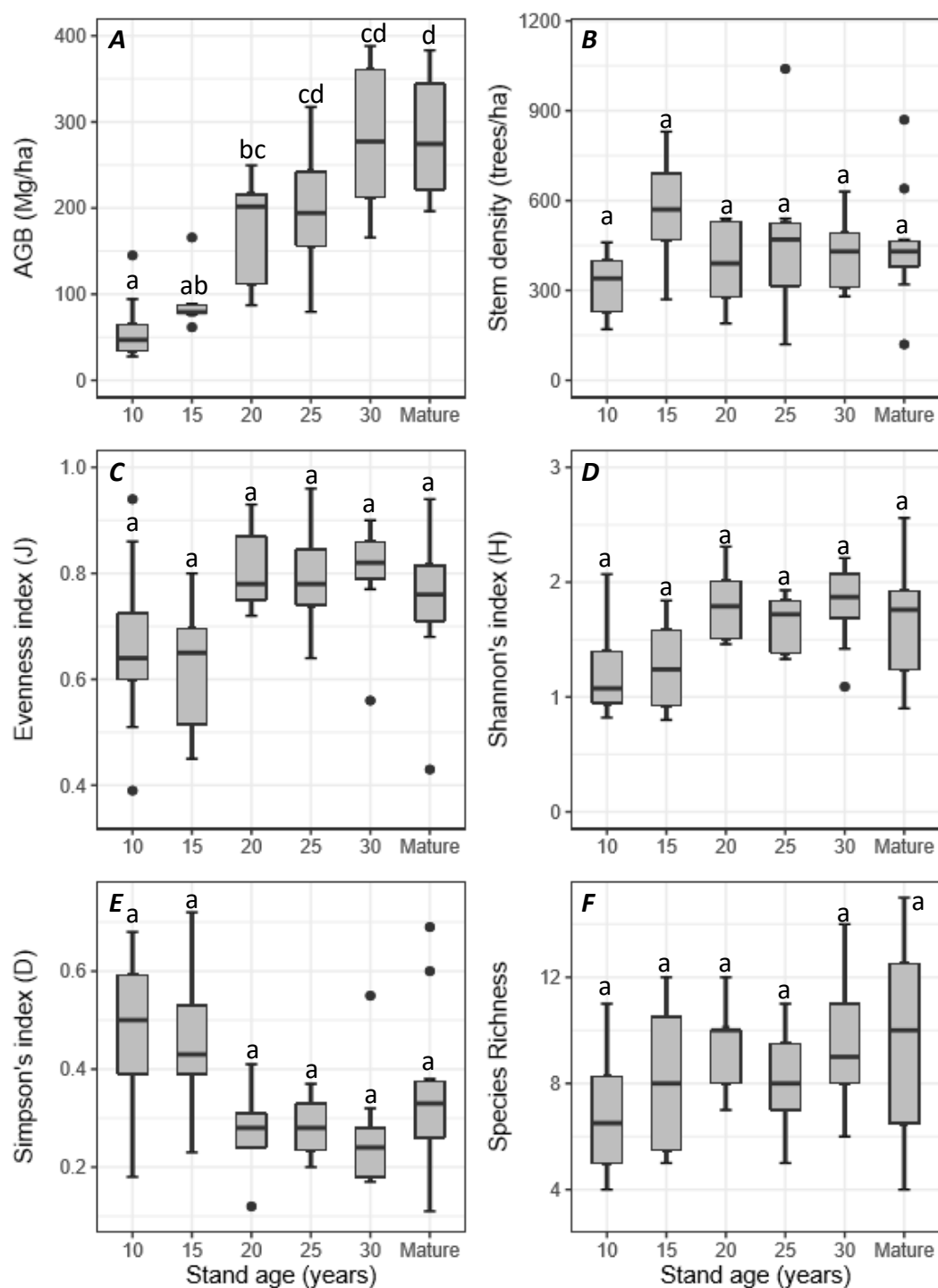


Figure 3-4 Mean variations in the secondary forest structure, species richness, and diversity of the age up to 30 years ($n = 36$) with the stage they become statistically indistinguishable from old-growth (Mature) secondary forest ($n = 11$). (A) Variation in the mean AGB between the six forest classes based on the stand age in years, (B) Variation in stem density across the classes, (C) evenness diversity index, (D) Shannon's diversity index, (E) Simpson's diversity index and (F) Species richness across the six classes.

Stem density and species richness and diversity indices did not show significant relationships between the different forest classes at 95% Confidence interval as indicated in Fig. 3-4 (B – F).

3.3.3. Similarity to the old-growth forest: Species Composition

In total, 60 tree species from 39 families distributed in the three (3) blocks of the Mau forest complex were identified. The study found out that, *Neoboutonia macrocalyx* (Euphorbiaceae) was the most dominant species in the youngest secondary forest as well as in the forest with the age of 25 years by 36.3%, 20%, and 21.9% of all the tree species observed in the respective forest classes. In the forest class with the age of 20 and 30 years, *Tabernaemontana stapfiana* (Apocynaceae) was the most dominant species recorded with 23.6% and 27.8% respectively. *Trichocladus ellipticus* (Hamamelidaceae) was the most dominant species in the old growth secondary forest class with 18.9% of the total species recorded in the old growth forest class. *Psydrax schimperiana* (Rubiaceae) was also widely distributed in the forest classes with the age of 20 and 25 years with 11.8% and 19.2% compositions respectively. Other species with high rank include; *Acacia melanoxylon* (11.6%) and *Ehretia cymosa* (6.9%) in the youngest secondary forest of age less than 10 years, *Euclea divinorum* (14.3%). Detailed high-ranked species in terms of composition are shown in Tab. 3-3 and complete species composition can be found in Appendix 8.

Table 3-3: Three most dominant species under various family recorded for each forest classes (recovery stages) in the 3 blocks of Mau forest Complex

Forest Class	Family	Species	Number of Species	Composition (%)
10	<i>Euphorbiaceae</i>	<i>Neoboutonia macrocalyx</i>	110	36.3
	<i>Mimosaceae</i>	<i>Acasia melanoxylon</i>	35	11.6
	<i>Boraginaceae</i>	<i>Ehretia cymosa</i>	21	6.9
15	<i>Euphorbiaceae</i>	<i>Neoboutonia macrocalyx</i>	67	20.0
	<i>Ebenaceae</i>	<i>Euclea Divinorum</i>	48	14.3
	<i>Apocynaceae</i>	<i>Tabernaemontana stapfiana</i>	39	11.6
20	<i>Apocynaceae</i>	<i>Tabernaemontana stapfiana</i>	46	23.6
	<i>Rubiaceae</i>	<i>Psydrax schimperiana</i>	23	11.8
	<i>Euphorbiaceae</i>	<i>Neoboutonia macrocalyx</i>	23	11.8
25	<i>Euphorbiaceae</i>	<i>Neoboutonia macrocalyx</i>	73	21.9
	<i>Rubiaceae</i>	<i>Psydrax schimperiana</i>	64	19.2
	<i>Myrtaceae</i>	<i>Sygyzium guineense</i>	30	9.0
30	<i>Apocynaceae</i>	<i>Tabernaemontana stapfiana</i>	110	27.8
	<i>Flacourtiaceae</i>	<i>Casearia battiscombei</i>	45	11.4
	<i>Euphorbiaceae</i>	<i>Suregada procera</i>	33	8.3
Mature (old growth)	<i>Hamamelidaceae</i>	<i>Trichocladus ellipticus</i>	91	18.9
	<i>Apocynaceae</i>	<i>Tabernaemontana stapfiana</i>	64	13.3
	<i>Ebenaceae</i>	<i>Diospyros abyssinica</i>	43	8.9

NMDS using the metaMDS function showed a stress level of 0.19 and the Non-metric fit of $R^2 = 0.97$ and Linear fit of $R^2 = 0.844$ was obtained as shown in appendix 5 [A]. The PERMANOVA revealed that the Age groups that represent the 6 forest classes were significant with R^2 of 0.15 at $P < 0.0001$ and the forest blocks were also statistically significant with R^2 0.14 at $P < 0.0001$, using the Bray distance metrics. At 95% confidence level, there existed significant variation between the young secondary forest of age below 15 years (g10 and g15) forest classes with the Older secondary forest and the old growth secondary forest complex as indicated in appendix 5 [A]. The hull plots also show the variation between the 3 forest blocks as shown in Fig. 3-5 (i) and variations by age groups especially the old growth secondary forest and the young forest classes as indicated in Fig. 3-5 (ii).

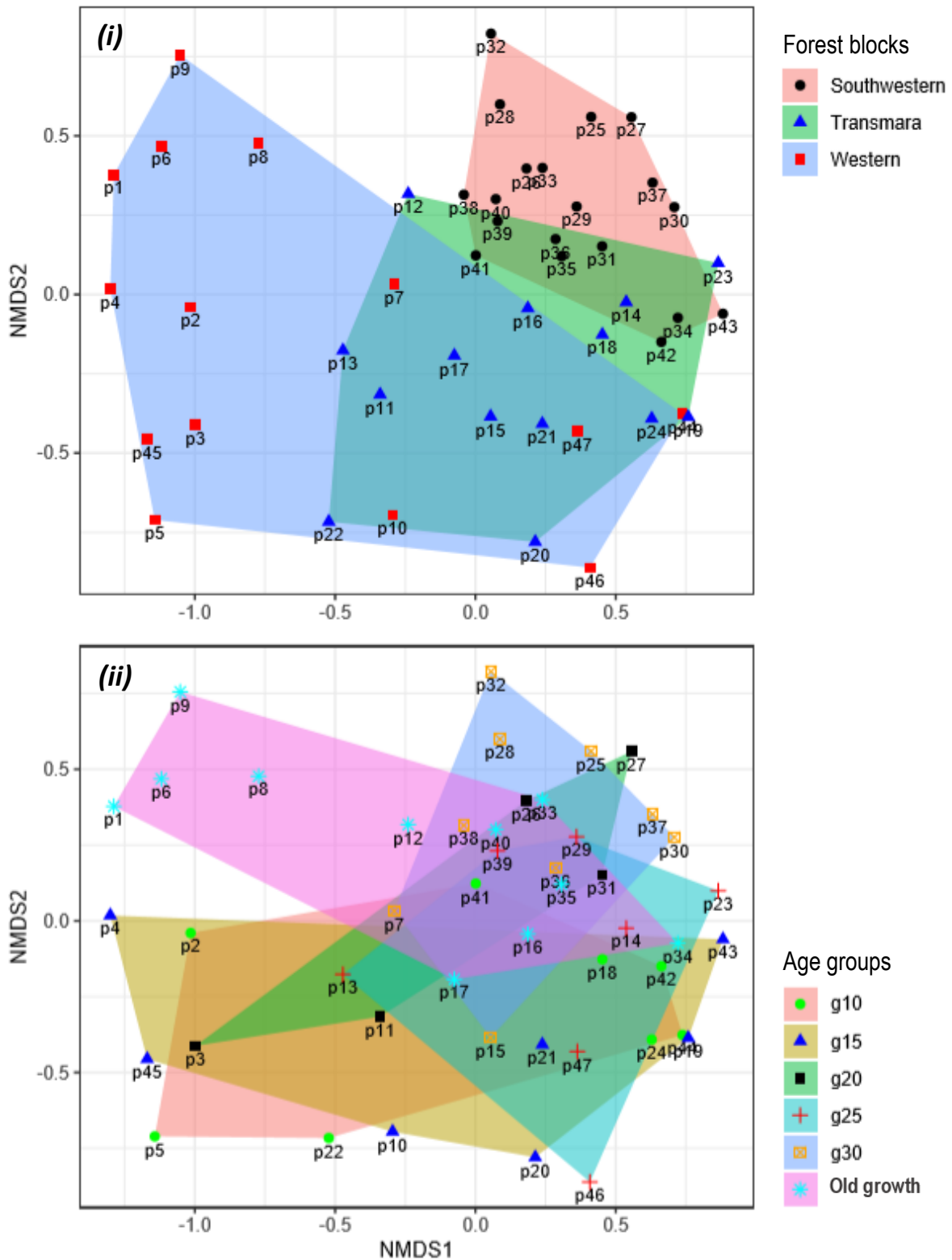


Figure 3-5 (i) Confidence Ellipses that suggests significance at < 0.05 and Overlaps between the different age groups, and (ii) Hull plots for the plots based on the Age groups. The old-growth plots, youngest (g10), (g15) show the greatest variance which can explain the significance of the age group in the adonis test (PERMANOVA)

3.4. Discussion

The rates of recovery and variation in the forest structure and composition in this study reflect the nature of undergoing processes and changes in the tropical montane forest that have faced degradation over time. The observed variations provide a vital basis for understanding the rates of forest recovery in the Mau forest complex. In this section, the study examines and discusses the distribution and variation in forest structure and composition i.e. BA, stem density and AGB, the rate of recovery of the AGB, the relationship between the AGB and forest structure, species diversity and richness as well as the time it takes the forest to recover the AGB and species diversity following clearance.

3.4.1. AGB Recovery rate

To the existing knowledge, the current study offers the first assessment of forest AGB recovery rates in the montane tropical forests of east Africa. The relationship between AGB and age (recovery period) was nonlinear. The AGB recovery of 6.42 Mg ha⁻¹ per year in the first 20 years of recovery is slightly higher than the refined default rates for African mountain systems which were reported as 5.5 Mg ha⁻¹ by Suarez et al., (2019) and based on just two chronosequences from another related region. These rates are slightly lower than those reported for lowland African forests: AGB recovery for intact African tropical rainforests (Lewis et al., 2009; Lopez-Gonzalez et al., 2011) and 8.03 Mg ha⁻¹ in the tropical moist forest following 24-year silvicultural experiment as reported by Gourlet-Fleury, et al., (2013). Other reported rates of AGB recovery within 20 – 25 years as shown in Tab. 3-3 demonstrate that the findings of the current study are in line with the reported rates of AGB recovery. The current study also revealed that the AGB recovery rate slows as the forest transitions into the old-growth secondary forest at an annual rate of 4.67 Mg ha⁻¹ to reach the level of AGB that was

measured in the old-growth secondary forests – although the current study recognizes that there is higher uncertainty about these latter rates, as the satellite time series only goes back to 1984 (as indicated in chapter 2), meaning the baseline for old-growth forests (many of the old growth forests could be secondary forests) is dependent on what has been determined by the existing satellite imagery.

The AGB recovery estimates in the current study for the young secondary forest can also further be refined based on the visible existence of remnant trees that influence the AGB estimates such as indicated in the (N’Guessan et al., 2019). The current study demonstrates that in 25 years, AGB of $198.32 \pm 78.11 \text{ Mg ha}^{-1}$ (mean \pm SD) becomes indistinguishable from the AGB measured in the old growth secondary forest i.e., 223.6 Mg ha^{-1} . The mean AGB determined at 25 years in this study is in line with the mean AGB reported IPCC default value of 190 Mg/ha for the tropical montane forests in Kenya (IPCC, 2006). The current study shows that the old growth secondary forest AGB was ($282.86 \pm 71.64 \text{ Mg ha}^{-1}$) which is slightly higher than the reported AGB of 223.6 Mg ha^{-1} by Kinyanjui et. al., (2014), however lower than the AGB of 391.6 Mg ha^{-1} from the moist tropical forests in Kenya (Otuoma et al., 2016).

Table 3-4: Estimated AGB recovery rates from previous studies across the tropical secondary forests compared to the current study

Period (years)	Rate (Mg/ha)	Site/Ecosystem Location	Reference
0 – 20	6.42	Mau Forest Complex, Kenya, East Africa	Current Study
0 – 20	5.50	Tropical Mountain System, Africa	Requena et. al., (2019)
0 – 20	7.60	Tropical rainforest	Gourlet-Fleury et. al., (2013)
0 – 24	8.03	Tropical Moist forest	Gourlet-Fleury et. al., (2013)
0 – 12	9.80	Montane forests in Southern Ecuador	Spracklen and Righelato, (2016)
0 – 20	6.20	Tropical Secondary forests	Poorter et. al., (2016)
0 – 20	7.80	Tropical Secondary forests	Bonner et. al., (2013)

3.4.2. Forest structural recovery

The study also assessed the recovery of other forest structure parameters especially Basal area, stem density, and found out that Basal area was also significantly increasing with the age of the secondary forest while stem density did not significantly change with the forest age and recovery stages i.e. between the youngest secondary forest and the old growth secondary forest as demonstrated in (Fig. 3-4B). The stem density could be affected by competition and dominance of certain species following forest clearance as has been reported by Kinyanjui, (2009). All the Species diversity and richness indices did not show any significant difference between the young and old growth secondary forests.

3.4.3. Species richness and diversity

The results of this current study demonstrate slow recovery of tree species diversity and richness in Mau forest, with a non-linear relationship between the evenness index and species richness and a linear relationship between Shannon's diversity index and Simpson's diversity index with stand age, although the Simpson's diversity index declines as the forest age increase. The slow increase in tree species diversity is consistent with the reports of similar studies undertaken in other montane forests of Kenya (Githae et al., 2008). Species richness and diversity recovery over time in montane forest in Kenya have not been widely undertaken, however, the findings of the other similar studies in tropical forest ecosystems suggest that forest species richness and diversity may take a longer time to recover to the old growth secondary forest status (Chapman et al., 2021; Goosem et al., 2016; H. Xu et al., 2015).

The slow recovery rate of species richness and diversity could also be associated with seed dispersion and seedling regeneration as reported by Wekesa et al., (2019). Overall, the findings of the current study suggest that AGB and Basal area recover quicker following forest clearance compared to species richness and diversity indices that recover slowly during the same recovery condition.

The species diversity and richness indices did not show any significant difference between the youngest secondary forest and the old growth secondary forest. This conforms with the reported slow recovery of forest tree species under different conditions associated (Wekesa et al., 2019; Wekesa, Maranga, Kirui, Muturi, and Gathara, 2018). However, in other forest ecosystems, species richness and diversity have been reported to have increased and stabilized between 20 – 25 years (Villa et al., 2018).

3.4.4. Species dominance and Composition

The study found out that, *Neoboutonia macrocalyx* (*Euphorbiaceae*) was the most dominant species in the age groups of 10, 15, and 25 years with the composition of 36.3%, 20%, and 21.9% respectively for the total species composition, while for age groups 20 and 30, *Tabernaemontana stapfiana* (*Apocynaceae*) was the most dominant species with 23.6% and 27.8% respectively, although, in the old-growth secondary forest, *Trichocladus ellipticus* (*Hamamelidaceae*) was also high in composition by 13.8%. The findings are in line with findings of Shisanya et al., (2014), although, *Tabernaemontana stapfiana* (*Apocynaceae*) was reported as the most dominant species as 22.7%, 22.9%, and 30.7% with a relative dominance of 14.3% distributed in Lower highland, and the two agro-ecological zones of Upper highland. However, the sampling approaches used in the study of Shisanya et al., (2014) differ

from those used in the current study, which focuses on the recovery stages based on the time when the last clearance occurred.

The multidimensional analysis in the current study revealed significant differences between the youngest secondary forest and the old growth secondary forest with $R^2= 0.14$, $p < 0.0001$, the turnover in species composition has been observed in other secondary forest chronosequences for example which revealed distinct local assemblages although did not conform to the expectations of intermediate disturbance hypothesis (Araia, Chirwa, and Assédé, 2020; X. Han et al., 2021; Hethcoat et al., 2019).

The significant PERMANOVA results demonstrates that the species do not vary in the different recovery as well as within the same groups. The PERMANOVA results offers new understanding of how the species vary across different recovery regimes which had not been undertaken before in the region, however insignificant results were observed in a comparison between human modified forest and state protected reserve in South Africa (Araia et al., 2020). A similar study that assessed tree species distribution in West Africa revealed a wider variation in tree species along disturbance gradients with a very low diversity in high disturbed forest compared to intermediate and non-stressed vegetation (Bentsi-Enchill, Dampsey, Pappoe, Ekumah, and Akotoye, 2022). Although, in this current study, species did not vary significantly across the disturbance gradients as compared with the findings of Bentsi-Enchill et al., 2022, this could be attributed to the differences in the forest types, environmental variables like altitude among others.

3.4.5. Study limitations and implications for policy planning and implementation

The study had limitations in terms of the age of the secondary forests, the old growth secondary forest sample plots were of unknown age since they existed before 1986 from the available remote sensing data which shows the forest cover change until up to the year 2017 which potentially represent a shifted baseline in terms of when the forest recovers to the level of the primary forest. Some of the plots could have been disturbed by cattle, fire, or logging with remnant trees that potentially affect the recovery rates of both the AGB and the species richness and diversity, therefore, further consideration should include assessing the effects of remnant trees that influence both the AGB and species responses to clearance as has been reported to significantly affect AGB in secondary forests (Carrière, Letourmy, and McKey, 2002; N'Guessan et al., 2019). Future research should focus on re-census of the plots to determine the actual changes in biomass, the role of growth and mortality dynamics, establish the age from other methods especially measure of tree rings (J. White, 1998) to supplement the remotely sensed data and minimize differences in age resulting from long rotations and natural regeneration of minors (Maltamo, Kinnunen, Kangas, and Korhonen, 2020) and extend the research to other blocks of the Mau forest complex that face different interaction from different communities adjacent to them.

The findings of the current study demonstrate the time needed for AGB to recover to the status of the old growth secondary forest (intact) as 25 years and the similarity in the tree species diversity and richness indices between the youngest secondary forest and the old growth secondary forest in this current study provide the basis for the design and development of policies that ensure effective restoration, use, and management of the tropical montane forests of East Africa. It is critical to incorporate

the findings of this research into the policy and plans to improve the resilience of the tropical montane forests (Nagel et al., 2017). The results also demonstrate how effective the tropical montane forests contribute to the curbing and mitigation of climate change by the amount of AGB and C sequestration which can be used to advance greenhouse gas (GHG) accounting and influence the policies towards the REDD+ initiatives in the Eastern Africa region and global scales.

3.5. Conclusion

In this study, it was discovered that forest recovers at a higher rate in the first 20 years after the forest was cleared, and then the rate of AGB recovery declines as the forest reaches the old growth secondary forest stage. Forest structure and composition especially basal area increase with the age following forest clearance. It was also discovered that forest areas that were recently disturbed were characterized by few dominant species. The current study contributes to the existing knowledge offers a comprehensive determination of the rate of recovery of aboveground AGB following forest clearance, information on species diversity in the montane forest ecosystem which has not been widely undertaken in Eastern Africa. The results provide insights and require information for the tropical montane forest restoration and monitoring.

4. QUANTIFICATION OF SOIL CARBON AND NITROGEN STOCKS ALONG FOREST RECOVERY STAGES IN TROPICAL MONTANE FOREST OF EAST AFRICA



Forest areas undergoing recovery following different forms of disturbance in the Mau Forest complex (a – c) with evidence of dead wood in the forest. Photographs taken from the Mau forest Complex during the field work in March 2019

Abstract

Tropical montane forests provide key ecological services and play a significant role as a carbon reservoir on a global scale. However, there is a lack of understanding of the variation in soil C and N stocks following forest clearance and how the forest recovery affects the soil C and N stock dynamics. This study assessed the changes in soil C and N stocks with the forest recovery process after forest clearance for the Mau forest Complex of Kenya. Soil samples from 47 forest plots were collected to assess the effect of recovery on the soil C and N stocks at three depths (0 – 10, 10 – 30, and 30 – 60 cm) and across six recovery stages ranging from <10 years, 10 – 15, 15 – 20, 20 – 25, 25 – 30 years and old-growth (mature) secondary forest. The forest plots were distributed within the three blocks of the Mau forest complex. This study found that soil properties (pH, soil organic matter concentrations, bulk density) did not significantly change with the forest recovery stages and that soil C and N stocks were also not significantly different across the recovery stages with the average soil C of 37.93 ± 12.96 Mg C ha⁻¹ from the 0 – 10 cm depth, 57.7 ± 13.67 Mg C ha⁻¹ (10 – 30 cm) and 88.48 ± 28.07 Mg C ha⁻¹ (30 – 60 cm) measured in the youngest secondary forest (<10 years of age) and 40.02 ± 14.64 Mg C ha⁻¹ (0 – 10 cm depth), 71.65 ± 12.34 Mg C ha⁻¹ (10 – 30 cm) and 106.25 ± 35.66 Mg C ha⁻¹ (30 – 60 cm depth) measured at the old-growth secondary forest. Likewise, total soil N stocks were also not significantly different between recovery regimes with 3.42 ± 0.85 Mg N ha⁻¹ (0 – 10 cm soil depth), 5.29 ± 1.81 Mg N ha⁻¹ (10 – 30 cm), and 7.64 ± 2.98 Mg N ha⁻¹ (30 – 60 cm depth) measured from the youngest secondary forest and 3.87 ± 1.36 Mg N ha⁻¹ (0 – 10 cm of soil depth), 6.79 ± 1.29 Mg N ha⁻¹ (10 – 30 cm), 9.41 ± 2.71 Mg N ha⁻¹ (30 – 60 cm) measured at the old-growth secondary forest. The findings in this

study suggest that the clearance of these secondary forests has a larger effect on aboveground C stocks, however, the soil C and N stocks do not significantly change with the recovery stages. The results provide empirical evidence of the capacity of the tropical montane forests of East Africa to store a considerable amount of soil C stocks and provide the vital information that can be used to design management policies towards conservation measures that can improve soil properties that ensure retention of the soil C stocks.

4.1. Introduction

Forest ecosystems store approximately 70% of the terrestrial carbon (C) of which the tropical montane forests play a significant role on a global scale (Spracklen and Righelato, 2014; Keenan et al., 2015; Taylor et al., 2017; de la Cruz-Amo, et al., 2020). Tropical montane forests cover approximately 8% of the total tropical forests (Spracklen and Righelato, 2016) and are recognized for their contribution to mitigation of climate change (Keith, Vardon, Stein, and Lindenmayer, 2019; Martínez et al., 2009), provision of hydrological services, and protection of biodiversity (Spracklen and Righelato, 2014; Stenfert Kroese, Jacobs, et al., 2020; Stenfert Kroese, Quinton, et al., 2020). Given that soil serves as a major reservoir of carbon (Saiz et al., 2012; de la Cruz-Amo, et al., 2020), the content of soil carbon (C) in areas with native vegetation such as forests, shrubs, among others sequester more soil C compared to the other land uses such as croplands (Sattler, Murray, Kirchner, and Lindner, 2014; Sun, Zhu, and Guo, 2015). Soil C sequestration is proposed as a key strategy to mitigate the effects of climate change (Liu et al., 2018). Understanding of the dynamics of soil C storage in secondary forest recovery following clearance is key to effective forest restoration and management (F. Huang et al., 2018; Long et al., 2018) because these forests contribute to up to 17% of global C emissions (Santini et al., 2020) resulting from the on-going land cover changes (Mendoza-Ponce, Corona-Núñez, Galicia, and Kraxner, 2019).

The variation in soil C and N stocks with soil physical and chemical properties has been widely studied in tropical forests (Quesada et al., 2020; Soong et al., 2020). The interaction between soil properties particularly an increase in nitrogen (N) capital can increase the capability of forests to sequester soil C (Yang, Luo, and Finzi, 2011).

Several studies have demonstrated that changes in land use influence soil C and N stocks (Don et al., 2011; Rahman et al., 2017), of these land-use changes, deforestation, is the one that influences most soil properties and functions (Martínez-Garza, Campo, Ricker, and Tobón, 2016; Veldkamp, Schmidt, Powers, and Corre, 2020). In the last few decades the knowledge of the carbon cycle in lowland tropical forest soils have increased significantly (Brienen et al., 2015b; Girardin et al., 2016; S. Moore et al., 2018) as well as for planted forest (Wang and Huang, 2020). However, for tropical montane forests (TMF) there are large gaps in knowledge, and the carbon cycling dynamics are understudied (Moser et al., 2011), especially the soil carbon dynamics following clearance and recovery (Nyirambangutse et al., 2017; Soh et al., 2019).

The storage of C in TMF ecosystems is under threat mainly due to the increasing human population, which contributes to the intensification of agriculture, and expansion of grazing (Ward et al., 2014), and undocumented logging (Santini et al., 2019). A study by Sherman et al., (2012) on changes in aboveground biomass and C along an altitudinal gradient in a disturbance prone TMF in the Dominican Republic reported variability in AGB and C stocks following a forest disturbance at different altitudes with AGB decreasing significantly with altitude.

Unlike TMFs, soil C stocks have been previously reported not to be affected during the forest recovery process in tropical forests in central and north Africa (Bauters et al., 2021, 2019; Djemel Merabtene et al., 2021) but these forests have different soil conditions from the tropical montane forests of Kenya particularly the Mau forest Complex. In the tropical montane forest, soil C has also been reported as relatively uniform along elevation gradients (Hagedorn et al., 2019; Phillips et al., 2019), at different succession stages (Nyirambangutse et al., 2017), although variations exist in

the altitude in the case of Yegof mountain natural vegetation in Ethiopia (Eshetu and Hailu, 2020). Berihu et al., (2017) and Muktar et al., (2018) reported a significant variation in soil C stocks from a dense forest, open forest, grazing land, farmland resulting from changes in land use. Soil C and N differed in different forest fragments that were affected by deforestation in the central highlands of Ethiopia (Tolessa and Senbeta, 2018). The high correlation of soil C and N stocks was established between different land uses with a decreasing trend with dept, increasing sequestration of soil C from cropland conversion to agroforestry in northern Ethiopia (Gelaw et. al., 2014). Land use and slope effects were found to significantly influence the soil physiochemical properties especially soil C and N stocks in the north-western Ethiopian highlands (Tamene, Adiss, and Alemu, 2020). Recent studies in the Mau forest complex particularly have demonstrated fluxes in soil carbon dioxide in both forest and agricultural lands (Arias-Navarro et al., 2017) and at different topographic positions (Arias-Navarro et al., 2017) with limited knowledge of how forest recovery from disturbances influence the soil C and N stocks.

The montane forests in East Africa are recognized as ecosystems that sequester carbon both within the vegetation cover and the soils especially in north-western Ethiopia (Gebeyehu et al., 2019). Elsewhere, soil C stocks vary with changes in land use and vegetation (Ge, Wang, Fan, Gongadze, and Wu, 2020; Sun et al., 2015; C. Zhang, Liu, Xue, and Sun, 2013; Zhao et al., 2017), and at a regional scale, climatic and soil properties significantly influence soil C stocks (Saiz et al., 2012), yet it is not clear how the soil C stocks in the East African montane forests respond to changes in the forest resulting from clearance and other forms of degradation.

Variation in forest soil C and N stocks with forest recovery has not been widely studied in the Afromontane vegetations in East Africa with exception of (Yimer, Ledin and

Abdelkadir, 2006, 2007; Gebrehiwot et al., 2018) who reported a significant relationship between elevation, topographic aspect, and soil moisture with the soil C stocks in the Bale Mountains and the Abune Yosef Afroalpine and sub-Afroalpine vegetation in Ethiopia. It is not clear how the soil C and N stocks vary with forest recovery dynamics in the TMFs of East Africa with an exception of studies by Tarus et al., (2019) and Kinjanjui et al., (2013) that assessed soil C dynamics in plantation forest with different management styles. Quantification of changes in soil C and N in the forested ecosystem that is undergoing recovery following disturbances are limited (Kizza et al., 2013), with little knowledge about the relationship and variation in soil C and N stocks from different forest recovery stages across the East African montane forests. The recent studies have focused on the evaluation of soil C and N stocks resulting from forest cover changes to agricultural land use and vice versa (Vittori Antisari et al., 2013; Gelaw, Singh and Lal, 2014). For example in Kenya and the Mau forest complex, in particular, previous studies have examined GHG fluxes in agricultural fields, forested land that has been converted to agriculture, and nutrient cycling in other land uses especially Kinjanjui, Karachi and Ondimu, (2013) who reported a significant difference between soil C concentration in an undisturbed forest as 6.6% and a disturbed forest (i.e. forest converted to farmland) as 4.9%.

In this study, the main objective was to quantify soil C and N stocks along the different stages of the forest recovery process following deforestation and forest clearance in the Mau forest complex, a montane forest in Kenya. Synthesize major changes in soil properties concerning the forest recovery stages i.e., from the youngest secondary forest to old growth secondary forest following clearance. The key research questions are:

Do the soil C and N stocks change with:

- (i) recovery time?
- (ii) aboveground biomass?

To answer these questions, the mapped area of forest loss and recovery in chapter three of this thesis was used to assess the aboveground forest biomass and species recovery as well as the forest structure and composition (in chapter three) which was then related with the below ground soil C and N stocks for this current chapter, the 47 forest plots which were used for assessing recovery in chapter 3 were also sampled with each having 4 replicates of depth ranging from 0 -10 cm, 10 – 30 cm, and 30 – 60 cm and investigated soil properties: soil organic matter content (SOM), bulk density, and calculated soil C and N stocks for different recovery stages. The analysis tested for associations between soil C and N stocks with the aboveground biomass, disturbance index (DI), and then determined variation between the blocks and the recovery regimes following deforestation.

4.2. Materials and methods

4.2.1. Study area and experimental design

The study was carried out in the 3 blocks of the Mau forest complex that have been assessed for the AGB and species diversity namely, Western (W), South Western (SW), and Transmara (T) in Western Kenya (Fig. 4-1). Fieldwork was undertaken between March – June 2019 and 47 plots were established within the six recovery regimes.

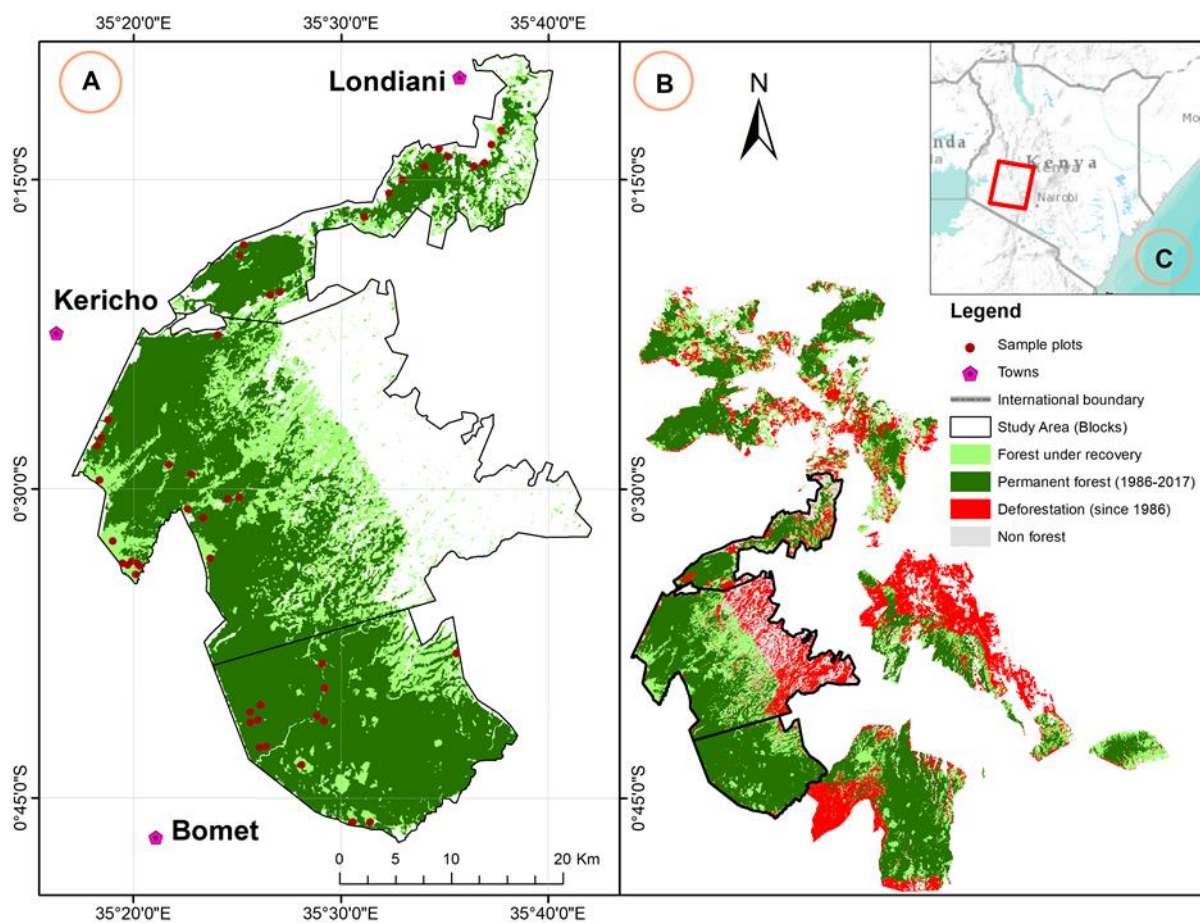


Figure 4-1: Location of the 3 forest blocks of the Mau forest complex, the red dots show the 47 sample plots that are distributed within the old-growth (permanent forest since 1986) and the forest undergoing recovery (A), map of the Mau forest Complex from which the 3 blocks were selected and showing areas that were deforested since 1986 (B) and (C) shows the location of the Mau forest complex within Kenya

The sample plots indicated in Fig. 4-1 were the same that were used for undertaking the aboveground biomass and recovery assessment (in Chapter 3) in this thesis.

Forest cover change classification was undertaken from the available Landsat satellite

data was used to determine the time since first and last forest clearance took place and areas that remained forest since 1986 as the oldest and old-growth secondary forest (Chapter two) of this current study.

4.2.2. Soil sampling and soil analysis

A total of 47 plots with dimensions of 20 m x 50 m (0.1 ha) were sampled as shown in Fig. 4-1. The plots were further subdivided to create 4 replicate subplots of 5 m x 5 m. Soil samples were collected within the three depths i.e., 0 – 10 cm, 10 – 30 cm, and 30 – 60 cm in each of the replicates. Within each of the 47 plots, evidence of forest disturbance was recorded which included signs of firewood collection, charcoal burning, livestock grazing, elephant damage, forest fires among others (Fig. 4-2)



Figure 4-2: Photographs taken at the sampling sites showing evidence of clearance and disturbance: (a) Evidence of forest fire in plot 44 in Western Mau block, (b) a spot in plot 2 in Western Mau block where charcoal was recently prepared, (c) Part of forest where a charcoal kiln is being established (d) Signs of firewood collection and cutting of trees for fuelwood in South Western Mau block (e) Evidence of damage by elephants ; (f) Areas disturbed as a result of livestock grazing.

Soil samples were collected using the Eijkkelkamp auger and soil sampling equipment.

The litter was cleared to the soil surface before soil samples were collected. The samples were collected in two sets (i) for determining the soil physical properties (bulk density, and soil organic matter) and (ii) to measure the soil chemical properties (i.e. soil pH, C and N). The collected samples were then air-dried and sieved using a 2 mm sieve to remove stones and large roots. In this current study, six soil chemical and

physical properties at different forest plots distributed in the 3 blocks of the Mau forest complex were evaluated.

4.2.3. Soil physical properties

The soil samples that were collected for the analysis of physical properties were oven-dried at 105°C until a constant weight was obtained and used to determine the soil bulk density (BD) following the direct method (Al-shammary et al., 2018; Han et al., 2016) and using Eq. 4-1. the oven-dried soils at 105°C were then further heated to 550 °C (loss-on-ignition) to determine and calculate soil organic matter (SOM) content (Adamczyk et al., 2019).

Equation 4-1: Estimation of soil bulk density (BD)

$$pb \text{ (units)} = M_s/V_s$$

Where:

pb is the Soil Bulk Density in ($Mg \text{ m}^{-3}$)

M_s is the weight of the dried sample (Mg)

V_s is the volume of the dry soil sample in (m^3)

4.2.4. Soil chemical properties

The air-dried soil samples were used to determine the pH, C, and N concentrations. To determine the pH, 10 g of the soil was mixed with 25ml of distilled water and thoroughly shaken using an orbital shaker for 30 minutes and then left to settle for 30 minutes in a 50 ml beaker. The pH was then measured at the soil-water interface using a pH meter (Mettler Toledo Seven Compact, Darmstadt, calibrated with standards at pH 4, 7, and 10. To determine the soil C and N concentrations, the air-dried samples were ground using the ball mill into powder form. A sub-sample of 20 mg of the powdered soil samples was wrapped using tin capsules and combusted at 950°C using an elemental micro-analyzer. Carbon and N concentrations were used to

calculate the total soil carbon (TSC) and total soil nitrogen (TSN) stocks following equations 4-2 and 4-3.

Equation 4-2: Estimation of the soil carbon stocks

$$TSC \text{ Stocks } (Mg \text{ ha}^{-1}) = BD \times C (\%) \times \text{Depth}$$

Equation 4-3: Estimation of the soil nitrogen stocks

$$TSN \text{ Stocks } (Mg \text{ ha}^{-1}) = BD \times N (\%) \times \text{Depth}$$

Where:

BD is the bulk density of the soil layers (g/cm^3),

Depth (cm),

C = Carbon concentration,

N = Nitrogen concentration

4.2.5. Statistical analysis

All analyses were carried out using the R statistical platform (R Core Team, 2020). Two-way ANOVA was used to assess the variation in the soil properties with the recovery regimes within the soil cores and the three forest blocks of the Mau forest complex and this was followed by a Turkey HSD. Spatial autocorrelation was used to determine the effects of location using the Moran's I test for spatial autocorrelation to minimize the influence of spatial correlation (Harisena, Groen, Toxopeus, and Naimi, 2021). Correlation analysis of the measured variables and Pearson correlation coefficient were used to assess the relationship between soil variables and to choose variables for mixed models.

Generalized Linear Mixed effect models (GLMMs) with both random and mixed effects (Bolker et al., 2009; Nakagawa, Johnson, and Schielzeth, 2017) were used to assess the relationship between age and changes in soil C and N stocks with the candidate soil variables selected as proxy from the Pearson's correlation analysis. Forest blocks

were used as random effect, and age, disturbance index, pH, and aboveground were fixed effects in the models. The accuracy of the models with different covariates was evaluated using minimum Akaike information criterion (AICs) following (Burnham, Kenneth P., Anderson, 2002) to select the best regression model to predict the soil C and N stocks from the measured variables.

4.3. Results

4.3.1. Soil Characteristics

Soils in the study area were found to be acidic to neutral with pH of 5.60 ± 0.81 (mean \pm SD) for 0 – 10 cm depth, 5.50 ± 0.77 in 10 – 30 cm and 5.39 ± 0.70 for 30 – 60 cm in the youngest secondary forest (<10 years of age) and for the old growth secondary forest were 5.22 ± 0.90 for 0 – 10 cm depth, 5.09 ± 0.80 in 10 – 30 cm and 5.03 ± 0.68 for 30 – 60 cm. Soil bulk density increased with the depth from 0.70 ± 0.09 (g/cm³) in 0 – 10 cm to 0.78 ± 0.12 (g/cm³) and 1.07 ± 0.27 (g/cm³) for 10 – 30 cm and 30 – 60 cm depth, respectively for the youngest secondary forest and 0.67 ± 0.11 (g/cm³) in 0 – 10 cm to 0.76 ± 0.08 (g/cm³) and 1.09 ± 0.29 (g/cm³) for 10 – 30 cm and 30 – 60 cm depth for the old growth secondary forest.

Soil C and N concentrations across the recovery stages were not significantly different for example, soil C concentration in the youngest secondary forest was 3.90 ± 0.70 (%) and N concentration for the same stage was 0.40 ± 0.10 (%) while for the old growth secondary forest were 4.60 ± 0.70 (%) for soil C and 0.40 ± 0.10 (%) of soil N concentration.

Soil properties did not significantly vary across sites and the recovery stages as shown in Tab. 4-1, soil C and N stocks were also not significantly different between the recovery stages across all the soil depths (of up to 60 cm) with the average soil C of 37.93 ± 12.96 Mg C ha⁻¹ from the 0 – 10 cm depth, 57.7 ± 13.67 Mg C ha⁻¹ (10 – 30 cm) and 88.48 ± 28.07 Mg C ha⁻¹ (30 – 60 cm) measured in the youngest secondary forest (<10 years of age) and 40.02 ± 14.64 Mg C ha⁻¹ (0 – 10 cm depth), 71.65 ± 12.34 Mg C ha⁻¹ (10 – 30 cm) and 106.25 ± 35.66 Mg C ha⁻¹ (30 – 60 cm depth) measured at the old growth secondary forest. Likewise, total soil N stocks were also not significantly different between recovery regimes with 3.42 ± 0.85 Mg N ha⁻¹ (0 –

10 cm soil depth), $5.29 \pm 1.81 \text{ Mg N ha}^{-1}$ (10 – 30 cm), and $7.64 \pm 2.98 \text{ Mg N ha}^{-1}$ (30 – 60 cm depth) measured from the youngest secondary forest and $3.87 \pm 1.36 \text{ Mg N ha}^{-1}$ (0 – 10 cm of soil depth), $6.79 \pm 1.29 \text{ Mg N ha}^{-1}$ (10 – 30 cm), $9.41 \pm 2.71 \text{ Mg N ha}^{-1}$ (30 – 60 cm) measured at the old growth secondary forest. Detailed distribution of the soil properties is indicated in Tab. 4-1.

Table 4-1: Soil physical and chemical properties for plots sampled at different recovery periods of the Mau Forest Complex. The values indicate the mean, standard deviation (SD), and Coefficient of Variation (CV) of the data for the 6 recovery periods for Bulk Density (BD), Soil organic matter (SOM), Carbon concentration (C), Nitrogen concentration (N), C:N Ratio, Soil organic carbon (SOC), Total soil Nitrogen (TSN) and Aboveground Carbon (AGC).

Soil Property	Depth (cm)	<10		10 – 15		15 – 20		20 – 25		25 – 30		Old growth	
		Mean ± SD	CV (%)	Mean ± SD	CV (%)	Mean ± SD	CV (%)	Mean ± SD	CV (%)	Mean ± SD	CV (%)	Mean ± SD	CV (%)
pH	0-10	5.6 ± 0.8a	14.4	5.7 ± 1.1a	19.6	5.5 ± 1.0a	18.9	5.3 ± 0.3a	6.3	4.9 ± 0.6a	12.1	5.2 ± 0.9a	17.3
	10-30	5.5 ± 0.8a	14.0	5.6 ± 1.1a	19.8	5.5 ± 0.9a	18.2	5.0 ± 0.4a	8.8	5.0 ± 0.6a	10.9	5.1 ± 0.8a	15.7
	30-60	5.4 ± 0.7a	12.9	5.5 ± 0.9a	16.1	5.2 ± 0.7a	13.7	4.9 ± 0.3a	4.9	4.8 ± 0.3a	5.9	5.0 ± 0.7a	13.5
C (%)	0-10	5.4 ± 1.4a	26.2	6.5 ± 2.1a	31.4	6.1 ± 1.1a	17.3	5.2 ± 0.9a	18.4	5.2 ± 1.2a	22.2	5.9 ± 1.6a	27.1
	10-30	3.7 ± 0.7a	18.9	4.8 ± 1.2a	24.9	4.9 ± 0.4a	7.9	4.1 ± 1.2a	28.6	3.9 ± 0.5a	13.6	4.7 ± 0.8a	17.4
	30-60	2.7 ± 0.5a	16.9	3.1 ± 0.8a	26.3	3.0 ± 0.3a	8.3	2.7 ± 0.9a	36.5	2.7 ± 0.5a	19.7	3.2 ± 0.4a	13.3
N (%)	0-10	0.5 ± 0.1a	20.6	0.6 ± 0.1a	19.5	0.6 ± 0.1a	14.5	0.5 ± 0.1a	17.1	0.5 ± 0.1a	20.7	0.6 ± 0.1a	24.9
	10-30	0.3 ± 0.1a	28.3	0.4 ± 0.1a	18.3	0.5 ± 0.04a	9.6	0.4 ± 0.1a	23.8	0.4 ± 0.1a	21.9	0.5 ± 0.1a	16.8
	30-60	0.2 ± 0.1a	23.8	0.3 ± 0.1a	27.1	0.3 ± 0.01a	4.6	0.2 ± 0.1a	24.6	0.3 ± 0.1a	27.0	0.3 ± 0.03a	11.2
C:N Ratio	0-10	11.0 ± 1.8a	16.1	12.2 ± 2.5a	20.1	11.6 ± 1.9a	17.2	10.5 ± 1.5a	14.1	11.5 ± 2.4a	20.8	11.3 ± 3.5a	31.0
	10-30	13.6 ± 5.6a	40.9	11.9 ± 1.9a	16.4	10.8 ± 0.9a	8.5	13.0 ± 6.5a	50.1	10.8 ± 1.7a	16.1	10.7 ± 1.3a	12.5
	30-60	12.1 ± 2.0a	16.6	12.8 ± 2.2a	17.4	10.8 ± 0.8a	7.2	12.3 ± 3.7a	29.9	12.3 ± 4.2a	34.1	11.3 ± 1.4a	12.0
SOC (Mg C ha ⁻¹)	0-10	37.9 ± 12.9a	34.2	44.4 ± 14.2a	31.9	32.0 ± 9.9a	30.9	36.0 ± 7.3a	20.2	33.4 ± 10.9a	32.6	40.0 ± 14.6a	36.6
	10-30	57.7 ± 13.7a	23.7	70.1 ± 14.1a	20.1	64.7 ± 8.7a	13.4	59.8 ± 20.0a	33.5	54.1 ± 7.9a	14.6	71.7 ± 12.3a	17.2
	30-60	88.5 ± 28.1a	31.7	102.9 ± 27.6a	26.8	98.3 ± 23.6a	24.0	99.7 ± 60.3a	60.5	86.3 ± 20.3a	23.5	106.3 ± 35.7a	33.6
TSN (Mg ha ⁻¹)	0-10	3.4 ± 0.8a	24.7	3.8 ± 0.9a	24.6	3.1 ± 1.1a	35.4	3.5 ± 0.7a	21.0	3.2 ± 1.0a	32.7	3.9 ± 1.4a	35.3
	10-30	5.3 ± 1.8 a	34.3	6.0 ± 1.5a	25.7	6.0 ± 1.0a	16.8	5.6 ± 1.7a	29.7	5.3 ± 1.1a	21.5	6.8 ± 1.3a	19.0
	30-60	7.6 ± 2.9 a	39.0	8.4 ± 2.2a	26.1	9.1 ± 2.4a	26.1	8.3 ± 3.5a	41.8	8.1 ± 2.5a	30.6	9.4 ± 2.7a	28.8
Bulk Density (g/cm ³)	0-10	0.7 ± 0.1a	12.7	0.7 ± 0.1a	13.5	0.5 ± 0.2a	35.0	0.7 ± 0.1a	14.4	0.6 ± 0.2a	25.8	0.7 ± 0.1a	17.1
	10-30	0.8 ± 0.1a	15.7	0.7 ± 0.1a	16.1	0.7 ± 0.1a	20.9	0.7 ± 0.1a	10.2	0.7 ± 0.1a	17.7	0.8 ± 0.1a	9.9
	30-60	1.1 ± 0.3a	25.2	1.1 ± 0.1a	12.5	1.1 ± 0.3a	28.1	1.2 ± 0.3a	23.5	1.1 ± 0.3a	24.7	1.1 ± 0.3a	26.6
SOM (%)	0-10	18.5 ± 5.4a	29.3	18.7 ± 2.9a	15.3	18.4 ± 3.2a	17.3	20.5 ± 2.9a	14.0	20.9 ± 1.6a	7.5	18.7 ± 2.2a	11.5
	10-30	15.4 ± 4.3a	27.6	15.2 ± 3.4a	22.3	15.5 ± 3.1a	19.9	16.9 ± 2.1a	12.6	18.1 ± 1.2a	6.8	16.0 ± 2.3a	14.5
	30-60	12.1 ± 3.7a	30.3	13.4 ± 2.8a	20.9	14.5 ± 4.4a	30.6	14.4 ± 2.9a	19.9	14.7 ± 1.7a	11.6	12.9 ± 2.8a	21.5
AGC (Mg C ha ⁻¹)		28.3 ± 18.9a	66.8	42.8 ± 16.0ab	37.4	81.4 ± 32.9bc	40.4	93.2 ± 36.7cd	39.4	132.7 ± 38.9cd	29.3	132.9 ± 33.7d	25.4

4.3.2. Relationship between the soil properties

Soil organic matter (SOM) concentration was significantly correlated with the soil bulk density ($p = -0.41$, $p < 0.05$ for 10 – 30 cm depth and $p = -0.39$, $p < 0.05$ for the 30 – 60 cm soil depths respectively), C:N ratio across all the soil cores with ($p = 0.94$, $p = 0.71$, $p = 0.85$ at $p < 0.05$) for 0 – 10, 10 – 30 and 30 – 60 cm respectively. SOM (%) was also significantly correlated with pH ($p = -0.44$ and -0.31 respectively for the 10 – 30 cm and 30 – 60 cm). Soil C (%) concentration was positively correlated with Nitrogen (%) concentration at ($p = 0.81$; $p < 0.05$ for 0 – 10 cm depth, 0.79 , $p < 0.05$ for 10 – 30 cm and the 10 – 30 cm) and negatively correlated with the soil N (%) at ($p = -0.39$; $p < 0.05$) for the topsoil (0 – 10 cm depth). C:N ratio was also significantly correlated with the soil C for the 10 – 30 and 30 – 60 cm by ($p = 0.79$ and $p = 0.77$; $p < 0.05$ respectively) and soil C (%) was also correlated negatively with soil N (%) for the sub soil cores i.e. ($p = -0.56$ and $p = -0.5$; $p < 0.05$) for 10 – 30 and 30 – 60 cm respectively.

There was significant negative correlation between SOM (%) and disturbance index ($p = -0.32$; $p < 0.05$) for the 30 – 60 cm depth as well as with the C:N ratio ($p = -0.32$; $p < 0.05$) at 10 – 30 cm soil depth. Soil C stocks was significantly correlated with the N concentration with $p = 0.81$, $p < 0.05$ (0 – 10 cm), $p = 0.79$, $p < 0.05$ (10 – 30 cm) and $p = 0.77$, $p < 0.05$ (30 – 60 cm) and was not correlated with the other physical and chemical properties that were measured across all the soil cores as shown in Tab. 4-2.

Table 4-2: Correlation analysis for all the variables i.e. Bulk Density (BD), Soil Organic Matter (SOM), pH, Carbon concentration (C), Nitrogen concentration (N), C:N Ratio and Disturbance Index (DI). Note: Bold coefficients represent significance at ($p < 0.05$)

	BD (g/cm ³)			SOM (%)			pH			C (%)			N (%)			C:N Ratio			
	0-10	10-30	30-60	0-10	10-30	30-60	0-10	10-30	30-60	0-10	10-30	30-60	0-10	10-30	30-60	0-10	10-30	30-60	
BD (g/cm ³)	1.00	1.00	1.00																
SOM (%)	-0.24	-0.41	-0.39	1.00	1.00	1.00													
pH	0.13	0.37	0.03	-0.15	-0.44	-0.35	1.00	1.00	1.00										
C (%)	0.00	-0.23	0.10	-0.22	-0.02	-0.04	0.06	-0.06	-0.13	1.00	1.00	1.00							
N (%)	0.04	-0.11	-0.09	0.02	0.14	0.12	0.02	-0.04	-0.05	0.81	0.79	0.77	1.00	1.00	1.00				
C:N Ratio	-0.24	-0.12	0.14	-0.19	-0.32	-0.13	-0.16	-0.02	-0.14	0.04	-0.18	-0.04	-0.39	-0.56	-0.50	1.00	1.00	1.00	
DI	0.01	0.27	0.15	-0.13	-0.25	-0.32	0.55	0.53	0.49	-0.11	-0.09	-0.12	0.09	0.13	0.02	-0.27	-0.18	-0.24	

In order, to select proxy variables for predicting and determining the response of soil C and N stocks, the study used the correlation relationships presented in Tab. 4-2 to identify variables that were not correlated.

4.3.3. Response of soil C and N stocks to recovery stages and Aboveground C

In this study eight (8) candidate models were fitted to predict the soil C and N from the soil physical and chemical properties that were collected from the field. Of the 8 models, 2 Null models were fitted each for soil C and N stocks with no predictor and compared its AIC with the 3 other models for both soil C and N stocks using the Age, DI, pH, and AGC as the covariates as shown in Tab. 4-3.

Table 4-3: Candidate models fitted to determine the relationship between the Total Soil Carbon (TSC) and Total Soil Nitrogen (TSN). The asterisk between covariates shows their interactive effects

Model/Description	Rank	AIC	BIC	Δ AIC
TSC = $\beta_0 + \beta_1$ (Age) + β_2 (DI) * β_3 (Soil pH) + β_4 (AGC)	1	477.54	492.35	0.00
TSC = $\beta_0 + \beta_1$ (Age) + β_2 (DI) + β_3 (Soil pH) + β_4 (AGC)	2	486.05	499.00	8.51
TSC = $\beta_0 + \beta_1$ (Age)	3	496.32	503.72	18.78
TSC = $\beta_0 + \beta_1$ (NULL)	4	501.13	506.68	23.59
TSN = $\beta_0 + \beta_1$ (Age) + β_2 (DI) * β_3 (Soil pH)	1	267.83	280.79	0.00
TSN = $\beta_0 + \beta_1$ (Age) + β_2 (DI)	2	271.62	280.87	3.79
TSN = $\beta_0 + \beta_1$ (Age) + β_2 (DI) * β_3 (Soil pH) + β_4 (AGC)	3	274.59	289.39	6.76
TSN = $\beta_0 + \beta_1$ (NULL)	4	275.29	280.84	7.46

The model which comprised of Age, DI, soil pH, and AGC as covariates with an interaction term between DI and pH performed better with a delta AIC of 8.51 compared to the next best model that did not include the interaction term between DI and pH as shown in Tab. 4-3. A similar model was also developed and fitted for the soil N stocks, with the detailed model coefficients for the best-fitted model at each soil depth as well as the combined (0 – 60 cm depth) plot level for the soil C stocks are indicated in Tab. 4-4.

Table 4-4: Mixed effect models for predicting the soil C stocks for 0 – 10, 10 -30, and 30 – 60 m soil profiles as well as the combined total soil carbon for 0 – 60 cm profile in the Mau forest complex. DI = Disturbance Index, AGC = Aboveground C derived from AGB. Average pH across the soil profile (0 – 60 cm) was used to determine the soil C stocks for the whole (Overall) profile. σ^2 = Residual Variance, ICC = Intra-class correlation coefficient, N = Number of groups (random), est. = Estimates

Predictors	0 – 10			10 – 30 cm			30 – 60 cm			0 – 60 cm (Overall soil profile)		
	Est.	CI	p	Est.	CI	p	Est.	CI	p	Est.	CI	p
(Intercept)	33.12	-36.05 – 102.29	0.35	47	-32.27 – 126.27	0.25	236.38	-23.17 – 495.93	0.07	274.69	-56.26 – 605.64	0.10
Age [years]	-2.42	-9.80 – 4.96	0.52	1.77	-7.13 – 10.66	0.69	-4.68	-23.90 – 14.55	0.63	-5.55	-36.25 – 25.15	0.72
DI	-9.46	-135.72 – 116.80	0.88	-26.23	-171.05 – 118.58	0.72	-255.25	-682.27 – 171.78	0.24	-253.3	-836.12 – 329.52	0.39
pH	2.35	-10.35 – 15.05	0.72	1.86	-12.98 – 16.70	0.81	-28.03	-77.85 – 21.79	0.27	-15.24	-77.49 – 47.02	0.63
AGC	0.04	-0.07 – 0.16	0.43	0.01	-0.12 – 0.15	0.84	0.18	-0.12 – 0.47	0.24	0.26	-0.21 – 0.73	0.28
DI * pH	-0.14	-23.39 – 23.10	0.99	4.85	-21.97 – 31.68	0.72	49.8	-33.51 – 133.12	0.24	45.71	-65.05 – 156.48	0.42
Random Effects												
σ^2	146.50			216.84			995.74			2520.38		
T ₀₀	27.15 Forest blocks			0.00 Forest blocks			491.62 Forest blocks			807.89 Forest blocks		
ICC	0.16						0.33			0.24		
N	3 Forest blocks			3 Forest blocks			3 Forest blocks			3 Forest blocks		
Observations	47			47			47			47		
Marginal R ² / Conditional R ²	0.03/ 0.18			0.050/NA			0.06/0.37			0.04/0.27		

From the four (4) models that were fitted to determine soil N stocks, the model with age, disturbance index, and soil pH without the AGC performed better with the lowest AIC of 267.83 and BIC of 280.79, the model was fitted with low marginal R^2 of 0.063. The detailed coefficients of the best fitted model for the soil N stocks based on the AIC are indicated in Tab. 4-5.

Table 4-5: Mixed effect models for predicting the soil N stocks for 0 – 10, 10 -30, and 30 – 60 m soil profiles as well as the combined total soil carbon for 0 – 60 cm profile in the Mau forest complex. DI = Disturbance Index, Average pH across the soil profile (0 – 60 cm) was used to determine the soil N stocks for the whole (overall) profile. σ^2 = Residual Variance, ICC = Intra-class correlation coefficient, N = Number of groups (random)

Predictors	0 – 10 cm			10 – 30 cm			30 – 60 cm			Overall (0 – 60 cm)		
	Est.	CI	p	Est.	CI	p	Est.	CI	p	Est.	CI	p
(Intercept)	3.29	-2.38 – 8.97	0.26	4.29	-3.59 – 12.18	0.29	18.04	-3.51 – 39.60	0.10	22.05	-4.66 – 48.76	0.11
Age [years]	0.04	-0.40 – 0.48	0.86	0.33	-0.24 – 0.90	0.26	0.44	-0.69 – 1.56	0.45	0.86	-0.93 – 2.65	0.35
DI	-0.81	-11.24 – 9.63	0.88	-1.62	-16.04 – 12.80	0.83	-17.87	-52.89 – 17.16	0.32	-17.92	-64.41 – 28.56	0.45
pH	0	-1.04 – 1.04	0.99	0.03	-1.47 – 1.52	0.97	-2.23	-6.37 – 1.91	0.29	-1.53	-6.57 – 3.50	0.55
DI * pH	0.18	-1.71 – 2.07	0.85	0.48	-2.24 – 3.21	0.73	3.67	-3.11 – 10.44	0.29	3.85	-4.83 – 12.53	0.39
Random Effects												
σ^2	1.16			1.94			7.24			19.15		
T ₀₀	0.00 Forest blocks			0.31 Forest blocks			0.34 Forest blocks			0.00 Forest blocks		
ICC							0.05					
N	3 Forest blocks			3 Forest blocks			3 Forest blocks			3 Forest blocks		
Observations	47			47			47			47		
Marginal R ² / Conditional R ²	0.01/NA			0.08/0.20			0.05/0.09			0.06/NA		

Forest age had a negative coefficient on the overall model with an estimate of confidence interval (CI) of -36.25 – 25.15 with a model $p = 0.104$ as shown in Tab. 4-4. Similar patterns were observed in the topsoil (0 – 10 cm) i.e., -2.42 and -4.68 for the 30 – 60 cm depth except for the 10 – 30 cm depth which indicated a positive coefficient of 1.77. AGC had a positive effect on soil C stocks across all the soil depths as well as the model for the whole soil profile with a coefficient of 0.04 for the topsoil as well as 0.01 and 0.18 for 10 – 30 cm and 30 – 60 cm depths respectively and 0.26 for the whole soil profile as presented in Tab. 4-4.

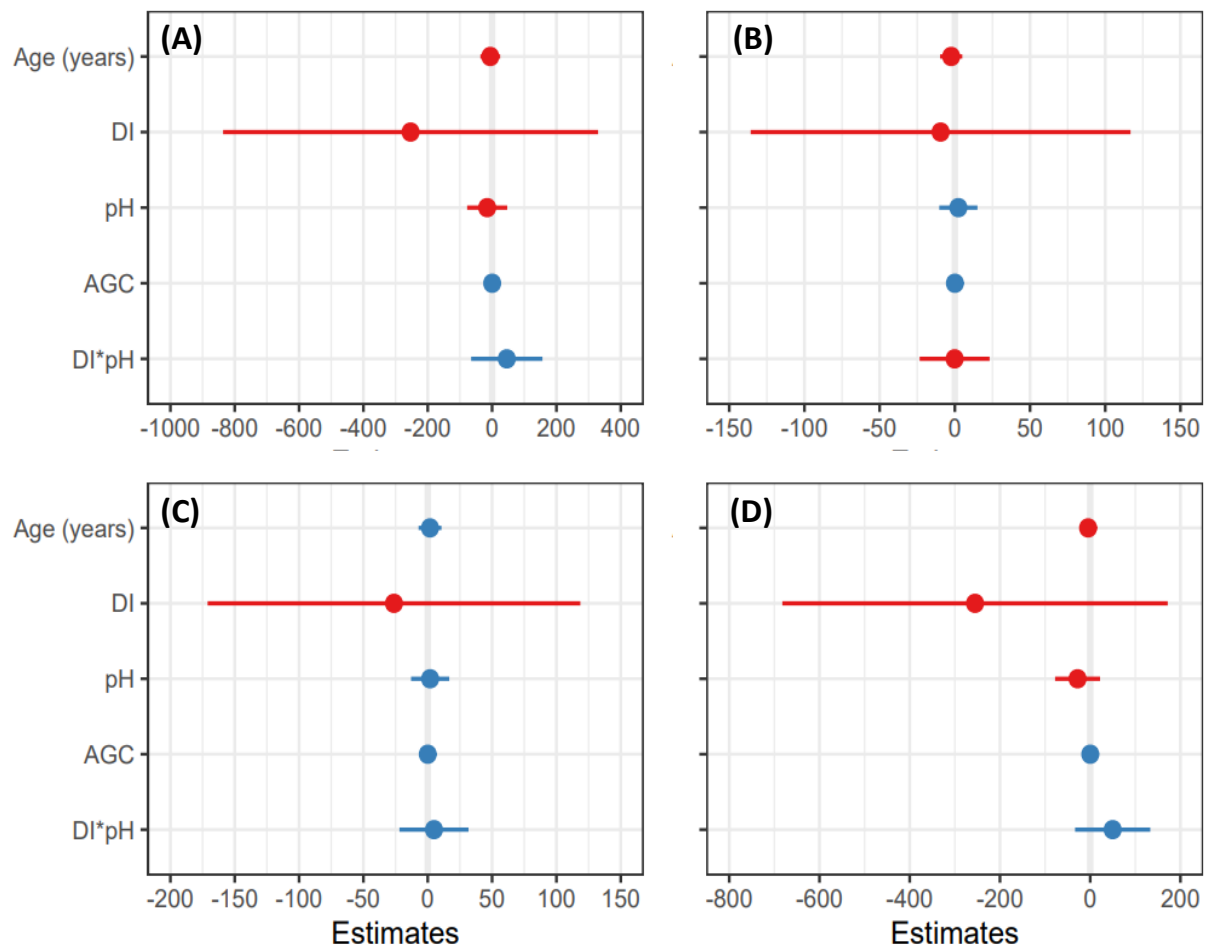


Figure 4-3: Soil C stocks estimation model coefficient with Age, Disturbance index (DI), soil pH, aboveground C, and the interaction effects between DI and soil pH as the model predictors for (A) overall model fitted with the best AIC for the whole soil profile, (B) shows the model effects of the predictors at 0 - 10 cm depth, (C) for 10 - 30 cm and (D) for 30 - 60 cm. The red dots and the confidence line indicate the negative effects while the blue dots and the lines indicate the positive effects.

For the soil C stocks, the model showed positive interaction effects between DI and the soil pH in the overall model (0 – 60 cm), model for 10 – 30 cm depth and 30 – 60 cm as shown in Fig. 4-3 (A), (C) and (D), however for negative interaction effect for the topsoil of 0 – 10 cm depth as shown in Fig. 4-3 (B).

While for the soil N stocks, the interaction effect between Di and soil pH was positive in all the layers including the overall soil profile. Age showed positive effect on the models at all soil profiles as well as the overall combined soil profile as shown in Fig 4-4.

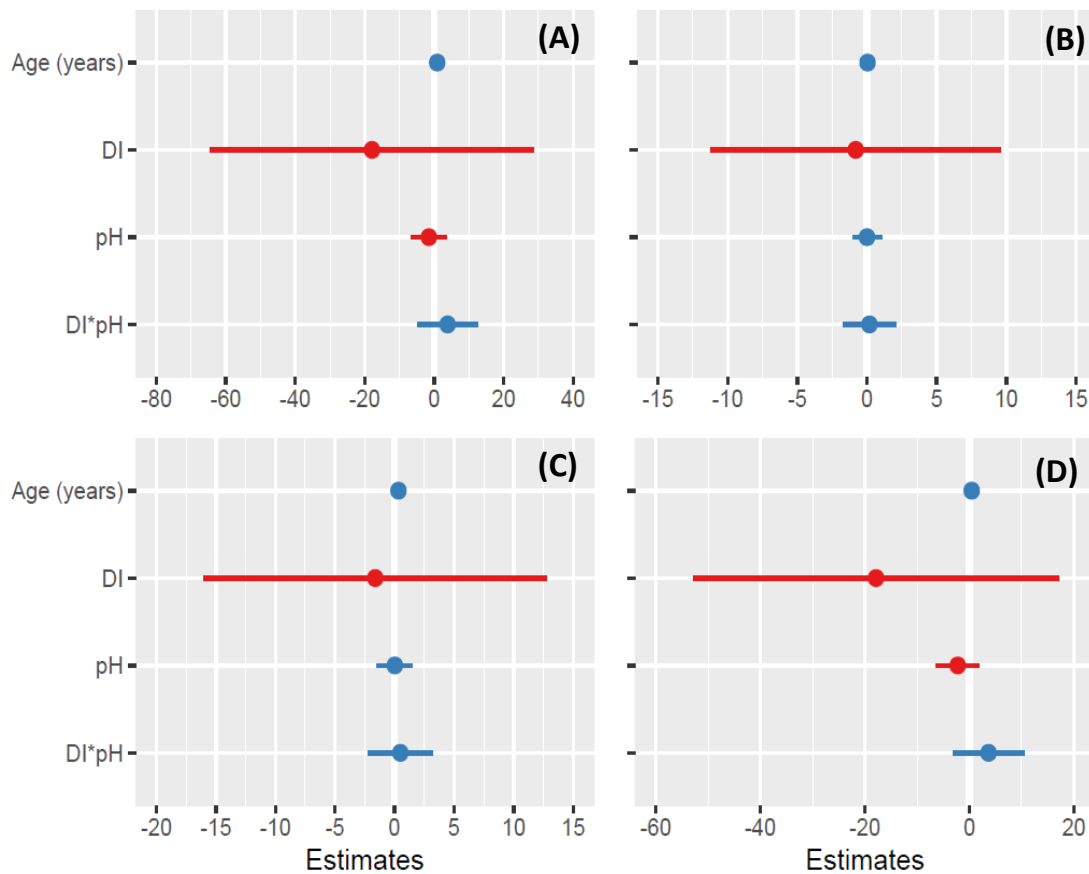


Figure 4-4: Soil N stock estimation model coefficient and the interaction effect with Age, Disturbance index (DI), soil pH and the interaction effects between DI and soil pH as predictors (A) shows the overall model fitted with the best AIC for the whole soil profile, (B) shows the model effect of the predictors at 0 - 10 cm depth, (C) for 10 - 30 cm and (D) for 30 - 60 cm. The red dots and the confidence line indicate the negative effects while the blue dots and the lines indicate the positive effects

4.4. Discussion

4.4.1. Distribution of the soil properties

Determination of accurate soil carbon stocks depends on accurate measurement of soil BD and soil C concentrations (Saiz et al., 2012). In this study, the soil BD and soil C concentrations were not correlated across the different soil depths as has been reported to be correlated in other landscapes (Liu, Li, Sun, and Yu, 2016). This study found that both BD and soil C were not significantly different between the recovery periods. The estimated soil C stocks were 37.93 ± 12.96 Mg C ha⁻¹ of soil C in the topsoil (0 – 10 cm), 57.7 ± 13.67 Mg C ha⁻¹ (10 – 30 cm), and 88.48 ± 28.07 Mg C ha⁻¹ (30 – 60 cm) in the youngest forest and there were no significant differences between young and old growth secondary forest.

The measured soil C stocks in this current study are in the same range as those measured by Berihu et al., (2017), who reported soil C stocks in four different land cover categories in Ethiopia (i.e. dense forest had 48.5 t ha⁻¹, open forest 38.60 t ha⁻¹, farmland 32.45, and grassland 40.09 t ha⁻¹ of up to 40 cm depth) which was significantly higher than grassland open forest and farmland, although differences exist in the classification of the forest from the current study which focused on the time taken by the secondary forest under-recovery. The findings of Berihu et al., (2017) indicate that there was no significant difference in soil C stocks by elevation (upper and lower), and soil C concentration significantly declined by depth (i.e. from upper elevation 44.89 t ha⁻¹ and for the lower was 34.95 t ha⁻¹) and the C/N Ratio in open/dense forest (i.e. open forest was 6.92:1 for the dense forest was 7.29:1) were not statistically significant as found in the current study.

This study's findings are also comparable with the findings reported by Tolessa and Senbeta, (2018) who reported soil C stocks for Jibat and Chillimo forest fragments in Ethiopia with different soil C and N stocks. The current study found that soil C and N stocks were not with the DI across all the soil, although the reported findings from a semi-arid watershed in northern Ethiopia (Gelaw et al., 2014) indicate that soil C and N stocks response to land-use change mainly rainfed crop production (RF), agroforestry based crop production (AF), open communal pasture (OP), silvopasture (SP) and irrigation-based fruit production (IR) were estimated from 0–5, 5–10, 10–20 and 20–30 cm soil layers showed a significant relationship. Generally, both magnitude and difference in soil C and N concentrations showed a decreasing trend with depth within and among most land uses in line with the reported pattern (Yimer et al., 2007). Soil C and N concentrations were also highly correlated in all land use and depths.

Soil bulk density, SOM, pH, and C:N ratio have shown variation across the soil cores and forest blocks. The current study findings conformed with the previous estimates of the soil properties in the Mau forest complex for example Wanyama et al., (2018) with a reported bulk density of $0.65 \pm 0.03 \text{ g/cm}^{-3}$ in the forest area that classified as smallholder affected, while forest adjacent to tea plantation was reported at $0.60 \pm 0.03 \text{ g/cm}^{-3}$ for the topsoil which was comparable with the bulk density of $0.66 \pm 0.13 \text{ g/cm}^{-3}$ for the topsoil (0 – 10 cm) in the current study. Soil pH in the current study was $5.33 \pm 0.82 \text{ g/cm}^{-3}$ for topsoil which was also comparable with $5.1 \pm 0.0 \text{ g/cm}^{-3}$ from the previous study in the Mau forest complex. Similar patterns of the C:N ratio were also observed across the forest blocks without significant differences. SOM, pH, and C:N ratio have demonstrated significant differences in topsoil between the blocks i.e., C:N ratio of 11.34 ± 2.41 for this current study compared to 10.8 ± 0.1 as reported in the study of Wanyama et al., (2018).

The role of SOM and soil properties influencing the soil C stocks has been well documented for example in West African landscapes (Saiz et al., 2012), however, in the current study, the approach focused on the different recovery periods based on the time when the forest recovery period other than the conversion of land from other land uses to the forest and vice versa with the results indicating that SOM was not related to the soil C. In this study, it was found that SOM was highly correlated with C:N ratio, and disturbance index across all soil cores, while bulk density was correlated with N concentration (%) in the sub-layer only i.e. 10 – 30 cm and 30 – 60 cm which conforms with the findings of Liu et al., (2016) who reported a similar correlation of bulk density and soil N concentration (%).

4.4.2. Determination of soil organic carbon and nitrogen stocks

With the assessment of contrasting soil chemical and physical properties, this study established a model to predict the soil C and N in the Mau forest complex by a combination of variables notable the DI, pH, and AGC offering the best fit. The study results show that soil C and N stocks were not significantly affected by the disturbance processes over time. From the six models that were fitted, the current study further revealed that with forest age, disturbance index did not influence the soil C and N, with both interactions and without interaction between the DI and soil pH, AGC. Although disturbance has been reported to have influence on the soil C stocks especially in the topsoil particularly if forest is converted to other land uses like agriculture (Cai and Chang, 2020; Mayer et al., 2020). Previous studies such as Gebeyehu et al., (2019) carried out in Afromontane forest in northeastern Ethiopia have reported a correlation between soil C and N stocks, and AGC. However, it is challenging to find indisputable evidence on the role of disturbance, pH, and AGC especially given that the predictor used in the model may be correlated with other variables hence it is not clear whether

or not the relationships are causative (Saiz et al., 2012). Soil properties (pH, SOM, N) were found to vary across land cover types in the semi-arid areas in Eastern Africa (Egeru et al., 2019), yet this does not represent the vegetation recovery process in the tropical montane forests following deforestation and forest clearance.

Tropical montane forest soils C stocks are influenced by the soil C in the roots resulting from the photosynthetic processes (Kuzyakov and Gavrichkova, 2010) that also determines the AGC, this explains the correlation between the AGC and the rooting systems that are correlated with the SOM (%) and consequently influence the soil C and N stocks. This study found out that soil C and N did not significantly vary with the recovery stages contrary to the AGC where at the age of 25 - 30 years the AGC attained the level of the old growth secondary forest and was significantly different from the youngest secondary forest. Previously similar observations were reported in the African tropical forests of Tshuapa province in the Democratic Republic of the Congo (DRC) which is a semi-deciduous lowland rain forest (Bauters et al., 2019), although the current study was conducted in a montane tropical forest in East Africa. The comparison of AGC with soil C stocks in this study indicated that while AGB and consequently AGC recovers and increases to the amount equalling to the old growth secondary forest, soil C stocks did not change with the recovery stages (Fig.4-4).

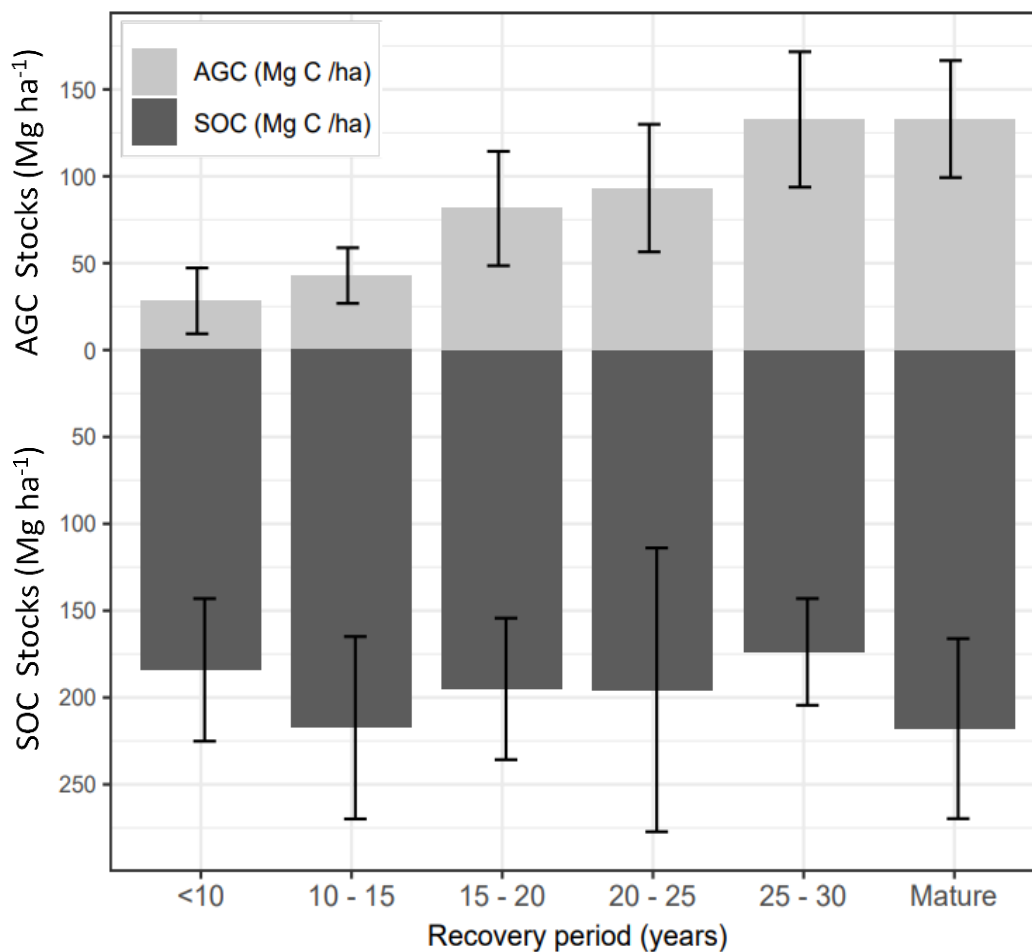


Figure 4-5: Variation of aboveground carbon (AGC) and soil organic carbon (SOC) along the forest recovery periods in the Mau forest complex. Error bars represent standard deviations.

The findings of this study suggest that soil C and N stocks did not change during the recovery regimes. Mean C stocks ranged from $173.8 \pm 30.7 \text{ Mg C ha}^{-1}$ to $217.9 \pm 51.8 \text{ Mg C ha}^{-1}$ across the recovery period (Fig. 4-5) within the 0 – 60 cm depth. Equally, soil N stocks ranging from $16.4 \pm 4.8 \text{ Mg N ha}^{-1}$ in <10 years forest recovery regime to $20.1 \pm 3.9 \text{ Mg N ha}^{-1}$ in the old growth secondary forest Complex in Kenya. The non-significant change in soil C and N stocks over different recovery periods in the Mau forest complex from this study provide new information which contributes to knowledge on how the soil C and N stocks in the montane forests of East Africa respond to forest clearance and the following recovery stages which had not been widely reported in the

montane tropical forest as similar studies focus on the tropical lowland forests (Moore et al., 2018).

The findings in this current study provide knowledge that has been lacking for the montane tropical forests of East Africa which demonstrate how the soil C and N stocks do not change with forest cover changes resulting from forest clearance and other forms of degradation. The study provides the distribution of the forest soil properties i.e. organic matter content across the soil profiles, bulk density, and pH which influence critical soil functions and provide indicators for awareness rising relating to land and soil degradation (Lorenz, Lal, and Ehlers, 2019). The findings on soil C, N, pH, SOM, and DI can be used to identify which of the soil properties can be managed to retain soil C and N stocks (Bai et al., 2021). This study also provides information on the tropical montane forests of East Africa such as soil C and N stocks from the youngest forest ($184.1 \pm 41.0 \text{ Mg C ha}^{-1}$) and the old-growth secondary forest ($217.9 \pm 51.8 \text{ Mg C ha}^{-1}$), the relationship between the various soil physical and chemical properties such as BD, SOM, pH and the ongoing disturbance processes especially; firewood collection, charcoal burning, logging, grazing and elephant damage to predict soil C and N stocks in forested montane forests.

These results in the current study indicate that soil C and N stocks do not change with the recovery period that was observed as shown in Tab. 4-1, which suggest that the soil C and N requires much more time to recover to the level and magnitude of the old-growth primary forests. The results of this study are limited to up to 60 cm soil profile, it should be noted that the soil C and N dynamics may vary or decrease with the soil depth (Xu, Pan, Johnson, and Plante, 2016). The current study did not include the

carbon in the plant roots for the live trees as they can increase decomposition which influences soil C and N stocks (Adamczyk et al., 2019; J. A. M. Moore et al., 2015).

4.5. Conclusion

Understanding the recovery rate and process of soil organic carbon recovery and stocks from the tropical montane forest has been a challenge yet these montane forests act as reservoirs of soil C. The current study determined the forest soil C and N stocks within different recovery stages following clearance and disturbance processes in the Mau forests complex which have not been studied previously. The findings further revealed that soil properties were stable and did not significantly vary across the recovery stages. The findings can further be used for designing management strategies for improving the soil nutrients and increasing the sequestration of soil C, designing forest restoration plans in terms of tree species can be supported as well as designing policies for the management of the tropical montane forests at the national level.

5. GENERAL DISCUSSION AND CONCLUSION



A recovering forest following disturbance with shrubs and bushes with visible remnant trees (fire) in Western Mau (a), moderate mature forest (b – d) with numerous small trees (saplings). The Photographs were taken from the Mau forest Complex during the field work in March 2019.

5.1. Discussion and conclusion

Tropical forests in sub-Saharan Africa are expected to be more vulnerable to clearance and loss due to the rapidly growing population which increases the demand for land to extend subsistence farming (Gibbs et al., 2010). The tropical montane forests of East Africa that are characterized by rich fertile volcanic soils provide a feasible option for the local communities to expand and increase food production to support the population. This chapter provides a synthesis of the findings and assesses the relevance of the findings for planning for the management and restoration of tropical montane forests.

5.2. Summary of the research findings

This section provides the summary of the findings from the chapters of this thesis that assessed the rate of forest cover changes due to deforestation, rate of recovery of the aboveground biomass and species, and how the effects on soil carbon and nitrogen stocks following clearance in the Mau forest Complex and how the results contribute to the knowledge on the tropical montane forests of East Africa.

5.2.1. Recovery of the aboveground biomass, species diversity, and richness

Chapter 2 of this thesis identified areas that were cleared and undergoing recovery. From these areas that were identified as recovering and intact, the study established 47 forest plots of 20 x 50-meter plots (0.1 ha plots) to assess the rate of AGB and species richness and diversity recovery. It was found that AGB varied significantly between the recovery periods for example; AGB measured from the youngest secondary forest of less than 10 years of age was $238 \pm 26 \text{ Mg ha}^{-1}$ and was significantly different from the old growth secondary forest with a mean AGB of $318 \pm$

78 Mg ha⁻¹. The measured AGB could be associated with the pan tropical allometric model used as the global models have been reported to underestimate AGB in young forest and overestimate AGB in mature forests (Novotný, Navrátilová, Janoutová, Oulehle, and Homolová, 2020), however the findings of Novotny et al (2020) were tested in a temperate forest dominated by Norway spruce as opposed to the current study area which is characterised by various species as well as remnant trees following disturbance. Stem density within the different recovery stages was not significantly different within the different recovery stages especially, in the youngest secondary forest (less than 10 years of age), the stem density showed no significant difference across the different recovery stages ranging from the youngest secondary forest (Less than 10 years) and the oldest old growth secondary forest. Species diversity and richness indices did not vary with the recovery stages. The research found out that AGB recovers rapidly in the first 20 years following forest clearance at an annual rate of 6.4 Mg ha⁻¹. After 20 years, the recovery rate slows down to 4.2 Mg ha⁻¹ to attain the level of AGB measured in the old growth secondary forest. The rate of recovery found in the current study is comparable to the redefined IPCC default values by Requena Suarez et al., (2019) for African mountain systems, however, according to Cook-Patton et al., (2020) the reported IPCC values underestimate the aboveground carbon estimation by 53% in the tropics. The current study revealed that species recovery across the Mau forest was slow and did not show significant change during the various recovery stages. The PERMANOVA results revealed a significant variation within the recovery periods with r^2 of 0.88, $p < 0.0001$. A total of 60 tree species were identified from 39 families, in the youngest secondary forest, *Neoboutonia macrocalyx* (*Euphorbiaceae*) was the most dominant species recorded during the field inventory, which composed of 36.3% of all the species observed,

identified and recorded in the <10, 15, and 25 years old secondary forests, while *Tabernaemontana stapfiana* which is an endangered species according to the Botanic Gardens Conservation International (BGCI) and IUCN SSC Global Tree Specialist Group (2019) was the most dominant in the 20, 30 and the old growth secondary forest recovery stages.

5.2.2. Effects of recovery on soil C and N stocks

From the plots 47 plots that were established in the Mau forest complex, the study collected soil samples from 0 – 10 cm, 10 – 30 cm, and 30 - 60 cm depths to determine the response of soil C and N stocks to the recovery process as indicated in Chapter 4 of this thesis. Soil C and N stocks did not significantly change with the recovery process in the Mau Forest Complex. The current study revealed that, much as soil C stocks were not significantly different across the recovery stages with an average of $184.1 \pm 41 \text{ Mg C ha}^{-1}$ in the youngest secondary forest and $217.9 \pm 51.8 \text{ Mg C ha}^{-1}$, while AGC was significantly different between the young secondary forest i.e., $28.3 \pm 18.9 \text{ Mg C ha}^{-1}$ and $132.9 \pm 33.7 \text{ Mg C ha}^{-1}$ for the old growth secondary forest as shown in Fig. 4-5. The mean soil C in this study is in line with the findings by Ramos Scharrón, Castellanos and Restrepo, (2012) who reported a soil C of $229.00 \text{ Mg C ha}^{-1}$ following landslide disturbance in a tropical montane ecosystem in Guatemala,

Chapter 4 of this thesis also examined the relationship between forest recovery and changes in soil physical and chemical properties mainly bulk density, SOM, pH, C, and N concentrations in the Mau forest complex. The current study shows that soil C stocks in the youngest secondary forest were $184.1 \pm 41 \text{ Mg C ha}^{-1}$ which was not significantly different from the soil C measured from the old growth secondary forest with $217.9 \pm 51 \text{ Mg C ha}^{-1}$, N stocks ranged from $16.4 \pm 4.8 \text{ Mg N ha}^{-1}$ in the youngest

secondary forest to 20.1 ± 3.9 Mg N ha⁻¹ in the old growth secondary forest. Mean bulk density was 0.9 ± 0.2 g/cm⁻³ for the youngest secondary forest (less than 10 years of age) and 0.8 ± 0.1 g/cm⁻³ for the old growth secondary forest. The soil bulk density across all the recovery regimes did not vary significantly and was not significantly correlated with the soil C and N concentrations across all the recovery stages as well as the soil profile. Soil pH ranged from medium acidic to slightly acidic, although not significantly different within the recovery stages, for example, pH of 5.5 ± 0.7 in the youngest forest and 5.1 ± 0.8 in the old growth secondary forest and was not significantly different across the recovery stages. However, soil pH was significantly correlated with the disturbance index, SOM, and BD. Soil Organic Matter (SOM) in the Mau forest complex did not also significantly vary with 15.3 ± 4.4 (%) in the youngest secondary forest and 15.9 ± 2.2 (%) for the old growth secondary forest. Soil BD, pH, SOM, and C:N ratio however varied significantly with the different depths and blocks. Bulk density across the forest blocks for the 0 – 10 cm and 30 – 60 cm were not significantly different; however, variations were observed in the 10 – 30 cm depths. SOM varied significantly between the different soil profiles. While soil pH and C:N ratio varied significantly within the three soil depths. Although the soil pH and BD in this current study did not vary with recovery stages within the forest, the results were in line with measured pH and BD for forest by Wanyama et al., (2018; 2019) and Owuor et al., (2018) who reported soil pH of 6.60 ± 0.10 and bulk density of 0.65 ± 0.03 g/cm⁻³ in the forest in 0 – 5 cm soil depth, soil pH of 5.70 ± 0.10 and BD of 0.79 ± 0.02 g/cm⁻³ in the forest in 20 – 30 cm depth. The soil C and N concentrations in this current study i.e. 4.6 ± 0.70 (%) and 0.4 ± 0.1 (%) respectively were also comparable with those reported by Arnhold et al., (2015) in the Lambwe Valley in Kenya i.e. 5.9 and

0.42% for C and N, respectively, although Lambwe Valley is not a Montane forest ecosystem.

Soil BD and SOM were correlated with a Pearson correlation coefficient of $r = -0.41$; $p < 0.05$, soil pH was also correlated with BD with $r = 0.37$; $p < 0.05$, and with SOM, $r = -0.44$; $p < 0.05$, there was also a significant correlation between disturbance index and pH with $r = 0.53$; $p < 0.05$. Other significant correlations were between C (%) and (N%) with $r = 0.79$, $p < 0.05$ as well as C:N Ratio and N (%) with $r = 0.56$, $p < 0.05$. Soil properties that were not correlated were selected as the proxy variable to be used in the model for determining the effects of the recovery period on the soils.

This study provides the amount of soil C and N stocks that revealed that the soil C and N are not significantly affected by clearance and disturbance processes such as forest fires, fuelwood collection, grazing (livestock), elephant damage, logging, and charcoal burning. Similar studies reported 68 Mg ha^{-1} of soil C from 0 – 30 cm soil depth in the Bwindi highlands in western Uganda (Twongyirwe et al., 2013). While previous studies compared the soil C in the forest lands with soil C in other Land use types or plantations for example (Omoro et al., 2013), this study assessed the dynamics with different forest recovery stages, with the estimates in the forest area that was comparable with the other measurements within the indigenous forests in Kenya.

Although there was no significant variation in the soil C stocks from different recovery stages, the amount of soil C measured from the tropical montane forest in the Mau forest complex in Kenya are comparable to the amount of soil C measured in other montane forests at both continental and global level for example in the current study the mean soil C was $217.90 \pm 51.80 \text{ Mg C ha}^{-1}$ which is comparable with soil C of $223.70 \text{ Mg C ha}^{-1}$ measured by Berihu et al., (2017) in northern Ethiopia, 217.60 Mg

C ha⁻¹ for altitude ranging between 900 -1870 m.a.s.l. from 0 – 100 cm depth in Himalayas reported by Tashi et al., (2016) and soil C stocks ranging from 106.00 ± 7.00 – 204.00 ± 27.00 Mg C ha⁻¹ between elevation of 1050 – 3060 m.a.s.l in tropical mountain forests of South Ecuador with no trend between 1050 – 2380 m.a.s.l but higher value close to 3060 m as reported by Moser et al., (2011) The insignificant difference in soil C and N in relation to recovery time could indicate the need for a longer recovery period after forest clearance to observe a change in soil C, especially as has been reported by (Xiaoju Liu and Pan, 2019) who reported 43 years period required for recovery of soil C following fires.

The current study found that most soil physical and chemical properties were not statistically significant across the recovery stages. Although there existed a correlation between some of the properties, hence, were selected proxy variables based on their correlation coefficients to avoid the causation effects on the models for assessing the effects of recovery on the soil C and N in the Mau forest complex.

5.2.3. Limitations of the study and policy planning implications

In this study, the forest cover change period was limited to the available remote sensing data to estimate the age of the forest. This means that it was not possible to establish the age of the forest that existed before 1984 periods until 2017 hence a shift in the basis for analysis. Reliance on Landsat satellite data would introduce the limitations of Landsat imagery and challenges associated with cloud cover on the imagery and 30 m x 30 m resolution. Future studies could integrate the findings from previous surveys (aerial photography) before the launch of Landsat and newly introduced sensors for example the European Space Agency (ESA's) sentinel imagery which offers higher resolution (up to 10 m x 10 m resolution).

The assessment of AGB, AGC, soil C, and N stocks was only limited to the 3 blocks of the Mau forest complex, this limited the findings of this study to only the 3 blocks that were surveyed. However, other blocks of Mau forest may have different forms of interaction with the neighbouring forest blocks. The adjacent communities to the forest also impact the forest-based on their interaction with the forest. Future studies would incorporate the assessment of remnant trees following disturbance (forest clearance), rate of mortality, and biomass in the litter and dead trees. Soil property assessment was only undertaken to the depth of 60 cm within each plot that was surveyed (n = 47), hence it is not clear how the soil cores beyond 60 cm depth respond to the recovery of the montane forest. Although previous studies report that there is not much soil variation in C and N stocks in the deeper soil cores.

The findings from this study provide information on the current state of the forest i.e., structure AGB and AGC, forest tree species, and soil C and N stocks that can be used as the basis for designing the policies that ensure sustainable and effective management of the Montane tropical forests. Enable effective restoration programs and design policies that are participatory in nature to involve the local communities in the management and protection of the forest ecosystem. The information regarding areas where deforestation took place and forest clearance can be used to plan for restoration activities in terms of species that can be introduced depending on the soil characteristics that have been reported in this study (chapter 4), protection plan based on the rate of clearance (chapter 2).

5.2.1. Relevance of the study and Future work

The results of the study offer relevant insights to the changes in the forest cover to the local, national, and international stakeholders. The local authorities can visualize how

the forest cover has changed over time as a result of interaction with the local communities. At the national scale, the government can use the results of the study to inform the policy development process to establish enabling policies that can help to curb the identified losses due to deforestation and clearance. Deforestation has been reported to have contributed to cost of the economy especially in Kenya. At the global scale, the findings of the study contribute to the gap in the knowledge on tropical montane ecosystems and provide information regarding the amount of C stocks from the Tropical montane forests in East Africa which can be used by the programs like the UN-REDD and UNFCCC for the appropriate climate action planning.

The trend in the forest cover change based on the historical data can then be used to relate with how the authorities in Kenya have moved from the historical and colonial approaches to the conservation, allocation of the forest land by the past governments and how the effects of these political actions could be reversed following the appropriate restoration and management plans that maybe adopted.

The results can also be used for the planning of the restoration activities by different stakeholders and authorities like conservationists, researchers for the planning purposes. The limitation and recommendations for the future work as a result of the finding of the study can help to guide the future studies in the tropical montane forests of East Africa.

The findings of the study especially the rate of recovery of the forest Aboveground Biomass and Carbon stocks as well as the Soil C and N stocks can be used to determine the overall C budget of the whole Mau forest Complex.

5.3. Conclusion

The study revealed the extent and rate of forest cover change (loss and recovery) following forest clearance and degradation in the Mau forest complex. The study also revealed the changes in forest structure and composition (mainly AGB, species richness, and diversity) following deforestation and disturbance processes and provided the quantification of forest soil C and N in the Montane tropical forest. Below are the main conclusions resulting from the study.

- Forest cover was lost to deforestation in both Mau forest complex and Elgon at a rate of $-0.88\% \text{ yr}^{-1}$ and $-1.03\% \text{ yr}^{-1}$ respectively during the period between 1984 and 2017 equating to the total area of 88,493 ha (21.9%) and 27,201 ha (12.5%) of the Mau forest complex and Mt Elgon forest respectively. During the same period, the two montane forests experienced recovery (forest gain) of 75,438 (18.6%) for the Mau forest complex and 59,047 ha (27.2%) for Mt Elgon forest. Areas, where these changes occurred, were also mapped and the time when the loss or recovery happened was also determined from the available remote sensing data (Chapter 2).
- The research also revealed the amount of AGB from the different recovery periods, the rate at which the Mau forest complex recovers AGB, and the rate of species recovery was also established. The study found that there was a significant difference in AGB between the youngest secondary forest (<10 years) and moderately mature 20 – 25 years of age and old growth secondary forest. It was further noted that the AGB recovers rapidly in the first 20 years following forest clearance and then the rate slows as the forest matures into the old growth secondary stage. AGB would require 25 years to be indistinguishable from the AGB in the oldest old growth secondary forest. Species recovery did not show any

significant change between the youngest secondary forest and the old growth secondary forest (*Chapter 3*).

- The study also quantified soil C and N across different recovery regimes and revealed that soil C and N stocks were static and did not vary significantly with recovery stages. Soil C in this study could be predicted using the AGC, pH, and the disturbance index. The results from the analysis of soil C and N dynamics suggest that it could take a longer period for soil C to be altered by forest clearance and recovery cycles in the Mau forest complex (*Chapter 4*).

REFERENCES

- Achard, F., Beuchle, R., Mayaux, P., Stibig, H. J., Bodart, C., Brink, A., Carboni, S., Desclee, B., Donnay, F., Eva, H. D., Lupi, A., Rastisluv, R., Seliger, R., Simonetti, D. (2014). Determination of tropical deforestation rates and related carbon losses from 1990 to 2010. *Global Change Biology*, 20(8), 2540–2554. <https://doi.org/10.1111/gcb.12605>
- Achard, F., Eva, H. D., Stibig, H.-J., Mayaux, P., Gallego, J., Richards, T., and Malingreau, J.-P. (2002). Determination of deforestation rates of the world's humid tropical forests. *Science* (New York, N.Y.), 297(5583), 999–1002. <https://doi.org/10.1126/science.1070656>
- Acharya, B. K., Chettri, B., and Vijayan, L. (2011). Distribution pattern of trees along an elevation gradient of Eastern Himalaya, India. *Acta Oecologica*, 37(4), 329–336. <https://doi.org/10.1016/J.ACTAO.2011.03.005>
- Adamczyk, B., Sietiö, O. M., Straková, P., Prommer, J., Wild, B., Hagner, M., Pihlatie, M., Fritze, H., Richter, A., Heinonsalo, J. (2019). Plant roots increase both decomposition and stable organic matter formation in boreal forest soil. *Nature Communications*, 10(1). <https://doi.org/10.1038/s41467-019-11993-1>
- Ahrends, A., Bulling, M. T., Platts, P. J., Swetnam, R., Ryan, C., Doggart, N., Peter M., Hollingsworth, P. M., Marchant, R., Balmford, A., Harris, D, J., Gross-Camp, N., Sumbi, P., Munishi, P., Madoffe, S., Mhoro, B., Leonard, C., Bracebridge, C., Doody, K., Wilkins, V., Owen, N., Marshall, A, R., Schaafsma, M., Pfliegner, K., Jones, T., Robinson, J., Topp-Jørgensen, E., Brink, H., Burgess, N. D. (2021). Detecting and predicting forest degradation:

- A comparison of ground surveys and remote sensing in Tanzanian forests. *Plants People Planet*, 3(3), 268–281. <https://doi.org/10.1002/ppp3.10189>
- Al-shammary, A. A. G., Kouzani, A. Z., Kaynak, A., Khoo, S. Y., Norton, M., and Gates, W. (2018). Soil Bulk Density Estimation Methods: A Review. *Pedosphere*, 28(4), 581–596. [https://doi.org/10.1016/S1002-0160\(18\)60034-7](https://doi.org/10.1016/S1002-0160(18)60034-7)
- Albertazzi, S., Bini, V., Lindon, A., and Trivellini, G. (2018). Relations of power driving tropical deforestation: a case study from the Mau Forest (Kenya). *Belgeo*, (2). <https://doi.org/10.4000/belgeo.24223>
- Alberto Quesada, C., Paz, C., Oblitas Mendoza, E., Lawrence Phillips, O., Saiz, G., and Lloyd, J. (2020). Variations in soil chemical and physical properties explain basin-wide Amazon forest soil carbon concentrations. *SOIL*, 6(1), 53–88. <https://doi.org/10.5194/soil-6-53-2020>
- Araia, M. G., Chirwa, P. W., and Assédé, E. S. P. (2020). Contrasting the effect of forest landscape condition to the resilience of species diversity in a human modified landscape: Implications for the conservation of tree species. *Land*, 9(1), 1–19. <https://doi.org/10.3390/land9010004>
- Arias-Navarro, C., Díaz-Pinés, E., Klatt, S., Brandt, P., Rufino, M. C., Butterbach-Bahl, K., and Verchot, L. V. (2017). Spatial variability of soil N₂O and CO₂ fluxes in different topographic positions in a tropical montane forest in Kenya. *Journal of Geophysical Research: Biogeosciences*, 122(3), 514–527. <https://doi.org/10.1002/2016JG003667>
- Arias-Navarro, C., Díaz-Pinés, E., Zuazo, P., Rufino, M. C., Verchot, L. V., and Butterbach-Bahl, K. (2017). Quantifying the contribution of land use to N₂O, NO and CO₂ fluxes in a montane forest ecosystem of Kenya.

- Biogeochemistry*, 134(1–2), 95–114. <https://doi.org/10.1007/s10533-017-0348-3>
- Arjasakusuma, S., Kamal, M., Hafizt, M., and Forestriko, H. F. (2018). Local-scale accuracy assessment of vegetation cover change maps derived from Global Forest Change data , ClasLite , and supervised classifications : case study at part of Riau Province , Indonesia. *Applied Geomatics*, 10(3), 205–217. <https://doi.org/10.1007/s12518-018-0226-2>
- Arnhold, S., Otieno, D., Onyango, J., Koellner, T., Huwe, B., and Tenhunen, J. (2015). Soil properties along a gradient from hillslopes to the savanna plains in the Lambwe Valley, Kenya. *Soil and Tillage Research*, 154, 75–83. <https://doi.org/10.1016/j.still.2015.06.021>
- Asner, G. P. (2013). Geography of forest disturbance. *Proceedings of the National Academy of Sciences of the United States of America*, 110(10), 3711–3712. <https://doi.org/10.1073/pnas.1300396110>
- Asner, G. P., Knapp, D. E., Balaji, A., and Paez-Acosta, G. (2009). Automated mapping of tropical deforestation and forest degradation: CLASlite. *Journal of Applied Remote Sensing*, 3(1), 033543. <https://doi.org/10.1117/1.3223675>
- Ayuyo, O. I., and Sweta, L. (2014). Land Cover and Land Use Mapping and Change Detection of Mau Complex in Kenya Using Geospatial Technology. *International Journal of Science and Research*, 3(3). Retrieved from www.ijsr.net
- Bai, J., Zong, M., Li, S., Li, H., Duan, C., Feng, Y., Peng, C., Zhang, X., Sun, D., Lin, C., Shi, Y., Zheng, G., Wang, H., Liu, D., Li, F., Huang, W. (2021). Nitrogen, water content, phosphorus and active iron jointly regulate soil organic carbon

- in tropical acid red soil forest. *European Journal of Soil Science*, 72(1), 446–459. <https://doi.org/10.1111/ejss.12966>
- Bailis, R., Drigo, R., Ghilardi, A., and Masera, O. (2015). The carbon footprint of traditional woodfuels. *Nature Climate Change*, 5(3), 266–272. <https://doi.org/10.1038/nclimate2491>
- Bakx, W., Janssen, L., Schetselaar, E., Tempfli, K., and Tolpekin, V. (2012). The core of GIScience: a systems-based approach (V. Tolpekin and A. Stein, Eds.). Enschede: *The International Institute for Geo-Information Science and Earth Observation (ITC)*, Hengelosestraat 99, Enschede, The Netherlands.
- Baldyga, T. J., Miller, S. N., Driese, K. L., and Gichaba, C. M. (2007). Assessing land cover change in Kenya's Mau Forest region using remotely sensed data. *African Journal of Ecology*, 46(1), 46–54. <https://doi.org/10.1111/j.1365-2028.2007.00806.x>
- Bauer, M., and Albrecht, H. (2020). Vegetation monitoring in a 100-year-old calcareous grassland reserve in Germany. *Basic and Applied Ecology*, 42, 15–26. <https://doi.org/10.1016/J.BAAE.2019.11.003>
- Bauters, M., Moonen, P., Summerauer, L., Doetterl, S., Wasner, D., Griepentrog, M., Mumbanza, F. M., Kearsley, E., Ewango, C., Boyemba, F., Six, J., Muys, B., Verbist, B., Boeckx, P., Verheyen, K. (2021). Soil Nutrient Depletion and Tree Functional Composition Shift Following Repeated Clearing in Secondary Forests of the Congo Basin. *Ecosystems*. <https://doi.org/10.1007/s10021-020-00593-6>
- Bauters, M., Vercleyen, O., Vanlauwe, B., Six, J., Bonyoma, B., Badjoko, H., Hubau, W., Hoyt, A., Boudin, M., Verbeeck, H., Boeckx, P. (2019). Long-term recovery of the functional community assembly and carbon pools in an

- African tropical forest succession. *Biotropica*, 51(3), 319–329.
<https://doi.org/10.1111/btp.12647>
- Bawa, K. S., and Hadley, M. (1991). Reproductive ecology of tropical forest plants. The role of disturbance in the regeneration. In *CRC Press*.
- Becknell, J. M., Kissing Kucek, L., and Powers, J. S. (2012, July 15). Aboveground biomass in mature and secondary seasonally dry tropical forests: A literature review and global synthesis. *Forest Ecology and Management*, Vol. 276, pp. 88–95. <https://doi.org/10.1016/j.foreco.2012.03.033>
- Bentsi-Enchill, F., Dampney, F. G., Pappoe, A. N. M., Ekumah, B., and Akotoye, H. K. (2022). Impact of anthropogenic disturbance on tree species diversity, vegetation structure and carbon storage potential in an upland evergreen forest of Ghana, West Africa. *Trees, Forests and People*, 8(March), 100238. <https://doi.org/10.1016/j.tfp.2022.100238>
- Berihu, T., Girmay, G., Sebhatleab, M., Berhane, E., Zenebe, A., and Sigua, G. C. (2017). Soil carbon and nitrogen losses following deforestation in Ethiopia. *Agronomy for Sustainable Development*, 37(1). <https://doi.org/10.1007/s13593-016-0408-4>
- BETA. (2019). National Equestrian Survey 2015 shows increased consumer spending. Retrieved August 28, 2019, from *British Equestrian Trade Association (BETA)* website: <http://www.beta-uk.org/pages/news-amp-events/news/national-equestrian-survey-2015-shows-increased-consumer-spending.php>
- BirdLife International. (2017). BirdLife International. Retrieved September 3, 2017, from Important Bird Areas factsheet: Mau forest complex. website: <http://datazone.birdlife.org/site/factsheet/6441>

- Boitt, M. K. (2016). Impacts of Mau Forest Catchment on the Great Rift Valley Lakes in Kenya. *Journal of Geoscience and Environment Protection*, 4(4), 137–145. <https://doi.org/10.4236/gep.2016.45014>
- Bolker, B. M., Brooks, M. E., Clark, C. J., Geange, S. W., Poulsen, J. R., Stevens, M. H. H., and White, J. S. S. (2009, March). Generalized linear mixed models: a practical guide for ecology and evolution. *Trends in Ecology and Evolution*, Vol. 24, pp. 127–135. <https://doi.org/10.1016/j.tree.2008.10.008>
- Bonner, M. T. L., Schmidt, S., and Shoo, L. P. (2013). A meta-analytical global comparison of aboveground biomass accumulation between tropical secondary forests and monoculture plantations. *Forest Ecology and Management*, 291, 73–86. <https://doi.org/10.1016/J.FORECO.2012.11.024>
- Brandt, M., Rasmussen, K., Peñuelas, J., Tian, F., Schurgers, G., Verger, A., Mertz, O., Palmer, J. R. B., Fensholt, R. (2017). Human population growth offsets climate-driven increase in woody vegetation in sub-Saharan Africa. *Nature Ecology and Evolution*, 1(4), 0081. <https://doi.org/10.1038/s41559-017-0081>
- Brandt, P., Hamunyela, E., Herold, M., de Bruin, S., Verbesselt, J., and Rufino, M. C. (2018). Sustainable intensification of dairy production can reduce forest disturbance in Kenyan montane forests. *Agriculture, Ecosystems and Environment*, 265, 307–319. <https://doi.org/10.1016/j.agee.2018.06.011>
- Bray, J. R., and Curtis, J. T. (1957). An Ordination of the Upland Forest Communities of Southern Wisconsin. *Ecological Monographs*, 27(4), 325–349. <https://doi.org/10.2307/1942268>
- Brienen, R. J. W., Phillips, O. L., Feldpausch, T. R., Gloor, E., Baker, T. R., Lloyd, J., Lopez-Gonzalez, G., Monteagudo-Mendoza, A., Malhi, Y., Lewis, S. L., Vásquez Martínez, R., Alexiades, M., Álvarez Dávila, E., Alvarez-Loayza, P.,

- Andrade, A., Aragaõ, L. E.O.C., Araujo-Murakami, A., Arets, E. J.M.M., Arroyo, L., Aymard C., G. A., Bánki, O. S., Baraloto, C., Barroso, J., Bonal, D., Boot, R. G.A., Camargo, J. L.C., Castilho, C. V., Chama, V., Chao, K. J., Chave, J., Comiskey, J. A., Cornejo Valverde, F., Da Costa, L., De Oliveira, E. A., Di Fiore, A., Erwin, T. L., Fauset, S., Forsthofer, M., Galbraith, D. R., Grahame, E. S., Groot, N., Hérault, B., Higuchi, N., Honorio Coronado, E. N., Keeling, H., Killeen, T. J., Laurance, W. F., Laurance, S., Licona, J., Magnussen, W. E., Marimon, B. S., Marimon-Junior, B. H., Mendoza, C., Neill, D. A., Nogueira, E. M., Núñez, P., Pallqui Camacho, N. C., Parada, A., Pardo-Molina, G., Peacock, J., Penã-Claros, M., Pickavance, G. C., Pitman, N. C.A., Poorter, L., Prieto, A., Quesada, C. A., Ramírez, F., Ramírez-Angulo, H., Restrepo, Z., Roopsind, A., Rudas, A., Salomaõ, R. P., Schwarz, M., Silva, N., Silva-Espejo, J. E., Silveira, M., Stropp, J., Talbot, J., Ter Steege, H., Teran-Aguilar, J., Terborgh, J., Thomas-Caesar, R., Toledo, M., Torello-Raventos, M., Umetsu, R. K., Van Der Heijden, G. M.F., Van Der Hout, P., Guimarães Vieira, I. C., Vieira, S. A., Vilanova, E., Vos, V. A., Zagt, R. J. (2015). Long-term decline of the Amazon carbon sink. *Nature*, 519(7543), 344–348. <https://doi.org/10.1038/nature14283>
- Brink, A. B., Bodart, C., Brodsky, L., Defourney, P., Ernst, C., Donney, F., Lupi, A., Tuckova, K. (2014). Anthropogenic pressure in East Africa-Monitoring 20 years of land cover changes by means of medium resolution satellite data. *International Journal of Applied Earth Observation and Geoinformation*, 28, 60–69. <https://doi.org/10.1016/j.jag.2013.11.006>

- Bruijnzeel, L. A., Scatena, F. N., Hamilton, L. S., Bubb, P., and Das, S. (2010). *Tropical Montane Cloud Forests: Science for Conservation and Management*. Cambridge University Press.
- Burnham, Kenneth P., Anderson, D. R. (2002). *Model Selection and Multimodel Inference - A Practical Information-Theoretic Approach* (2nd ed.). <https://doi.org/10.1007/b97636>
- Bussmann, R. W. (2001). Succession and regeneration patterns of East African mountain forests A review. *Systematics and Geography of Plants Geogr. Pl*, 71(71), 959–974. <https://doi.org/10.2307/3668731>
- Bussmann, R. W. (2002). Vegetation Ecology and Regeneration of Tropical Mountain Forests. *In Modern Trends in Applied Terrestrial Ecology* (pp. 195–223). https://doi.org/10.1007/978-1-4615-0223-4_11
- Buyinza, M., and Nabalegwa, M. (2008). Socioeconomic Impacts of Land Degradation in Mid-Hills of Uganda: A Case Study in Mt. Elgon Catchment, Eastern Uganda. *Environmental Research*, 2, 226–231.
- Cai, Y., and Chang, S. X. (2020). Disturbance effects on soil carbon and greenhouse gas emissions in forest ecosystems. *Forests*, 11(3), 1–5. <https://doi.org/10.3390/f11030297>
- Cao, M., and Zhang, J. (1997). Tree species diversity of tropical forest vegetation in Xishuangbanna, SW China. *Biodiversity and Conservation*, 6(7), 995–1006. <https://doi.org/10.1023/A:1018367630923>
- Carr, D. L., Suter, L., and Barbieri, A. (2005). Population Dynamics and Tropical Deforestation: State of the Debate and Conceptual Challenges. *Population and Environment*, 27(1), 89–113. <https://doi.org/10.1007/s11111-005-0014-x>

- Carrière, S. M., Letourmy, P., and McKey, D. B. (2002). Effects of remnant trees in fallows on diversity and structure of forest regrowth in a slash-and-burn agricultural system in southern Cameroon. *Journal of Tropical Ecology*, 18(3), 375–396. <https://doi.org/10.1017/S0266467402002262>
- Cavanagh, C. (2017). Paying for carbon at Mount Elgon: two contrasting approaches at a transboundary park in East Africa. In M. P. Namirembe S, Leimona B, van Noordwijk M (Ed.), *Co-investment in ecosystem services: global lessons from payment and incentive schemes*. Nairobi: (pp. 1–10). Nairobi.
- Ceddia, M. G. (2020). The super-rich and cropland expansion via direct investments in agriculture. *Nature Sustainability*, 3(4), 312–318. <https://doi.org/10.1038/s41893-020-0480-2>
- Chapman, C. A., Galán-Acedo, C., Gogarten, J. F., Hou, R., Lawes, M. J., Omeja, P. A., Sarkar, D., Sugiyama, A., Kalbitzer, U. (2021). A 40-year evaluation of drivers of African rainforest change. *Forest Ecosystems*, 8(1). <https://doi.org/10.1186/s40663-021-00343-7>
- Chave, J., Andalo, C., Brown, S., Cairns, M. A., Chambers, J. Q., Eamus, D., Fölster, H., Fromard, F., Higuchi, N., Kira, T., Lescure, J. P., Nelson, B. W., Ogawa, H., Puig, H., Riéra, B., Yamakura, T. (2005). Tree allometry and improved estimation of carbon stocks and balance in tropical forests. *Oecologia*, 145(1), 87–99. <https://doi.org/10.1007/s00442-005-0100-x>
- Chave, J., Réjou-Méchain, M., Búrquez, A., Chidumayo, E., Colgan, M. S., Delitti, W. B. C., Duque, A., Eid, T., Fearnside, P. M., Goodman, R. C., Henry, M., Martínez-Yrizar, A., Mugasha, W. A., Muller-Landau, H. C., Mencuccini, M., Nelson, B. W., Ngomanda, A., Nogueira, E. M., Ortiz-Malavassi, E., Pélissier, R., Ploton, P., Ryan, C. M., Saldarriaga, J., Vieilledent, G. (2014). Improved

- allometric models to estimate the aboveground biomass of tropical trees. *Global Change Biology*, 3177–3190. <https://doi.org/10.1111/gcb.12629>
- Chave, Jerome, Coomes, D., Jansen, S., Lewis, S. L., Swenson, N. G., and Zanne, A. E. (2009). Towards a worldwide wood economics spectrum. *Ecology Letters*, 12(4), 351–366. <https://doi.org/10.1111/j.1461-0248.2009.01285.x>
- Chave, Jérôme, Muller-Landau, H. C., Baker, T. R., Easdale, T. A., ter Steege, H., and Webb, C. O. (2006). Regional and phylogenetic variation of wood density across 2456 Neotropical tree species. *Ecological Applications: A Publication of the Ecological Society of America*, 16(6), 2356–2367. Retrieved from <http://www.ncbi.nlm.nih.gov/pubmed/17205910>
- Chazdon, R. L., Broadbent, E. N., Rozendaal, D. M. A., Bongers, F., Zambrano, A. M. A., Aide, T. M., Balvanera, P., Becknell, J. M., Boukili, V., Brancalion, P. H. S., Craven, D., Almeida-Cortez, J. S., Cabral, G. A. L., De Jong, B., Denslow, J. S., Dent, D. H., DeWalt, S. J., Dupuy, J. M., Durán, S. M., Espírito-Santo, M. M., Fandino, M. C., César, R. G., Hall, J. S., Hernández-Stefanoni, J. L., Jakovac, C. C., Junqueira, A. B., Kennard, D., Letcher, S. G., Lohbeck, M., N., Martínez-Ramos, M., Massoca, P., Meave, J. A., Mesquita, R., Mora, F., Muñoz, R., Muscarella, R., Nunes, Y. R. F., Ochoa-Gaona, S., Orihuela-Belmonte, E., Peña-Claros, M., Pérez-García, E. A., Piotto, D., Powers, J. S., Rodríguez-Velazquez, J., Romero-Pérez, I. E., Ruíz, J., Saldarriaga, J. G., Sanchez-Azofeifa, A., Schwartz, N. B., Steininger, M. K., Swenson, N. G., Uriarte, M., Van Breugel, M., Van Der Wal, H., Veloso, M.D. M., Vester, H., Vieira, I. C. G., Bentos, T. V., Williamson, G. B., Poorter, L. (2016). Carbon sequestration potential of

- second-growth forest regeneration in the Latin American tropics. *Science Advances*, 2(5), e1501639. <https://doi.org/10.1126/sciadv.1501639>
- Chen, Y., Guerschman, J. P., Cheng, Z., and Guo, L. (2019). Remote sensing for vegetation monitoring in carbon capture storage regions: A review. *Applied Energy*, 240 (2), 312–326. <https://doi.org/10.1016/j.apenergy.2019.02.027>
- Choksi, P. (2019). Examining Patterns and Impacts of Forest Resource Extraction and Forest Degradation in Tropical Dry Forests. <https://doi.org/10.4018/978-1-7998-0014-9.ch009>
- Chrisphine, M. O., Maryanne, A. O., and Mark, B. K. (2015). Assessment of Hydrological Impacts of Mau Forest, Kenya. *Journal of Waste Water Treatment and Analysis*, 07(01), 1–7. <https://doi.org/10.4172/2157-7587.1000223>
- Cohen, W. B., and Goward, S. N. (2004). Landsat's Role in Ecological Applications of Remote Sensing. *BioScience*, 54(6), 535–545. [https://doi.org/10.1641/0006-3568\(2004\)054\[0535:Irieao\]2.0.co;2](https://doi.org/10.1641/0006-3568(2004)054[0535:Irieao]2.0.co;2)
- Cohen, W. B., Healey, S. P., Yang, Z., Zhu, Z., and Gorelick, N. (2020). Diversity of algorithm and spectral band inputs improves landsat monitoring of forest disturbance. *Remote Sensing*, 12(10), 1673. <https://doi.org/10.3390/rs12101673>
- Cohen, W. B., Yang, Z., and Kennedy, R. (2010). Detecting trends in forest disturbance and recovery using yearly Landsat time series: 2. TimeSync - Tools for calibration and validation. *Remote Sensing of Environment*, 114(12), 2911–2924. <https://doi.org/10.1016/j.rse.2010.07.010>

- Cole, L. E. S., Bhagwat, S. A., and Willis, K. J. (2014). Recovery and resilience of tropical forests after disturbance. *Nature Communications*, 5. <https://doi.org/10.1038/ncomms4906>
- Cook-Patton, S. C., Leavitt, S. M., Gibbs, D., Harris, N. L., Lister, K., Anderson-Teixeira, K. J., Briggs, R. D., Chazdon, R. L., Crowther, T. W., Ellis, P. W., Griscom, H. P., Herrmann, V., Holl, K. D., Houghton, R. A., Larrosa, C., Lomax, G., Lucas, R., Madsen, P., Malhi, Y., Paquette, A., Parker, J. D., Paul, K., Routh, D., Roxburgh, S., Saatchi, S., van den Hoogen, J., Walker, W. S., Wheeler, C. E., Wood, S. A., Xu, L., Griscom, B. W. (2020). Mapping carbon accumulation potential from global natural forest regrowth. *Nature*, 585(7826), 545–550. <https://doi.org/10.1038/s41586-020-2686-x>
- Crafford, J., Strohmaier, R., Muñoz, P., Oliveira, T. De, Christian, L. M. W., Burger, A., and Bosch, J. (2012). The Role and Contribution of Montane Forests and Related Ecosystem Services to the Kenyan Economy. In *United Nations Environment Programme (UNEP)*, Nairobi 00100, Kenya. Nairobi.
- Crausbay, S. D., and Martin, P. H. (2016). Natural disturbance, vegetation patterns and ecological dynamics in tropical montane forests. *Journal of Tropical Ecology*, 32(05), 384–403. <https://doi.org/10.1017/S0266467416000328>
- Cuni-Sanchez, A., Sullivan, M. J. P., Platts, P. J., Lewis, S. L., Marchant, R., Imani, G., ... Zibera, E. (2021). High aboveground carbon stock of African tropical montane forests. *Nature*, 596(7873), 536–542. <https://doi.org/10.1038/s41586-021-03728-4>
- Curtis, P. G., Slay, C. M., Harris, N. L., Tyukavina, A., and Hansen, M. C. (2018). Classifying drivers of global forest loss. *Science (New York)*, 361(6407), 1108–1111. <https://doi.org/10.1126/science.aau3445>

- D'Almeida, C., Vörösmarty, C. J., Hurtt, G. C., Marengo, J. A., Dingman, S. L., and Keim, B. D. (2007). The effects of deforestation on the hydrological cycle in Amazonia: a review on scale and resolution. *International Journal of Climatology*, 27(5), 633–647. <https://doi.org/10.1002/joc.1475>
- Dale, V. H., Joyce, L. A., McNulty, S., Neilson, R. P., Ayres, M. P., Flannigan, M. D., ... Wotton, B. M. (2001). Climate Change and Forest Disturbances Climate change can affect forests by altering the frequency, intensity, duration, and timing of fire, drought, introduced species, insect and pathogen outbreaks, hurricanes, windstorms, ice storms, or landslides. *Bioscience*, 51(9), 723–734. [https://doi.org/10.1641/0006-3568\(2001\)051\[0723:CCAFD\]2.0.CO;2](https://doi.org/10.1641/0006-3568(2001)051[0723:CCAFD]2.0.CO;2)
- de la Cruz-Amo, L., Bañares-de-Dios, G., Cala, V., Granzow-de la Cerda, Í., Espinosa, C. I., Ledo, A., ... Cayuela, L. (2020). Trade-Offs Among Aboveground, Belowground, and Soil Organic Carbon Stocks Along Altitudinal Gradients in Andean Tropical Montane Forests. *Frontiers in Plant Science*, 11, 106. <https://doi.org/10.3389/fpls.2020.00106>
- De Marzo, T., Pflugmacher, D., Baumann, M., Lambin, E. F., Gasparri, I., and Kuemmerle, T. (2021). Characterizing forest disturbances across the Argentine Dry Chaco based on Landsat time series. *International Journal of Applied Earth Observation and Geoinformation*, 98, 102310. <https://doi.org/10.1016/j.jag.2021.102310>
- Deklerck, V., De Mil, T., Ilondea, B. A., Nsenga, L., De Caluwé, C., Van den Bulcke, J., ... Hubau, W. (2019). Rate of forest recovery after fire exclusion on anthropogenic savannas in the Democratic Republic of Congo. *Biological Conservation*, 233, 118–130. <https://doi.org/10.1016/j.biocon.2019.02.027>

- Devries, B., Pratihast, A. K., Verbesselt, J., Kooistra, L., De Bruin, S., and Herold, M. (2013). Near real-time tropical forest disturbance monitoring using Landsat time series and local expert monitoring data. *MultiTemp 2013 - 7th International Workshop on the Analysis of Multi-Temporal Remote Sensing Images: "Our Dynamic Environment", Proceedings*, 1–4. <https://doi.org/10.1109/Multi-Temp.2013.6866022>
- DeVries, B., Verbesselt, J., Kooistra, L., and Herold, M. (2015). Robust monitoring of small-scale forest disturbances in a tropical montane forest using Landsat time series. *Remote Sensing of Environment*, 161, 107–121. <https://doi.org/10.1016/j.rse.2015.02.012>
- Ding, Y., Zang, R., Lu, X., and Huang, J. (2017). The impacts of selective logging and clear-cutting on woody plant diversity after 40 years of natural recovery in a tropical montane rain forest, south China. *Science of the Total Environment*, 579, 1683–1691. <https://doi.org/10.1016/j.scitotenv.2016.11.185>
- Djemel Merabtene, M., Faraoun, F., Mlih, R., Djellouli, R., Latreche, A., and Bol, R. (2021). Forest Soil Organic Carbon Stocks of Tessala Mount in North-West Algeria-Preliminary Estimates. *Frontiers in Environmental Science*, 8, 277. <https://doi.org/10.3389/fenvs.2020.520284>
- Don, A., Schumacher, J., and Freibauer, A. (2011). Impact of tropical land-use change on soil organic carbon stocks - a meta-analysis. *Global Change Biology*, 17(4), 1658–1670. <https://doi.org/10.1111/j.1365-2486.2010.02336.x>
- Douglas Bates, Martin Maechler, Ben Bolker, Steven Walker, Rune Haubo Bojesen Christensen, Henrik Singmann, Bin Dai, Fabian Scheipl, Gabor Grothendieck, Peter Green, J. F. (2015). *Linear and Nonlinear Mixed Effects*

- Models [R package nlme version 3.1-143]. Retrieved from <https://cran.r-project.org/web/packages/nlme/index.html>
- EAC, UNEP, and GRID-Arendal. (2016). Sustainable mountain development in East Africa in a changing climate - Mountain Adaptation Outlook Series.
- Edwards, D. P., Massam, M. R., Hugaasen, T., and Gilroy, J. J. (2017). Tropical secondary forest regeneration conserves high levels of avian phylogenetic diversity. *Biological Conservation*, 209, 432–439. <https://doi.org/10.1016/j.biocon.2017.03.006>
- Egeru, A., Wasonga, O., Gabiri, G., MacOpiyo, L., Mburu, J., and Mwanjalolo Majaliwa, J. G. (2019). Land Cover and Soil Properties Influence on Forage Quantity in a Semiarid Region in East Africa. *Applied and Environmental Soil Science*, 2019. <https://doi.org/10.1155/2019/6874268>
- Ellison, D., Morris, C. E., Locatelli, B., Sheil, D., Cohen, J., Murdiyarsa, D., ... Sullivan, C. A. (2017). Trees, forests and water: Cool insights for a hot world. *Global Environmental Change*, 43, 51–61. <https://doi.org/10.1016/j.gloenvcha.2017.01.002>
- Eshetu, E. Y., and Hailu, T. A. (2020). Carbon sequestration and elevational gradient: The case of Yegof mountain natural vegetation in North East, Ethiopia, implications for sustainable management. *Cogent Food and Agriculture*, 6(1), 1733331. <https://doi.org/10.1080/23311932.2020.1733331>
- FAO. (2014). Global Forest Resources Assessment 2015. *Country Report Kenya*, Rome. Retrieved from <http://www.fao.org/3/a-az251e.pdf>
- FAO. (2015). Global Forest Resources Assessment 2015. *In Desk Reference*. <https://doi.org/10.1002/2014GB005021>

-
- FAO, and UNEP. (2020). The State of the World's Forests 2020. <https://doi.org/10.4060/ca8642en>
- Fortier, J., Rogan, J., Woodcock, C. E., and Runfola, D. M. (2011). Utilizing temporally invariant calibration sites to classify multiple dates and types of satellite imagery. *Photogrammetric Engineering and Remote Sensing*, 77(2), 181–189. <https://doi.org/10.14358/PERS.77.2.181>
- Frazier, R. J., Coops, N. C., and Wulder, M. A. (2015). Boreal Shield forest disturbance and recovery trends using Landsat time series. *Remote Sensing of Environment*, 170, 317–327. <https://doi.org/10.1016/j.rse.2015.09.015>
- Frelich, L. E. (2002). Forest Dynamics and Disturbance Regimes. <https://doi.org/10.1017/CBO9780511542046>
- Frolking, S., Palace, M. W., Clark, D. B., Chambers, J. Q., Shugart, H. H., and Hurtt, G. C. (2009). Forest disturbance and recovery: A general review in the context of spaceborne remote sensing of impacts on aboveground biomass and canopy structure. *Journal of Geophysical Research: Biogeosciences*, 114(3), n/a-n/a. <https://doi.org/10.1029/2008JG000911>
- Gallegos, S. C., Beck, S. G., Hensen, I., Saavedra, F., Lippok, D., and Schleuning, M. (2016). Factors limiting montane forest regeneration in bracken-dominated habitats in the tropics. *Forest Ecology and Management*, 381, 168–176. <https://doi.org/10.1016/j.foreco.2016.09.014>
- Ge, J., Wang, S., Fan, J., Gongadze, K., and Wu, L. (2020). Soil nutrients of different land-use types and topographic positions in the water-wind erosion crisscross region of China's Loess Plateau. *Catena*, 184, 104243. <https://doi.org/10.1016/j.catena.2019.104243>

- Gebeyehu, G., Soromessa, T., Bekele, T., and Teketay, D. (2019). Carbon stocks and factors affecting their storage in dry Afroalpine forests of Awi Zone, northwestern Ethiopia. *Journal of Ecology and Environment*, 43(1), 1–18. <https://doi.org/10.1186/s41610-019-0105-8>
- Gebrehiwot, K., Desalegn, T., Woldu, Z., Demissew, S., and Teferi, E. (2018). Soil organic carbon stock in Abune Yosef afroalpine and sub-afroalpine vegetation, northern Ethiopia. *Ecological Processes*, 7(1). <https://doi.org/10.1186/s13717-018-0117-9>
- Gelaw, A. M., Singh, B. R., and Lal, R. (2014). Soil organic carbon and total nitrogen stocks under different land uses in a semi-arid watershed in Tigray, Northern Ethiopia. *Agriculture, Ecosystems and Environment*, 188, 256–263. <https://doi.org/10.1016/j.agee.2014.02.035>
- Gerland, P., Raftery, A. E., Ševčíková, H., Li, N., Gu, D., Spoorenberg, T., ... Wilmoth, J. (2014). World population stabilization unlikely this century. *Science*, 346(6206), 234–237. <https://doi.org/10.1126/science.1257469>
- Gibbs, H. K., Ruesch, A. S., Achard, F., Clayton, M. K., Holmgren, P., Ramankutty, N., and Foley, J. A. (2010). Tropical forests were the primary sources of new agricultural land in the 1980s and 1990s. *Proceedings of the National Academy of Sciences*, 107(38), 16732–16737. <https://doi.org/10.1073/pnas.0910275107>
- Gichuhi, M. (2013). Ecological management of the Mau catchment area and its impact on Lake Nakuru national park. *Journal of Agriculture, Science and Technology*, Vol. 15, pp. 81–101.
- Girardin, C. A. J., Malhi, Y., Doughty, C. E., Metcalfe, D. B., Meir, P., del Aguila-Pasquel, J., ... Rowland, L. (2016). Seasonal trends of Amazonian rainforest

- phenology, net primary productivity, and carbon allocation. *Global Biogeochemical Cycles*, 30(5), 700–715.
<https://doi.org/10.1002/2015GB005270>
- Githae, E. W., Chuah-Petiot, M., Mworira, J. K., and Odee, D. W. (2008). A botanical inventory and diversity assessment of Mt. Marsabit forest, a sub-humid montane forest in the arid lands of northern Kenya. *African Journal of Ecology*, 46(1), 39–45. <https://doi.org/10.1111/j.1365-2028.2007.00805.x>
- GoK. (2012). Kenya's Vision 2030. In "Kenya aims to be a nation living in a clean, secure, and sustainable environment by 2030" (Vol. 2030). Retrieved from https://na.unep.net/atlas/datlas/sites/default/files/unepsiouxfalls/atlasbook_1135/Kenya_Screen_Chapter1.pdf
- Goosem, M., Paz, C., Fensham, R., Preece, N., Goosem, S., and Laurance, S. G. W. (2016). Forest age and isolation affect the rate of recovery of plant species diversity and community composition in secondary rain forests in tropical Australia. *Journal of Vegetation Science*, 27, 504–514.
<https://doi.org/10.1111/jvs.12376>
- Gourlet-Fleury, S., Mortier, F., Fayolle, A., Baya, F., Ouedraogo, D., Benedet, F., and Picard, N. (2013). Tropical forest recovery from logging: a 24 year silvicultural experiment from Central Africa. *Philosophical Transactions of the Royal Society B: Biological Sciences*, 368(1625), 20120302–20120302.
<https://doi.org/10.1098/rstb.2012.0302>
- Government of Kenya. (2017). Forest Management Information System. Retrieved November 7, 2020, from Kenya Forest Service (KFS) website: http://www.kenyaforestservice.org/index.php?option=com_content&view=article&id=472&Itemid=633

- Goward, S. N., Masek, J. G., Cohen, W. B., Moisen, G. G., Collatz, G. J., Healey, S. P., ... Wulder, M. A. (2008). Forest Disturbance and North American Carbon Flux. *Eos*, 89(11), 28–30.
- Grantham, H. S., Costa, H. M., Elsen, P. R., Laurance, W. F., and Watson, J. E. M. (2020). Modification of forests by people means only 40% of remaining forests have high ecosystem integrity. *BioRxiv*, 10017. <https://doi.org/10.1101/2020.03.05.978858>
- Griffiths, P., Kuemmerle, T., Baumann, M., Radeloff, V. C., Abrudan, I. V., Lieskovsky, J., ... Hostert, P. (2014). Forest disturbances, forest recovery, and changes in forest types across the carpathian ecoregion from 1985 to 2010 based on landsat image composites. *Remote Sensing of Environment*, 151, 72–88. <https://doi.org/10.1016/j.rse.2013.04.022>
- Grinand, C., Rakotomalala, F., Gond, V., Vaudry, R., Bernoux, M., and Vieilledent, G. (2013). Estimating deforestation in tropical humid and dry forests in Madagascar from 2000 to 2010 using multi-date Landsat satellite images and the random forests classifier. *Remote Sensing of Environment*, 139, 68–80. <https://doi.org/10.1016/j.rse.2013.07.008>
- Gu, H., Williams, C. A., Ghimire, B., Zhao, F., and Huang, C. (2016). High-resolution mapping of time since disturbance and forest carbon flux from remote sensing and inventory data to assess harvest, fire, and beetle disturbance legacies in the Pacific Northwest. *Biogeosciences*, 13(22), 6321–6337. <https://doi.org/10.5194/bg-13-6321-2016>
- Guan, F., Tang, X., Fan, S., Zhao, J., and Peng, C. (2015). Changes in soil carbon and nitrogen stocks followed the conversion from secondary forest to

- Chinese fir and Moso bamboo plantations. *Catena*, 133, 455–460.
<https://doi.org/10.1016/j.catena.2015.03.002>
- Guzha, A. C., Rufino, M. C., Okoth, S., Jacobs, S., and Nóbrega, R. L. B. (2018). Impacts of land use and land cover change on surface runoff, discharge and low flows: Evidence from East Africa. *Journal of Hydrology: Regional Studies*, 15, 49–67. <https://doi.org/10.1016/j.ejrh.2017.11.005>
- Hagedorn, F., Gavazov, K., and Alexander, J. M. (2019). Vegetation To Climate Change. *Science*, 1123(September), 1119–1123.
- Hamunyela, E., Brandt, P., Shirima, D., Do, H. T. T., Herold, M., and Roman-Cuesta, R. M. (2020). Space-time detection of deforestation, forest degradation and regeneration in montane forests of Eastern Tanzania. *International Journal of Applied Earth Observation and Geoinformation*, 88. <https://doi.org/10.1016/j.jag.2020.102063>
- Han, X., Huang, J., Yao, J., Xu, Y., Ding, Y., and Zang, R. (2021). Effects of logging on the ecological strategy spectrum of a tropical montane rain forest. *Ecological Indicators*, 128, 107812. <https://doi.org/10.1016/j.ecolind.2021.107812>
- Han, Y., Zhang, J., Mattson, K. G., Zhang, W., and Weber, T. A. (2016). Sample Sizes to Control Error Estimates in Determining Soil Bulk Density in California Forest Soils. *Soil Science Society of America Journal*, 80(3), 756. <https://doi.org/10.2136/sssaj2015.12.0422>
- Hansen, M. C., Potapov, P. V., Moore, R., Hancher, M., Turubanova, S. A., Tyukavina, A., ... Townshend, J. R. G. (2013). High-resolution global maps of 21st-century forest cover change. *Science*, 342(6160), 850–853. <https://doi.org/10.1126/science.1244693>

- Hansen, M. C., Stehman, S. V, and Potapov, P. V. (2010). Quantification of global gross forest cover loss. *Proceedings of the National Academy of Sciences*, 107(19), 8650–8655. <https://doi.org/10.1073/pnas.0912668107>
- Hansen, M. C., Stehman, S. V, Potapov, P. V, Loveland, T. R., Townshend, J. R. G., DeFries, R. S., ... Dimiceli, C. (2008). Humid tropical forest clearing from 2000 to 2005 quantified by using multitemporal and multiresolution remotely sensed data. *Proceedings of the National Academy of Sciences of the United States of America*, 105(27), 9439–9444. <https://doi.org/10.1073/pnas.0804042105>
- Harisena, N. V., Groen, T. A., Toxopeus, A. G., and Naimi, B. (2021). When is variable importance estimation in species distribution modelling affected by spatial correlation? *Ecography*. <https://doi.org/10.1111/ecog.05534>
- Harris, N. L., Gibbs, D. A., Baccini, A., Birdsey, R. A., de Bruin, S., Farina, M., ... Tyukavina, A. (2021). Global maps of twenty-first century forest carbon fluxes. *Nature Climate Change*, 22. <https://doi.org/10.1038/s41558-020-00976-6>
- Hector, A., Philipson, C., Saner, P., Chamagne, J., Dzulkifli, D., O'Brien, M., ... Godfray, H. C. J. (2011). The Sabah Biodiversity Experiment: A long-term test of the role of tree diversity in restoring tropical forest structure and functioning. *Philosophical Transactions of the Royal Society B: Biological Sciences*, 366(1582), 3303–3315. <https://doi.org/10.1098/rstb.2011.0094>
- Hemp, A. and Hemp, C. (2018) 'Broken bridges: The isolation of Kilimanjaro's ecosystem', *Global Change Biology*, 24(8), pp. 3499–3507. doi: 10.1111/gcb.14078.

- Hermosilla, T., Wulder, M. A., White, J. C., Coops, N. C., and Hobart, G. W. (2015). Regional detection, characterization, and attribution of annual forest change from 1984 to 2012 using Landsat-derived time-series metrics. *Remote Sensing of Environment*, 170, 121–132. <https://doi.org/10.1016/j.rse.2015.09.004>
- Hesslerová, P., and Pokorný, J. (2011). Effect of mau forest clear cut on temperature distribution and hydrology of catchment of lakes nakuru and naivasha: Preliminary study. In *Water and Nutrient Management in Natural and Constructed Wetlands*, (pp. 263–273). https://doi.org/10.1007/978-90-481-9585-5_19
- Hethcoat, M. G., King, B. J., Castiblanco, F. F., Ortiz-Sepúlveda, C. M., Achiardi, F. C. P., Edwards, F. A., ... Edwards, D. P. (2019). The impact of secondary forest regeneration on ground-dwelling ant communities in the Tropical Andes. *Oecologia*, 191(2), 475–482. <https://doi.org/10.1007/s00442-019-04497-8>
- Hirata, Y., Gen, T., Tamotsu, S., and Jumpei, T. (2012). REDD-plus Cookbook, how to measure and monitor forest carbon. In H. Yasumasa, T. Gen, S. Tamotsu, and T. Jumpei (Eds.), *REDD-plus Cookbook, how to measure and monitor forest carbon*.
- Hirschmugl, M., Gallaun, H., Dees, M., Datta, P., Deutscher, J., Koutsias, N., and Schardt, M. (2017). Methods for Mapping Forest Disturbance and Degradation from Optical Earth Observation Data: a Review. *Current Forestry Reports*, 3(1), 32–45. <https://doi.org/10.1007/s40725-017-0047-2>

- Hofer, T., and Zingari, P. C. (2014). The Multiple Functions of Forests in Sustainable Mountain Development and the Challenge of their Management. <https://www.fao.org/3/XII/0810-B1.htm>
- Holeksa, J., Jaloviar, P., Kucbel, S., Saniga, M., Svoboda, M., Szewczyk, J., ... Żywiec, M. (2017). Models of disturbance driven dynamics in the West Carpathian spruce forests. *Forest Ecology and Management*, 388, 79–89. <https://doi.org/10.1016/j.foreco.2016.08.026>
- Holl, K. D. (2012). Restoration of Tropical Forests. In *Restoration Ecology* (pp. 103–114). <https://doi.org/10.1002/9781118223130.ch9>
- Hosonuma, N., Herold, M., De Sy, V., De Fries, R. S., Brockhaus, M., Verchot, L., ... Romijn, E. (2012). An assessment of deforestation and forest degradation drivers in developing countries. *Environmental Research Letters*, Vol. 7, p. 044009. <https://doi.org/10.1088/1748-9326/7/4/044009>
- Houghton, R. A., Byers, B., and Nassikas, A. A. (2015). A role for tropical forests in stabilizing atmospheric CO₂. *Nature Climate Change*, 5(12), 1022–1023. <https://doi.org/10.1038/nclimate2869>
- Houghton, R. A., (2012). Carbon emissions and the drivers of deforestation and forest degradation in the tropics This review comes from a themed issue on Climate systems. *Current Opinion in Environmental Sustainability*, 4, 597–603. <https://doi.org/10.1016/j.cosust.2012.06.006>
- Huang, C., Goward, S. N., Masek, J. G., Thomas, N., Zhu, Z., and Vogelmann, J. E. (2010). An automated approach for reconstructing recent forest disturbance history using dense Landsat time series stacks. *Remote Sensing of Environment*, 114(1), 183–198. <https://doi.org/10.1016/j.rse.2009.08.017>

- Huang, F., Zhang, W., Gan, X., Huang, Y., Guo, Y., and Wen, X. (2018). Changes in vegetation and soil properties during recovery of a subtropical forest in South China. *Journal of Mountain Science*, 15(1), 46–58. <https://doi.org/10.1007/s11629-017-4541-6>
- Huang, W. (2015). Assessing forest biomass and monitoring changes from disturbance and recovery with LiDAR and SAR. *University of Maryland*.
- Hubau, W., Lewis, S. L., Phillips, O. L., Affum-Baffoe, K., Beeckman, H., Cuni-Sanchez, A., ... Zemagho, L. (2020). Asynchronous carbon sink saturation in African and Amazonian tropical forests. *Nature*, 579(7797), 80–87. <https://doi.org/10.1038/s41586-020-2035-0>
- Imani, G., Boyemba, F., Lewis, S., Nabahungu, N. L., Calders, K., Zapfack, L., ... Cuni-Sanchez, A. (2017). Height-diameter allometry and above ground biomass in tropical montane forests: Insights from the Albertine Rift in Africa. *PloS One*, 12(6), e0179653. <https://doi.org/10.1371/journal.pone.0179653>
- IPCC. (2006). Guidelines for National Greenhouse Gas Inventories. Volume 4: Agriculture, Forestry and Other Land Use. The Intergovernmental Panel on Climate Change. In and N. H. R. Harald Aalde, Patrick Gonzalez, Michael Gytarsky, Thelma Krug, Werner A. Kurz, Stephen Ogle, John Raison, Dieter Schoene and Z. S. Nagmeldin G. Elhassan, Linda S. Heath, Niro Higuchi, Samuel Kainja, Mitsuo Matsumoto, María José Sanz Sánchez (Eds.), *Forest Land*. https://doi.org/10.1007/978-3-642-41714-6_62425
- Jacobs, S. R., Breuer, L., Butterbach-Bahl, K., Pelster, D. E., and Rufino, M. C. (2017). Land use affects total dissolved nitrogen and nitrate concentrations in tropical montane streams in Kenya. *Science of The Total Environment*, 603–604, 519–532. <https://doi.org/10.1016/j.scitotenv.2017.06.100>

- Jensen, J. R. (2007). *Remote Sensing of Environment: an earth resource pererspective* (Second Edi). *Upper Saddle River: Pearson Prentice Hall*.
- Jiang, B., Bamutaze, Y., and Pilesjö, P. (2014). Geo-spatial Information Science Climate change and land degradation in Africa: a case study in the Mount Elgon region, Uganda Climate change and land degradation in Africa: a case study in the Mount Elgon region, Uganda. *Geo-Spatial Information Science*, 17(1), 39–53. <https://doi.org/10.1080/10095020.2014.889271>
- Johnstone, J. F., Allen, C. D., Franklin, J. F., Frelich, L. E., Harvey, B. J., Higuera, P. E., ... Turner, M. G. (2016). Changing disturbance regimes, ecological memory, and forest resilience. *Frontiers in Ecology and the Environment*, Vol. 14, pp. 369–378. <https://doi.org/10.1002/fee.1311>
- Johnstone, J. F., and Chapin, F. S. (2006). Effects of soil burn severity on post-fire tree recruitment in boreal forest. *Ecosystems*, 9(1), 14–31. <https://doi.org/10.1007/s10021-004-0042-x>
- José Pinheiro, Douglas Bates, Saikat DebRoy, Deepayan Sarkar, Siem Heisterkamp, B. V. W. (2015). *Linear Mixed-Effects Models using “Eigen” and S4 [R package lme4 version 1.1-21]*.
- Joseck J, M., Khaemba, A., Mburu, N., and Ngaywa M, A. (2016). Effects of increased land use changes on runoff and sediment yield in the Upper River Nzoia Catchment. *International Journal of Civil Engineering and Technology* (IJCIET), 7(2), 76–94.
- Jung, M., Hill, S. L. L., Platts, P. J., Marchant, R., Siebert, S., Fournier, A., ... Newbold, T. (2017). Local factors mediate the response of biodiversity to land use on two African mountains. *Animal Conservation*, 20(4), 370–381. <https://doi.org/10.1111/acv.12327>

- Kanui, I. T., Kibwage, J. K., Murangiri, R. M., Qiu, Z., and K Rongoei, P. J. (2016). Water Tower Ecosystems Services and Diversification of Livelihood Activities to Neighbouring Communities; A Case Study of Chyulu Hills Water Tower in Kenya. *Journal of Geography, Environment and Earth Science International*, 6(4), 1–12. <https://doi.org/10.9734/JGEEESI/2016/26620>
- Kebede, B., and Soromessa, T. (2018). Allometric equations for aboveground biomass estimation of *Olea europaea* L. subsp. *cuspidata* in Mana Angetu Forest. *Ecosystem Health and Sustainability*, 4(1), 1–12. <https://doi.org/10.1080/20964129.2018.1433951>
- Keenan, R. J., Reams, G. A., Achard, F., de Freitas, J. V., Grainger, A., and Lindquist, E. (2015). Dynamics of global forest area: Results from the FAO Global Forest Resources Assessment 2015. *Forest Ecology and Management*, 352, 9–20. <https://doi.org/10.1016/j.foreco.2015.06.014>
- KEFRI. (2018). Economic Value of the Mau Forest Complex, Cherangany Hills and Mt. Elgon Water Towers in Kenya; *Supporting Decision Making and Conservation of Kenya's Important Ecosystems*.
- Keith, H., Vardon, M., Stein, J. A., and Lindenmayer, D. (2019). Contribution of native forests to climate change mitigation – A common approach to carbon accounting that aligns results from environmental-economic accounting with rules for emissions reduction. *Environmental Science and Policy*, 93, 189–199. <https://doi.org/10.1016/j.envsci.2018.11.001>
- Kennedy, R. E., Yang, Z., and Cohen, W. B. (2010). Detecting trends in forest disturbance and recovery using yearly Landsat time series: 1. LandTrendr - Temporal segmentation algorithms. *Remote Sensing of Environment*, 114(12), 2897–2910. <https://doi.org/10.1016/j.rse.2010.07.008>

- KFS. (2017). Kenya Forest Service - *Kenya Water Towers Status Report*. Retrieved July 23, 2017, from <http://www.kenyaforestservice.org/index.php/2016-04-25-20-08-29/news/501-kenya-water-towers-status-report>
- KFS. (2021). Kenya Forest Service - *Mau Forest*. Retrieved June 12, 2021, from http://www.kenyaforestservice.org/index.php?option=com_content&view=article&id=699:mau-forest&catid=183&Itemid=695
- Kim, D., Sexton, J. O., and Townshend, J. R. (2015). Tropics From the 1990s To the 2000s. *Geophysical Research Letters*, 42, 3495–3501. <https://doi.org/10.1002/2014GL062777>
- Kimutai, D. K., and Watanabe, T. (2016). Forest-cover change and participatory forest management of the lembus forest, Kenya. *Environments - MDPI*, 3(3), 1–18. <https://doi.org/10.3390/environments3030020>
- Kinjanjui, J. M., Karachi, M., and Ondimu, K. N. (2013). Natural regeneration and ecological recovery in Mau Forest complex, Kenya. *Open Journal of Ecology*, 03(06), 417–422. <https://doi.org/10.4236/oje.2013.36047>
- Kinyanjui, M. (2009). The effect of human encroachment on forest cover , composition and structure in the western blocks of the mau forest complex. <https://doi.org/10.13140/2.1.2110.4964>
- Kinyanjui, M. J., Latva-käyrä, P., and Bhuvneshwar, P. S. (2014). An Inventory of the Above Ground Biomass in the Mau Forest Ecosystem , Kenya. *Open Journal of Ecology*, 4(7), 619–627. <https://doi.org/10.4236/oje.2014.410052>
- Kissinger, G., Herold, M., and De Sy, V. (2012). Drivers of Deforestation and Forest Degradation: *A Synthesis Report for REDD+ Policymakers*.
- Kizza C., L., Majaliwa J. G. M., Nakileza, B., Eilu, G., Bahat, I., Kansiime, F., and Wilson, J. (2013). Soil and nutrient losses along the chronosequential forest

- recovery gradient in Mabira Forest Reserve, Uganda. *African Journal of Agricultural Research*, 8(1), 77–85. <https://doi.org/10.5897/ajar11.963>
- Klopp, J. M., and Sang, J. K. (2011). Maps, Power, and the Destruction of the Mau Forest in Kenya. *Georgetown Journal of International Affairs*, 12(1), 125–134.
- Kucuker, M. A., Guney, M., Oral, H. V., Coptu, N. K., and Onay, T. T. (2015). Impact of deforestation on soil carbon stock and its spatial distribution in the western black sea region of Turkey. *Journal of Environmental Management*, 147, 227–235. <https://doi.org/10.1016/j.jenvman.2014.08.017>
- Kuzyakov, Y., and Gavrichkova, O. (2010). REVIEW: Time lag between photosynthesis and carbon dioxide efflux from soil: A review of mechanisms and controls. *Global Change Biology*, Vol. 16, pp. 3386–3406. <https://doi.org/10.1111/j.1365-2486.2010.02179.x>
- KWTA. (2015). *Kenya Water Towers Status Report*. Retrieved from [http://www.kwta.go.ke/doc/Status of Water Towers Submission Final.pdf](http://www.kwta.go.ke/doc/Status%20of%20Water%20Towers%20Submission%20Final.pdf)
- Lambin, E. F., Geist, H. J., and Lepers, E. (2003). Dynamics of Land-Use and Land-Cover Change in Tropical Regions. *Annual Review of Environment and Resources*, 28(1), 205–241. <https://doi.org/10.1146/annurev.energy.28.050302.105459>
- Landmann, T., and Dubovyk, O. (2014). Spatial analysis of human-induced vegetation productivity decline over eastern Africa using a decade (2001-2011) of medium resolution MODIS time-series data. *International Journal of Applied Earth Observation and Geoinformation*, 33(1), 76–82. <https://doi.org/10.1016/j.jag.2014.04.020>

- Langat, D. K., Maranga, E. K., Aboud, A. A., and Cheboiwo, J. K. (2016). Role of Forest Resources to Local Livelihoods: The Case of East Mau Forest Ecosystem, Kenya. *International Journal of Forestry Research*, 2016. <https://doi.org/10.1155/2016/4537354>
- Lawrence, D., and Vandecar, K. (2015, December 18). Effects of tropical deforestation on climate and agriculture. *Nature Climate Change*, Vol. 5, pp. 27–36. <https://doi.org/10.1038/nclimate2430>
- Lewis, S. L., Lopez-Gonzalez, G., Sonké, B., Affum-Baffoe, K., Baker, T. R., Ojo, L. O., ... Wöll, H. (2009). Increasing carbon storage in intact African tropical forests. *Nature*, 457(7232), 1003–1006. <https://doi.org/10.1038/nature07771>
- Lewis, S. L., Sonké, B., Sunderland, T., Begne, S. K., Lopez-Gonzalez, G., van der Heijden, G. M. F., ... Zemagho, L. (2013). Above-ground biomass and structure of 260 African tropical forests. *Philosophical Transactions of the Royal Society B: Biological Sciences*, 368(1625), 20120295. <https://doi.org/10.1098/rstb.2012.0295>
- Lin, D., Lai, J., Yang, B., Song, P., Li, N., Ren, H., and Ma, K. (2015). Forest biomass recovery after different anthropogenic disturbances: relative importance of changes in stand structure and wood density. *European Journal of Forest Research*, 134(5), 769–780. <https://doi.org/10.1007/s10342-015-0888-9>
- Liu, Xiang, Yang, T., Wang, Q., Huang, F., and Li, L. (2018). Dynamics of soil carbon and nitrogen stocks after afforestation in arid and semi-arid regions: A meta-analysis. *Science of the Total Environment*, Vol. 618, pp. 1658–1664. <https://doi.org/10.1016/j.scitotenv.2017.10.009>
- Liu, Xiaoju, and Pan, C. (2019). Effects of recovery time after fire and fire severity on stand structure and soil of larch forest in the Kanas National Nature Reserve,

- Northwest China. *Journal of Arid Land*, 11(6), 811–823.
<https://doi.org/10.1007/s40333-019-0022-9>
- Liu, Y., Li, S., Sun, X., and Yu, X. (2016). Variations of forest soil organic carbon and its influencing factors in east China. *Annals of Forest Science*, 73(2), 501–511. <https://doi.org/10.1007/s13595-016-0543-8>
- Long, C., Yang, X., Long, W., Li, D., Zhou, W., and Zhang, H. (2018). Soil Nutrients Influence Plant Community Assembly in Two Tropical Coastal Secondary Forests. *Tropical Conservation Science*, 11, 194008291881795. <https://doi.org/10.1177/1940082918817956>
- Loo, L. C., Song, G. Z. M., and Chao, K. J. (2017). Characteristics of tropical human-modified forests after 20 years of natural regeneration. *Botanical Studies*, 58(1), 36. <https://doi.org/10.1186/s40529-017-0190-x>
- Lopez-Gonzalez, G., Lewis, S. L., Burkitt, M., and Phillips, O. L. (2011). ForestPlots.net: A web application and research tool to manage and analyse tropical forest plot data. *Journal of Vegetation Science*, 22(4), 610–613. <https://doi.org/10.1111/j.1654-1103.2011.01312.x>
- Lorenz, K., Lal, R., and Ehlers, K. (2019). Soil organic carbon stock as an indicator for monitoring land and soil degradation in relation to United Nations' Sustainable Development Goals. *Land Degradation and Development*, 30(7), 824–838. <https://doi.org/10.1002/ldr.3270>
- Lu, J. (2006). Modeling Hydrological Response to Forest Management and Climate Change at Contrasting Watersheds in the Southern United States. *North Carolina State University*.
- Lucas, R. M., Honzák, M., Do Amaral, I., Curran, P. J., Foody, G. M., Honza, M., and Amaral, I. DO. (2002). Forest regeneration on abandoned clearances in

- central Amazonia. *International Journal of Remote Sensing*, 23(5), 965–988.
<https://doi.org/10.1080/01431160110069791>
- Luo, P., Zhou, M., Deng, H., Lyu, J., Cao, W., Takara, K., ... Geoffrey Schladow, S. (2018). Impact of forest maintenance on water shortages: Hydrologic modeling and effects of climate change. *Science of The Total Environment*, 615, 1355–1363. <https://doi.org/10.1016/j.scitotenv.2017.09.044>
- MacDicken, K. G. (2015). Global Forest Resources Assessment 2015: What, why and how? *Forest Ecology and Management*, 352, 3–8.
<https://doi.org/10.1016/j.foreco.2015.02.006>
- Majumdar, K., Shankar, U., and Datta, B. K. (2014). Trends in Tree Diversity and Stand Structure during Restoration: A Case Study in Fragmented Moist Deciduous Forest Ecosystems of Northeast India. *Journal of Ecosystems*, 2014, 1–10.
<https://doi.org/10.1155/2014/845142>
- Maltamo, M., Kinnunen, H., Kangas, A., and Korhonen, L. (2020). Predicting stand age in managed forests using National Forest Inventory field data and airborne laser scanning. *Forest Ecosystems*, 7(1).
<https://doi.org/10.1186/s40663-020-00254-z>
- Margono, B. A., Turubanova, S., Zhuravleva, I., Potapov, P., Tyukavina, A., Baccini, A., ... Hansen, M. C. (2012). Mapping and monitoring deforestation and forest degradation in Sumatra (Indonesia) using Landsat time series data sets from 1990 to 2010. *Environmental Research Letters*, 7(3).
<https://doi.org/10.1088/1748-9326/7/3/034010>
- Marthews TR, Riutta T, Menor IO, Urrutia R, Moore S, Metcalfe D, Malhi Y, Phillips O, Huaraca Huasco W, Ruiz Jaen M, Girardin C, Butt N, C. R. (2014). Measuring Tropical Forest Carbon Allocation and Cycling: A RAINFOR-GEM

- Field Manual for Intensive Census Plots (v3.0). Retrieved from <http://gem.tropicalforests.ox.ac.uk/>
- Martínez-Garza, C., Campo, J., Ricker, M., and Tobón, W. (2016). Effect of initial soil properties on six-year growth of 15 tree species in tropical restoration plantings. *Ecology and Evolution*, 6(24), 8686–8694. <https://doi.org/10.1002/ece3.2508>
- Martínez, M. L., Pérez-Maqueo, O., Vázquez, G., Castillo-Campos, G., García-Franco, J., Mehlreter, K., ... Landgrave, R. (2009). Effects of land use change on biodiversity and ecosystem services in tropical montane cloud forests of Mexico. *Forest Ecology and Management*, 258(9), 1856–1863. <https://doi.org/10.1016/j.foreco.2009.02.023>
- Mayaux, P., Holmgren, P., Achard, F., Eva, H., Stibig, H.-J., and Branthomme, A. (2005). Tropical forest cover change in the 1990s and options for future monitoring. *Philosophical Transactions of the Royal Society B: Biological Sciences*, 360(1454), 373–384. <https://doi.org/10.1098/rstb.2004.1590>
- Mayer, M., Prescott, C. E., Abaker, W. E. A., Augusto, L., Cécillon, L., Ferreira, G. W. D., ... Vesterdal, L. (2020). Influence of forest management activities on soil organic carbon stocks: A knowledge synthesis. *Forest Ecology and Management*, 466(April), 118127. <https://doi.org/10.1016/j.foreco.2020.118127>
- Mbugua, M. W. (2011). Environmental degradation as a cause of conflict: a case study of the Mau Forest Degradation in Kenya (1963-2010). *University of Nairobi, Kenya*. <https://doi.org/10.4324/9781315731100-13>
- Mehr, M., Brandl, R., Kneib, T., and Müller, J. (2012). The effect of bark beetle infestation and salvage logging on bat activity in a national park. *Biodiversity*

- and Conservation*, 21(11), 2775–2786. <https://doi.org/10.1007/s10531-012-0334-y>
- Mekuria, W., Wondie, M., Amare, T., Wubet, A., Feyisa, T., and Yitaferu, B. (2018). Restoration of degraded landscapes for ecosystem services in North-Western Ethiopia. *Heliyon*, 4(8). <https://doi.org/10.1016/j.heliyon.2018.e00764>
- Mendoza-Ponce, A., Corona-Núñez, R. O., Galicia, L., and Kraxner, F. (2019). Identifying hotspots of land use cover change under socioeconomic and climate change scenarios in Mexico. *Ambio*, 48(4), 336–349. <https://doi.org/10.1007/s13280-018-1085-0>
- Menhinick, E. F. (1964). A Comparison of Some Species-Individuals Diversity Indices Applied to Samples of Field Insects. *Ecology*, 45(4), 859–861. <https://doi.org/10.2307/1934933>
- Mensah, S., Egeru, A., Assogbadjo, A. E., and Glèlè Kakaï, R. (2020). Vegetation structure, dominance patterns and height growth in an Afromontane forest, Southern Africa. *Journal of Forestry Research*, 31(2), 453–462. <https://doi.org/10.1007/s11676-018-0801-8>
- Milodowski, D. T., Mitchard, E. T. A., and Williams, M. (2017). Forest loss maps from regional satellite monitoring systematically underestimate deforestation in two rapidly changing parts of the Amazon. *Environmental Research Letters*, 12(9). <https://doi.org/10.1088/1748-9326/aa7e1e>
- Mitchard, E. T. A. (2018). The tropical forest carbon cycle and climate change. *Nature*, 559(7715), 527–534. <https://doi.org/10.1038/s41586-018-0300-2>
- Mitchell, A. L., Rosenqvist, A., and Mora, B. (2017). Current remote sensing approaches to monitoring forest degradation in support of countries

- measurement, reporting and verification (MRV) systems for REDD+. *Carbon Balance and Management*, 12(1), 9. <https://doi.org/10.1186/s13021-017-0078-9>
- Mohandass, D., Campbell, M. J., Hughes, A. C., Mammides, C., and Davidar, P. (2017). The effect of altitude, patch size and disturbance on species richness and density of lianas in montane forest patches. *Acta Oecologica*, 83, 1–14. <https://doi.org/10.1016/j.actao.2017.06.004>
- Mokria, M., Gebrekirstos, A., Aynekulu, E., and Bräuning, A. (2015). Tree dieback affects climate change mitigation potential of a dry afro-montane forest in northern Ethiopia. *Forest Ecology and Management*, 344, 73–83. <https://doi.org/10.1016/j.foreco.2015.02.008>
- Moore, J. A. M., Jiang, J., Patterson, C. M., Mayes, M. A., Wang, G., and Classen, A. T. (2015). Interactions among roots, mycorrhizas and free-living microbial communities differentially impact soil carbon processes. *Journal of Ecology*, 103(6), 1442–1453. <https://doi.org/10.1111/1365-2745.12484>
- Moore, S., Adu-Bredu, S., Duah-Gyamfi, A., Addo-Danso, S. D., Ibrahim, F., Mbou, A. T., ... Malhi, Y. (2018). Forest biomass, productivity and carbon cycling along a rainfall gradient in West Africa. *Global Change Biology*, 24(2), e496–e510. <https://doi.org/10.1111/gcb.13907>
- Moser, G., Leuschner, C., Hertel, D., Graefe, S., Soethe, N., and Iost, S. (2011). Elevation effects on the carbon budget of tropical mountain forests (S Ecuador): The role of the belowground compartment. *Global Change Biology*, 17(6), 2211–2226. <https://doi.org/10.1111/j.1365-2486.2010.02367.x>

- Mugagga, F, Kakembo, V., and Buyinza, M. (2012). Land use changes on the slopes of Mount Elgon and the implications for the occurrence of landslides. *Catena*, 90, 39–46. <https://doi.org/10.1016/j.catena.2011.11.004>
- Mugagga, Frank, Nagasha, B., Barasa, B., and Buyinza, M. (2015). The Effect of Land Use on Carbon Stocks and Implications for Climate Variability on the Slopes of Mount Elgon, Eastern Uganda. *International Journal of Regional Development*, 2(1), 58. <https://doi.org/10.5296/ijrd.v2i1.7537>
- Muhweezi, A. B., Sikoyo, G. M., and Chemonges, M. (2007). Introducing a Transboundary Ecosystem Management Approach in the Mount Elgon Region. *Mountain Research and Development*, 27(3), 215–219. [https://doi.org/10.1659/0276-4741\(2007\)27\[215:IATEMA\]2.0.CO;2](https://doi.org/10.1659/0276-4741(2007)27[215:IATEMA]2.0.CO;2)
- Mukadasi, B., Kaboggoza, J. R., and Nabalegwa, M. (2007). Agroforestry practices in the buffer zone area of Mt Elgon National Park, eastern Uganda. *African Journal of Ecology*, 45(SUPPL. 3), 48–53. <https://doi.org/10.1111/j.1365-2028.2007.00857.x>
- Muktar, M., Bobe, B., Kibebew, K., and Yared, M. (2018). Soil organic carbon stock under different land use types in Kersa Sub Watershed, Eastern Ethiopia. *African Journal of Agricultural Research*, 13(24), 1248–1256. <https://doi.org/10.5897/ajar2018.13190>
- Mutugi, M., and Kiiru, W. (2015). Biodiversity, local resource, national heritage, regional concern, and global impact: The case of Mau forest, Kenya. *European Scientific Journal*, ESJ, 11(10). <https://doi.org/10.19044/ESJ.2015.V11N10P%P>
- Mwangi, E., Cerutti, P., Doumenge, C., and Nasi, R. (2018). The current state of Eastern Africa's forests. <https://doi.org/10.2760/512555>

- N'Guessan, A. E., N'dja, J. K., Yao, O. N., Amani, B. H. K., Gouli, R. G. Z., Pioniot, C., ... Hérault, B. (2019). Drivers of biomass recovery in a secondary forested landscape of West Africa. *Forest Ecology and Management*, 433, 325–331. <https://doi.org/10.1016/j.foreco.2018.11.021>
- Nabutola, W. (2010). The Mau Forest in the Rift Valley: Kenya's Largest Water Tower: a Perfect Model for the Challenges and Opportunities of a Sustainable Development Project? *Climate Change and Environmental Threats*, (4) 24 11 – 16.
- Nagel, L. M., Palik, B. J., Battaglia, M. A., D'Amato, A. W., Guldin, J. M., Swanston, C. W., ... Roske, M. R. (2017). Adaptive silviculture for climate change: A national experiment in manager-scientist partnerships to apply an adaptation framework. *Journal of Forestry*, 115(3), 167–178. <https://doi.org/10.5849/jof.16-039>
- Nagel, T. A., Mikac, S., Dolinar, M., Klopčič, M., Keren, S., Diaci, J., ... Paulič, V. (2017). The natural disturbance regime in forests of the Dinaric Mountains: A synthesis of evidence. *Forest Ecology and Management*, 388, 29–42. <https://doi.org/10.1016/j.foreco.2016.07.047>
- Nakagawa, S., Johnson, P. C. D., and Schielzeth, H. (2017). The coefficient of determination R^2 and intra-class correlation coefficient from generalized linear mixed-effects models revisited and expanded. *Journal of the Royal Society Interface*, 14(134). <https://doi.org/10.1098/rsif.2017.0213>
- Noss, R. F., and Lindenmayer, D. B. (2006). The Ecological Effects of Salvage Logging after Natural Disturbance Introduction. *Conservation Biology*, 20(4), 946–948. <https://doi.org/10.1111/j.1523-1739.2006.00498.x>

- Novotný, J., Navrátilová, B., Janoutová, R., Oulehle, F., and Homolová, L. (2020). Influence of site-specific conditions on estimation of forest above ground biomass from airborne laser scanning. *Forests*, 11(3), 1–18. <https://doi.org/10.3390/f11030268>
- Nyirambangutse, B., Zibera, E., Uwizeye, F. K., Nsabimana, D., Bizuru, E., Pleijel, H., ... Wallin, G. (2017). Carbon stocks and dynamics at different successional stages in an Afrotropical forest. *Biogeosciences*, 14(5), 1285–1303. <https://doi.org/10.5194/bg-14-1285-2017>
- Olang, L. O., and Kundu, P. M. (2011). Land Degradation of the Mau Forest Complex in Eastern Africa: A Review for Management and Restoration Planning. In Dr Ema Ekundayo (Ed.), *Environmental Monitoring*. Retrieved from <http://etd-library.ku.ac.ke/handle/123456789/11626>
- Olang, L. O., Kundu, P., Bauer, T., and Fürst, J. (2011). Analysis of spatio-temporal land cover changes for hydrological impact assessment within the Nyando River Basin of Kenya. *Environmental Monitoring and Assessment*, 179(1–4), 389–401. <https://doi.org/10.1007/s10661-010-1743-6>
- Oliveras, I., Román-Cuesta, R. M., Urquiaga-Flores, E., Quintano Loayza, J. A., Kala, J., Huamán, V., ... Malhi, Y. (2018). Fire effects and ecological recovery pathways of tropical montane cloud forests along a time chronosequence. *Global Change Biology*, 24(2), 758–772. <https://doi.org/10.1111/gcb.13951>
- Olofsson, P., Foody, G. M., Herold, M., Stehman, S. V, Woodcock, C. E., and Wulder, M. A. (2014). Good practices for estimating area and assessing accuracy of land change. *Remote Sensing of Environment*, Vol. 148, pp. 42–57. <https://doi.org/10.1016/j.rse.2014.02.015>

- Omoding, J., Walters, G., Andama, E., Carvalho, S., Colomer, J., Cracco, M., Eilu, G., Kiyingi, G., Kumar, C., Langoya, C. D., Bugembe, N. B., Reinhard, F., Schelle, C. (2020). Analysing and applying stakeholder perceptions to improve protected area governance in Ugandan conservation landscapes. *Land*, 9(6). <https://doi.org/10.3390/LAND9060207>
- Omoro, L. M. A., Starr, M., and Pellikka, P. K. E. (2013). Tree biomass and soil carbon stocks in indigenous forests in comparison to plantations of exotic species in the Taita Hills of Kenya. *Silva Fennica*, 47(2), 1–18. <https://doi.org/10.14214/sf.935>
- Ongugo, P., Njuguna, J., Obonyo, E., and Sigu, G. (2001). Livelihoods, natural resource entitlements and protected areas: The case of Mt. Elgon forest in Kenya. 11.
- Otieno, K. O. (2016). Forestry carbon sequestration and trading : a case of Mau Forest Complex in Kenya Forest Change detection and carbon trading. *University of Gavle*. Retrieved from <https://www.diva-portal.org/smash/get/diva2:882491/FULLTEXT02.pdf>
- Otuoma, J., Anyango, B., Ouma, G., Okeyo, D., Muturi, G. M., and Oindo, B. (2016). Determinants of aboveground carbon offset additionality in plantation forests in a moist tropical forest in western Kenya. *Forest Ecology and Management*, 365, 61–68. <https://doi.org/10.1016/j.foreco.2016.01.028>
- Owuor, S. O., Butterbach-Bahl, K., Guzha, A. C., Jacobs, S., Merbold, L., Rufino, M. C., Pelster, D. E., Díaz-Pinés, E., Breuer, L. (2018). Conversion of natural forest results in a significant degradation of soil hydraulic properties in the highlands of Kenya. *Soil and Tillage Research*, 176, 36–44. <https://doi.org/10.1016/j.still.2017.10.003>

- Panayotov, M., Gogushev, G., Tsavkov, E., Vasileva, P., Tsvetanov, N., Kulakowski, D., and Bebi, P. (2017). Abiotic disturbances in Bulgarian mountain coniferous forests – An overview. *Forest Ecology and Management*, 388, 13–28. <https://doi.org/10.1016/j.foreco.2016.10.034>
- Patterson, T. (2012). East African montane forests. Retrieved April 23, 2022, from *Terrestrial Ecoregions, Natural Earth II* website: <https://www.worldwildlife.org/ecoregions/at0108>
- Paulo, V. B., Roeland, K., Jens-Peter, B. L., and Lars, G. (2015). An alternative simplified version of the VECEA potential natural vegetation map for eastern Africa. <https://doi.org/10.6084/m9.figshare.1306936.v1>
- Pederson, N., Dyer, J. M., McEwan, R. W., Hessel, A. E., Mock, C. J., Orwig, D. A., Rieder, H. E., Cook, B. I. (2014). The legacy of episodic climatic events in shaping temperate, broadleaf forests. *Ecological Monographs*, 84(4), 599–620. <https://doi.org/10.1890/13-1025.1>
- Peterson, C. J., Cannon, J. B., and Godfrey, C. M. (2016). First Steps Toward Defining the Wind Disturbance Regime in Central Hardwoods Forests. https://doi.org/10.1007/978-3-319-21527-3_5
- Petursson, J. G., Vedeld, P., and Sassen, M. (2013). An institutional analysis of deforestation processes in protected areas: The case of the transboundary Mt. Elgon, Uganda and Kenya. *Forest Policy and Economics*, 26, 22–33. <https://doi.org/10.1016/j.forpol.2012.09.012>
- Phillips, J., Ramirez, S., Wayson, C., and Duque, A. (2019). Differences in carbon stocks along an elevational gradient in tropical mountain forests of Colombia. *Biotropica*, 51(4), 490–499. <https://doi.org/10.1111/btp.12675>

- Pielou, E. C. (1966). The measurement of diversity in different types of biological collections. *Journal of Theoretical Biology*, 13(C), 131–144. [https://doi.org/10.1016/0022-5193\(66\)90013-0](https://doi.org/10.1016/0022-5193(66)90013-0)
- Plumptre, A. J., Ayebare, S., Behangana, M., Forrest, T. G., Hatanga, P., Kabuye, C., Kirunda, B., Kityo, R., Mugabe, H., Namaganda, M., Nampindo, S., Nangendo, G., Nkuutu, D. N., Pomeroy, D., Tushabe, H., Prinsloo, S. (2019). Conservation of vertebrates and plants in Uganda: Identifying Key Biodiversity Areas and other sites of national importance. *Conservation Science and Practice*, 1(2), e7. <https://doi.org/10.1002/csp2.7>
- Poorter, L., Bongers, F., Aide, T. M., Almeyda Zambrano, A. M., Balvanera, P., Nunes, Y. R..F., Ochoa-Gaona, S., De Oliveira, A. A., Orihuela-Belmonte, E., Peña-Claros, M., Pérez-García, E. A., Piotta, D., Powers, J. S., Rodríguez-Velázquez, J., Romero-Pérez, I. E., Ruíz, J., Saldarriaga, J. G., Sanchez-Azofeifa, A., Schwartz, N. B., Steininger, M. K., Swenson, N. G., Toledo, M., Uriarte, M., Van Breugel, M., Van Der Wal, H., Veloso, M. D. M., Vester, H. F. M., Vicentini, A., Vieira, I. C. G., Bentos, T. V., Williamson, G. B., Rozendaal, D. M. A. (2016). Biomass resilience of Neotropical secondary forests. *Nature*, 530(7589), 211–214. <https://doi.org/10.1038/nature16512>
- Potapov, P., Li, X., Hernandez-Serna, A., Tyukavina, A., Hansen, M. C., Kommareddy, A., Pickens, A., Turubanova, S., Tang, H., Silva, C. E., Armston, J., Dubayah, R., Blair, J. B., Hofton, M. (2021). Mapping global forest canopy height through integration of GEDI and Landsat data. *Remote Sensing of Environment*, 253(10), 112165. <https://doi.org/10.1016/j.rse.2020.112165>
- Potapov, P. V., Turubanova, S. A., Hansen, M. C., Adusei, B., Broich, M., Altstatt, A., Mane, L., Justice, C. O. (2012). Quantifying forest cover loss in Democratic

- Republic of the Congo, 2000 – 2010, with Landsat ETM + data. *Remote Sensing of Environment*, 122, 106–116.
<https://doi.org/10.1016/j.rse.2011.08.027>
- Pratihast, A. K., DeVries, B., Avitabile, V., de Bruin, S., Kooistra, L., Tekle, M., and Herold, M. (2014). Combining satellite data and community-based observations for forest monitoring. *Forests*, 5(10), 2464–2489.
<https://doi.org/10.3390/f5102464>
- Price, M. F., Gratzner, G., Duguma, L. A., Kohler, T., Maselli, D., and Romeo, R. (2011). Mountain Forests in a Changing World Mountain Forests in a Changing World Realizing values, addressing challenges. In *FAO/MPS and SDC, Rome* (Vol. 29). <https://doi.org/10.13140/2.1.2386.5283>
- Pugh, T. A. M., Lindeskog, M., Smith, B., Poulter, B., Arneth, A., Haverd, V., and Calle, L. (2019). Role of forest regrowth in global carbon sink dynamics. *Proceedings of the National Academy of Sciences of the United States of America*, 116(10), 4382–4387. <https://doi.org/10.1073/pnas.1810512116>
- Puyravaud, J.-P. (2003). Standardizing the calculation of the annual rate of deforestation. *Forest Ecology and Management*, 177(1–3), 593–596.
[https://doi.org/10.1016/S0378-1127\(02\)00335-3](https://doi.org/10.1016/S0378-1127(02)00335-3)
- Rahman, M. M., Bárcena, T. G., and Vesterdal, L. (2017). Tree species and time since afforestation drive soil C and N mineralization on former cropland. *Geoderma*, 305, 153–161. <https://doi.org/10.1016/j.geoderma.2017.06.002>
- Ramos Scharrón, C. E., Castellanos, E. J., and Restrepo, C. (2012). The transfer of modern organic carbon by landslide activity in tropical montane ecosystems. *Journal of Geophysical Research: Biogeosciences*, 117(3), 3016.
<https://doi.org/10.1029/2011JG001838>

- Requena Suarez, D., Rozendaal, D. M. A., De Sy, V., Phillips, O. L., Alvarez-Dávila, E., Anderson-Teixeira, K., Araujo-Murakami, A., Arroyo, L., Baker, T. R., Bongers, F., Brienen, R. J.W., Carter, S., Cook-Patton, S. C., Feldpausch, T. R., Griscom, B. W., Harris, N., Hérault, B., Honorio Coronado, E. N., Leavitt, S. M., Lewis, S. L., Marimon, B. S., Monteagudo Mendoza, A., N'dja, J. K., N'Guessan, A. E., Poorter, L., Qie, L., Rutishauser, E., Sist, P., Sonké, B., Sullivan, M. J. P., Vilanova, E., Wang, M. M. H., Martius, C., Herold, M. (2019). Estimating aboveground net biomass change for tropical and subtropical forests: refinement of IPCC default rates using forest plot data. *Global Change Biology*, 00, 21. <https://doi.org/10.1111/gcb.14767>
- Richter, M. (2010). Tropical mountain forests – distribution and general features. In and D. G. (Göttingen: G. C. for B. and E. S. R. Gradstein, J. Homeier (Ed.), *Tropical Mountain Forest: Patterns and Processes in a Biodiversity Hotspot* (Vol. 2, pp. 7–24).
- Rosa, I. M. D., Purves, D., Carreiras, J. M. B., and Ewers, R. M. (2014). Modelling land cover change in the Brazilian Amazon: temporal changes in drivers and calibration issues. *Regional Environmental Change*, 15(1), 123–137. <https://doi.org/10.1007/s10113-014-0614-z>
- Roussel, J.-M., and Daval, E. (2012). Nile Equatorial Lakes Subsidiary Action Program: Nile Equatorial Lakes Subsidiary Action Program: Feasibility study and preparation of an Integrated Watershed Management program and investment proposal for Sio-Malaba-Malakisi sub basin. *Retrieved from* http://nileis.nilebasin.org/system/files/Main_report_010812.pdf
- Rutkowska, M., Dubalska, K., Bajger-Nowak, G., Konieczka, P., and Namieśnik, J. (2014). Organomercury Compounds in Environmental Samples: Emission

- Sources, Toxicity, Environmental Fate, and Determination. *Critical Reviews in Environmental Science and Technology*, 44(6), 638–704. <https://doi.org/10.1080/10643389.2012.728825>
- Rutten, G., Ensslin, A., Hemp, A., and Fischer, M. (2015). Forest structure and composition of previously selectively logged and non-logged montane forests at Mt. Kilimanjaro. *Forest Ecology and Management*, 337, 61–66. <https://doi.org/10.1016/j.foreco.2014.10.036>
- Saiz, G., Bird, M. I., Domingues, T., Schrodt, F., Schwarz, M., Feldpausch, T. R., Veenendaal, E., Djangbletey, G., Hien, F., Compaore, H., Diallo, A., Lloyd, J. (2012). Variation in soil carbon stocks and their determinants across a precipitation gradient in West Africa. *Global Change Biology*, 18(5), 1670–1683. <https://doi.org/10.1111/j.1365-2486.2012.02657.x>
- Salinas, N., Cosio, E. G., Silman, M., Meir, P., Nottingham, A. T., Roman-Cuesta, R. M., and Malhi, Y. (2021). Editorial: Tropical Montane Forests in a Changing Environment. *Frontiers in Plant Science*, 12(August), 1–5. <https://doi.org/10.3389/fpls.2021.712748>
- Sannier, C., McRoberts, R. E., and Fichet, L. V. (2016). Suitability of Global Forest Change data to report forest cover estimates at national level in Gabon. *Remote Sensing of Environment*, 173, 326–338. <https://doi.org/10.1016/j.rse.2015.10.032>
- Santini, N. S., Adame, M. F., Nolan, R. H., Miquelajauregui, Y., Piñero, D., Mastretta-Yanes, A., Cuervo-Robayo, Á. P., Eamus, D. (2019). Storage of organic carbon in the soils of Mexican temperate forests. *Forest Ecology and Management*, Vol. 446, pp. 115–125. <https://doi.org/10.1016/j.foreco.2019.05.029>

-
- Santini, N. S., Villarruel-Arroyo, A., Adame, M. F., Lovelock, C. E., Nolan, R. H., Gálvez-Reyes, N., González, E. J., Olivares-Resendiz, B., Mastretta-Yanes, A., Piñero, D. (2020). Organic Carbon Stocks of Mexican Montane Habitats: Variation Among Vegetation Types and Land-Use. *Frontiers in Environmental Science*, 8:581476. doi: 10.3389/fenvs.2020.581476
- Sasaki, N., and Putz, F. E. (2009). Critical need for new definitions of “forest” and “forest degradation” in global climate change agreements. *Conservation Letters*, 2(5), 226–232. <https://doi.org/10.1111/j.1755-263x.2009.00067.x>
- Sassen, M., and Sheil, D. (2013). Human impacts on forest structure and species richness on the edges of a protected mountain forest in Uganda. *Forest Ecology and Management*, 307, 206–218. <https://doi.org/10.1016/j.foreco.2013.07.010>
- Sassen, M., Sheil, D., Giller, K. E., and ter Braak, C. J. F. (2013). Complex contexts and dynamic drivers: Understanding four decades of forest loss and recovery in an East African protected area. *Biological Conservation*, 159, 257–268. <https://doi.org/10.1016/j.biocon.2012.12.003>
- Sattler, D., Murray, L. T., Kirchner, A., and Lindner, A. (2014). Influence of soil and topography on aboveground biomass accumulation and carbon stocks of afforested pastures in South East Brazil. *Ecological Engineering*, 73, 126–131. <https://doi.org/10.1016/j.ecoleng.2014.09.003>
- Schoene, D., Killmann, W., Lupke, H., LoycheWilkie, M., von Lüpke, H., and LoycheWilkie, M. (2007). Definitional issues related to reducing emissions from deforestation in developing countries. *Forests and Climate Change Working Paper 5*.

- Schulz, J. J., Cayuela, L., Echeverria, C., Salas, J., and Rey Benayas, J. M. (2010). Monitoring land cover change of the dryland forest landscape of Central Chile (1975-2008). *Applied Geography*, 30(3), 436–447. <https://doi.org/10.1016/j.apgeog.2009.12.003>
- Scott, P. (1998). From conflict to collaboration: people and forests at Mount Elgon, Uganda. From Conflict to Collaboration: People and Forests at Mount Elgon, Uganda, 149(32). Retrieved from <https://www.iucn.org/content/conflict-collaboration-people-and-forests-mount-elgon-uganda>
- Seidl, R., Schelhaas, M. J., Rammer, W., and Verkerk, P. J. (2014). Increasing forest disturbances in Europe and their impact on carbon storage. *Nature Climate Change*, 4(9), 806–810. <https://doi.org/10.1038/nclimate2318>
- Seidl, R., Thom, D., Kautz, M., Martin-Benito, D., Peltoniemi, M., Vacchiano, G., Wild, J., Ascoli, D., Petr, M., Honkaniemi, J., Lexer, M. J., Trotsiuk, V., Mairota, P., Svoboda, M., Fabrika, M., Nagel, T. A., Reyer, C. P. O. (2017). Forest disturbances under climate change. *Nature Climate Change*, Vol. 7, pp. 395–402. <https://doi.org/10.1038/nclimate3303>
- Shannon, C. E. (1948). A Mathematical Theory of Communication. *Bell System Technical Journal*, 27(3), 379–423. <https://doi.org/10.1002/j.1538-7305.1948.tb01338.x>
- Shapiro, A. C., Grantham, H. S., Aguilar-Amuchastegui, N., Murray, N. J., Gond, V., Bonfils, D., and Rickenbach, O. (2021). Forest condition in the Congo Basin for the assessment of ecosystem conservation status. *Ecological Indicators*, 122, 107268. <https://doi.org/10.1016/j.ecolind.2020.107268>

- Sheil, D. (2018). Forests, atmospheric water and an uncertain future: the new biology of the global water cycle. *Forest Ecosystems*, Vol. 5. <https://doi.org/10.1186/s40663-018-0138-y>
- Sheil, D., and Murdiyarso, D. (2009). How Forests Attract Rain: An Examination of a New Hypothesis. *BioScience*, 59(4), 341–347. <https://doi.org/10.1525/bio.2009.59.4.12>
- Sherman, R. E., Fahey, T. J., Martin, P. H., and Battles, J. J. (2012). Patterns of growth, recruitment, mortality and biomass across an altitudinal gradient in a neotropical montane forest, Dominican Republic. *Journal of Tropical Ecology*, 28(5), 483–495. <https://doi.org/10.1017/S0266467412000478>
- Shisanya, M. J., Nyabuti, C. A., Waqo, O. K., and Ojwala, W. P. (2014). Assessing Tree Species Dominance along an Agro Ecological Gradient in the Mau Forest Complex, Kenya. Kenya. *Open Journal of Ecology*, 4, 662–670. <https://doi.org/10.4236/oje.2014.411056>
- Simpson, E. H. (1949, April). Measurement of diversity [16]. *Nature*, Vol. 163, p. 688. <https://doi.org/10.1038/163688a0>
- Simula, M. (2009). Towards defining forest degradation: comparative analysis of existing definitions. In *Forest Resources Assessment Programme working Paper*. Retrieved from <http://www.iaeme.com/IJCIET/index.asp>
- Soh, M. C. K., Mitchell, N. J., Ridley, A. R., Butler, C. W., Puan, C. L., and Peh, K. S.-H. (2019). Impacts of Habitat Degradation on Tropical Montane Biodiversity and Ecosystem Services: A Systematic Map for Identifying Future Research Priorities. *Frontiers in Forests and Global Change*, 2, 83. <https://doi.org/10.3389/ffgc.2019.00083>

- Song, X. P., Hansen, M. C., Stehman, S. V., Potapov, P. V., Tyukavina, A., Vermote, E. F., and Townshend, J. R. (2018). Global land change from 1982 to 2016. *Nature*, 560(7720), 639–643. <https://doi.org/10.1038/s41586-018-0411-9>
- Soong, J. L., Janssens, I. A., Grau, O., Margalef, O., Stahl, C., Van Langenhove, L., Urbina, I., Chave, J., Dourdain, A., Ferry, B., Freycon, V., Herault, B., Sardans, J., Peñuelas, J., Verbruggen, E. (2020). Soil properties explain tree growth and mortality, but not biomass, across phosphorus-depleted tropical forests. *Scientific Reports*, 10(1). <https://doi.org/10.1038/s41598-020-58913-8>
- Spracklen, D. V., and Righelato, R. (2014). Tropical montane forests are a larger than expected global carbon store. *Biogeosciences*, 11(10), 2741–2754. <https://doi.org/10.5194/bg-11-2741-2014>
- Spracklen, D. V., and Righelato, R. (2016). Carbon storage and sequestration of re-growing montane forests in southern Ecuador. *Forest Ecology and Management*, 364, 139–144. <https://doi.org/10.1016/j.foreco.2016.01.001>
- Stenfert Kroese, J., Jacobs, S. R., Tych, W., Breuer, L., Quinton, J. N., and Rufino, M. C. (2020). Tropical Montane Forest Conversion Is a Critical Driver for Sediment Supply in East African Catchments. *Water Resources Research*, 56(10). <https://doi.org/10.1029/2020WR027495>
- Stenfert Kroese, J., Quinton, J., Jacobs, S., Breuer, L., and Rufino, M. (2020). Particulate macronutrient exports from tropical African montane catchments point to the impoverishment of agricultural soils. *SOIL Discussions*, 7(1), 1–30. <https://doi.org/10.5194/soil-2020-73>

- Strahler, A. H., Boschetti, L., Foody, G. M., Friedl, M. A., Hansen, M. C., Herold, M., Mayaux, P., Morissette, J. T., Stehman, S. E., Woodcock, C. E. (2006) Global Land Cover Validation: Recommendations for Evaluation and Accuracy Assessment of Global Land Cover Maps. *Office for Official Publications of the European Communities*, Luxemburg. http://nofc.cfs.nrcan.gc.ca/gofc-gold/Report Series/GOLD_25.pdf
- Suescún, D., Villegas, J. C., León, J. D., Flórez, C. P., García-Leoz, V., and Correa-Londoño, G. A. (2017). Vegetation cover and rainfall seasonality impact nutrient loss via runoff and erosion in the Colombian Andes. *Regional Environmental Change*, 17(3), 827–839. <https://doi.org/10.1007/s10113-016-1071-7>
- Sun, G., McNulty, S., Lu, J., Vose, J., Amayta, D., Zhou, G., and Zhang, Z. (2005). Modeling hydrologic responses to deforestation/forestation and climate change at multiple scales in the southern us and china. In: *Forest and Water in a Changing Environment*, Beijing, China, 8-2010. Retrieved from <https://www.srs.fs.usda.gov/pubs/28881>
- Sun, W., Zhu, H., and Guo, S. (2015). Soil organic carbon as a function of land use and topography on the Loess Plateau of China. *Ecological Engineering*, 83, 249–257. <https://doi.org/10.1016/j.ecoleng.2015.06.030>
- Swart, R. (2016). Monitoring 40 years of Landuse change in the Mau forest complex, Kenya a Landuse change driver analysis. *Wageningen University and Research*. Retrieved from <http://edepot.wur.nl/404611>
- Tamene, G. M., Adiss, H. K., and Alemu, M. Y. (2020). Effect of Slope Aspect and Land Use Types on Selected Soil Physicochemical Properties in North

- Western Ethiopian Highlands. *Applied and Environmental Soil Science*, 2020. <https://doi.org/10.1155/2020/8463259>
- Tarus, G. K., Kirui, B. K., and Obwoyere, G. (2019). Impacts of forest management type and season on soil carbon fluxes in Eastern Mau Forest, Kenya. *African Journal of Ecology*, 57(1), 113–121. <https://doi.org/10.1111/aje.12571>
- Tashi, S., Singh, B., Keitel, C., and Adams, M. (2016). Soil carbon and nitrogen stocks in forests along an altitudinal gradient in the eastern Himalayas and a meta-analysis of global data. *Global Change Biology*, 22(6), 2255–2268. <https://doi.org/10.1111/gcb.13234>
- Taylor, P. G., Cleveland, C. C., Wieder, W. R., Sullivan, B. W., Doughty, C. E., Dobrowski, S. Z., and Townsend, A. R. (2017). Temperature and rainfall interact to control carbon cycling in tropical forests. *Ecology Letters*, 20(6), 779–788. <https://doi.org/10.1111/ele.12765>
- Team, R. C. (2018). R: A language and environment for statistical computing. Retrieved from <https://www.r-project.org/>
- Team, R. C. (2020). R: A language and environment for statistical computing. R Foundation for Statistical Computing. Retrieved from <https://www.r-project.org/>
- Thomas, B. W., Hao, X., and Willms, W. D. (2017). Soil organic carbon, nitrogen, and phosphorus 13 yr after abruptly disturbing Northern Great Plains grassland. *Canadian Journal of Soil Science*, 97(2), 329–333. <https://doi.org/10.1139/cjss-2016-0113>
- Thorn, S., Bässler, C., Svoboda, M., and Müller, J. (2016). Effects of natural disturbances and salvage logging on biodiversity – Lessons from the

- Bohemian Forest. *Forest Ecology and Management*, Vol. 388, pp. 113–119.
<https://doi.org/10.1016/j.foreco.2016.06.006>
- Tolessa, T., and Senbeta, F. (2018). The extent of soil organic carbon and total nitrogen in forest fragments of the central highlands of Ethiopia. *Journal of Ecology and Environment*, 42(1). <https://doi.org/10.1186/s41610-018-0081-4>
- Trabucco, A., Zomer, R. J., Bossio, D. A., van Straaten, O., and Verchot, L. V. (2008). Climate change mitigation through afforestation/reforestation: A global analysis of hydrologic impacts with four case studies. *Agriculture, Ecosystems and Environment*, 126(1–2), 81–97.
<https://doi.org/10.1016/j.agee.2008.01.015>
- Twongyirwe, R., Sheil, D., Majaliwa, J. G. M., Ebanyat, P., Tenywa, M. M., van Heist, M., and Kumar, L. (2013). Variability of Soil Organic Carbon stocks under different land uses: A study in an afro-montane landscape in southwestern Uganda. *Geoderma*, 193–194, 282–289.
<https://doi.org/10.1016/j.geoderma.2012.09.005>
- Vásquez-Morales, S. G., Sánchez-Velásquez, L. R., Pineda-López, M. del R., Díaz-Fleischer, F., Flores-Estévez, N., and Viveros-Viveros, H. (2017). Moderate anthropogenic disturbance does not affect the demography of *Magnolia schiedeana*, an endangered species from Mexico. *Flora: Morphology, Distribution, Functional Ecology of Plants*, 234, 77–83.
<https://doi.org/10.1016/j.flora.2017.07.005>
- VECEA Team. (2020). Potential vegetation map for eastern Africa. Retrieved February 10, 2021, from *Potential vegetation map for eastern Africa website*: <https://vegetationmap4africa.org/Home.html>

- Veldkamp, E., Schmidt, M., Powers, J. S., and Corre, M. D. (2020). Deforestation and reforestation impacts on soils in the tropics. *Nature Reviews Earth and Environment*, 1(11), 590–605. <https://doi.org/10.1038/s43017-020-0091-5>
- Villa, P. M., Martins, S. V., Oliveira N, S. N., Rodrigues, A. C., Safar, N. V. H., Monsanto, L. D., Cancio, N, M., Ali, A. (2018). Woody species diversity as an indicator of the forest recovery after shifting cultivation disturbance in the northern Amazon. *Ecological Indicators*, 95, 687–694. <https://doi.org/10.1016/j.ecolind.2018.08.005>
- Vittori Antisari, L., Falsone, G., Carbone, S., and Vianello, G. (2013). Short-term effects of forest recovery on soil carbon and nutrient availability in an experimental chestnut stand. *Biology and Fertility of Soils*, 49(2), 165–173. <https://doi.org/10.1007/s00374-012-0708-z>
- Vogelmann, J. E., Khoa, V. P., Lan, D. X., Shermeyer, J., Shi, H., Wimberly, M. C., Duong, H. T., Huong, L. (2017). Assessment of Forest Degradation in Vietnam Using Landsat Time Series Data. *Forests*, 8(7), 238. <https://doi.org/10.3390/f8070238>
- Vollstädt, M. G. R., Ferger, S. W., Hemp, A., Howell, K. M., Töpfer, T., Böhning-Gaese, K., and Schleuning, M. (2017). Direct and indirect effects of climate, human disturbance and plant traits on avian functional diversity. *Global Ecology and Biogeography*, 26(8), 963–972. <https://doi.org/10.1111/geb.12606>
- Wang, R., and Gamon, J. A. (2019). Remote sensing of terrestrial plant biodiversity. *Remote Sensing of Environment*, 231, 111218. <https://doi.org/10.1016/j.rse.2019.111218>
- Wang, R., Gamon, J. A., Schweiger, A. K., Cavender-Bares, J., Townsend, P. A., Zygielbaum, A. I., and Kothari, S. (2018). Influence of species richness,

- evenness, and composition on optical diversity: A simulation study. *Remote Sensing of Environment*, 211, 218–228. <https://doi.org/10.1016/J.RSE.2018.04.010>
- Wang, S., and Huang, Y. (2020). Determinants of soil organic carbon sequestration and its contribution to ecosystem carbon sinks of planted forests. *Global Change Biology*, 26(5), 3163–3173. <https://doi.org/10.1111/gcb.15036>
- Wanyama, I., Pelster, D. E., Arias-Navarro, C., Butterbach-Bahl, K., Verchot, L. V., and Rufino, M. C. (2018). Management intensity controls soil N₂O fluxes in an Afromontane ecosystem. *Science of the Total Environment*, 624, 769–780. <https://doi.org/10.1016/j.scitotenv.2017.12.081>
- Wanyama, I., Pelster, D. E., Butterbach-Bahl, K., Verchot, L. V., Martius, C., and Rufino, M. C. (2019). Soil carbon dioxide and methane fluxes from forests and other land use types in an African tropical montane region. *Biogeochemistry*, 143(2), 171–190. <https://doi.org/10.1007/s10533-019-00555-8>
- Ward, A., Dargusch, P., Thomas, S., Liu, Y., and Fulton, E. A. (2014). A global estimate of carbon stored in the world's mountain grasslands and shrublands, and the implications for climate policy. *Global Environmental Change*, 28(1), 14–24. <https://doi.org/10.1016/j.gloenvcha.2014.05.008>
- Warton, D. I., Wright, S. T., and Wang, Y. (2012). Distance-based multivariate analyses confound location and dispersion effects. *Methods in Ecology and Evolution*, 3(1), 89–101. <https://doi.org/10.1111/j.2041-210X.2011.00127.x>
- Wekesa, C., Kirui, B. K., Maranga, E. K., and Muturi, G. M. (2019). Variations in forest structure, tree species diversity and above-ground biomass in edges to interior cores of fragmented forest patches of Taita Hills, Kenya. *Forest*

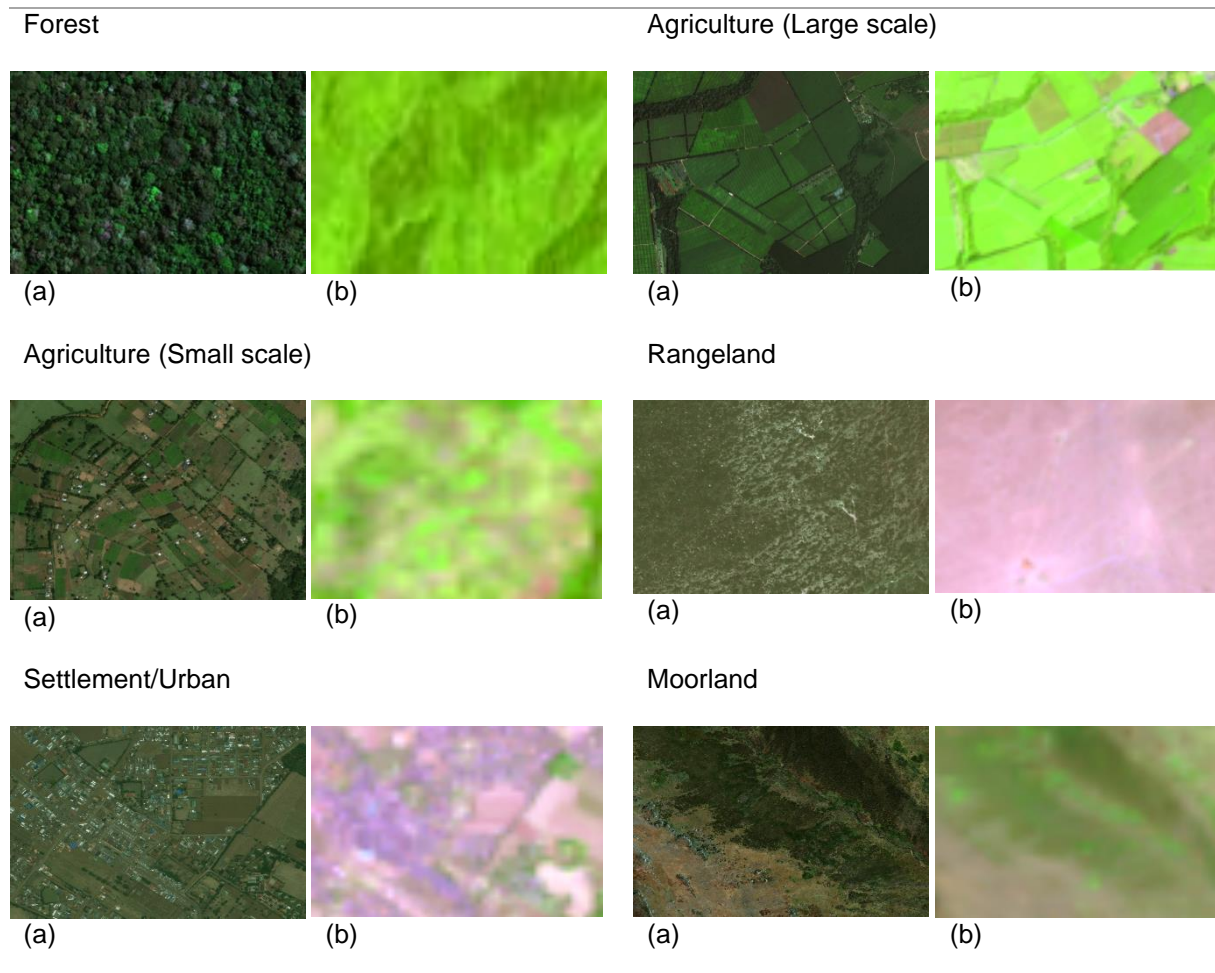
- Ecology and Management*, 440, 48–60.
<https://doi.org/10.1016/j.foreco.2019.03.011>
- Wekesa, C., Maranga, E. K., Kirui, B. K., Muturi, G. M., and Gathara, M. (2018). Interactions between native tree species and environmental variables along forest edge-interior gradient in fragmented forest patches of Taita Hills, Kenya. *Forest Ecology and Management*, 409, 789–798.
<https://doi.org/10.1016/j.foreco.2017.12.023>
- Were, K. O., Dick, T. B., and Singh, B. R. (2013). Remotely sensing the spatial and temporal land cover changes in Eastern Mau forest reserve and Lake Nakuru drainage basin, Kenya. *Applied Geography*, 41, 75–86.
<https://doi.org/10.1016/j.apgeog.2013.03.017>
- White, F. (1983). A descriptive memoir to accompany the Unesco/AETFAT/UNSO vegetation map of Africa. Paris: the United Nations Educational, Scientific and Cultural Organization.
- White, J. (1998). Estimating the age of large and veteran trees in Britain. Forestry Commission information note. *Forestry Commission*, Edinburgh. Retrieved from <http://www.forestry.gov.uk>
- Wielochowski, A., and West Col Productions. (1989). Mount Elgon : map and guide (1st ed.). Retrieved from <http://www.ewpnet.com/elgonmap.htm>
- World Agroforestry Centre. (2016). Wood Density Database. *World Agroforestry Centre*. Retrieved December 28, 2019, from website [website: http://www.worldagroforestry.org/publication/african-wood-density-database](http://www.worldagroforestry.org/publication/african-wood-density-database)
- WWF. (2005). Water towers of eastern Africa Policy, issues and vision for community-based protection and management of montane forests. In *WWF Eastern Africa Regional Programme Office*. Nairobi, Kenya.

- WWF. (2007). Water towers of eastern Africa Policy, issues and vision for community-based protection and management of montane forests. Retrieved from www.panda.org/earpo
- WWF. (2021). Eastern Africa: southern Sudan, central Kenya, *int Ecoregions*, World Wide Fund for Nature. Retrieved June 12, 2021, from <https://www.worldwildlife.org/ecoregions/at0108>
- Xu, B., Pan, Y., Johnson, A. H., and Plante, A. F. (2016). Method Comparison for Forest Soil Carbon and Nitrogen Estimates in the Delaware River Basin. *Soil Science Society of America Journal*, 80(1), 227–237. <https://doi.org/10.2136/sssaj2015.04.0167>
- Xu, H., Li, Y., Liu, S., Zang, R., He, F., and Spence, J. R. (2015). Partial recovery of a tropical rain forest a half-century after clear-cut and selective logging. *Journal of Applied Ecology*, 52(4), 1044–1052. <https://doi.org/10.1111/1365-2664.12448>
- Yang, Y., Luo, Y., and Finzi, A. C. (2011). Carbon and nitrogen dynamics during forest stand development: A global synthesis. *New Phytologist*, 190(4), 977–989. <https://doi.org/10.1111/j.1469-8137.2011.03645.x>
- Yimer, F., Ledin, S., and Abdelkadir, A. (2006). Soil organic carbon and total nitrogen stocks as affected by topographic aspect and vegetation in the Bale Mountains, Ethiopia. *Geoderma*, 135, 335–344. <https://doi.org/10.1016/j.geoderma.2006.01.005>
- Yimer, F., Ledin, S., and Abdelkadir, A. (2007). Changes in soil organic carbon and total nitrogen contents in three adjacent land use types in the Bale Mountains, south-eastern highlands of Ethiopia. *Forest Ecology and*

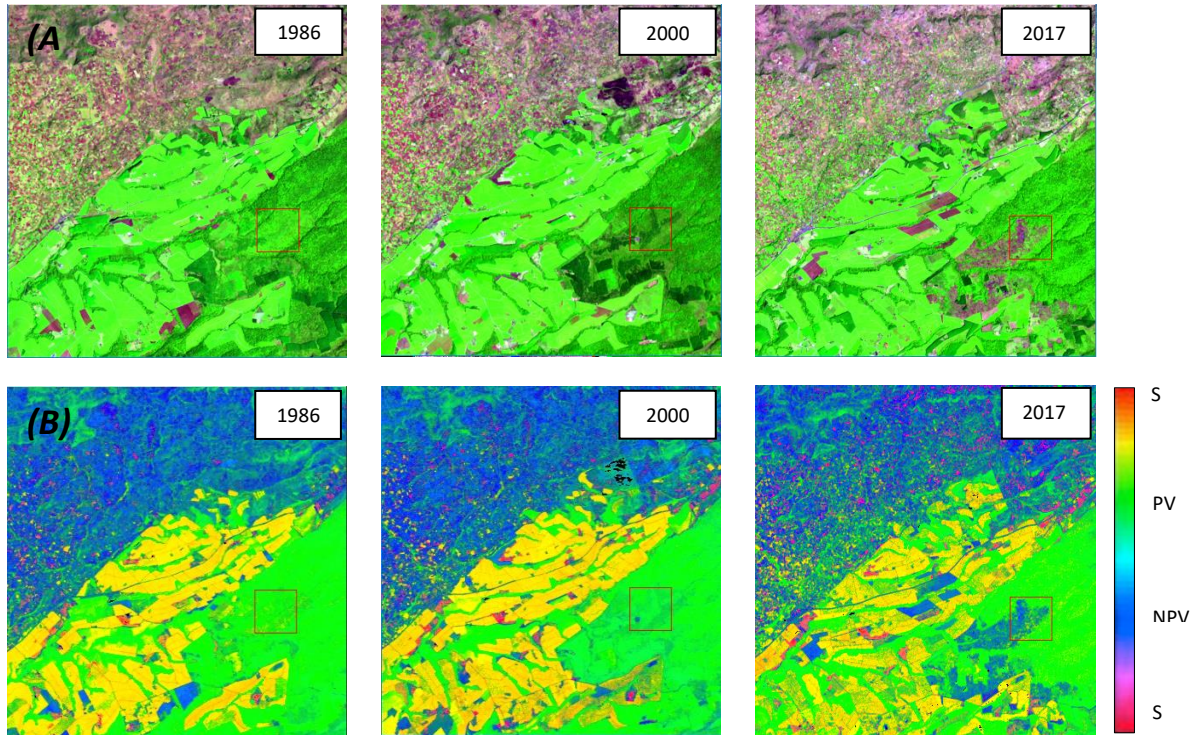
- Management*, 242(2–3), 337–342.
<https://doi.org/10.1016/j.foreco.2007.01.087>
- Zhang, C., Liu, G., Xue, S., and Sun, C. (2013). Soil organic carbon and total nitrogen storage as affected by land use in a small watershed of the Loess Plateau, China. *European Journal of Soil Biology*, 54, 16–24.
<https://doi.org/10.1016/j.ejsobi.2012.10.007>
- Zhang, M., Liu, N., Harper, R., Li, Q., Liu, K., Wei, X., Ning, D., Hou, Y., Liu, S. (2016). A global review on hydrological responses to forest change across multiple spatial scales: Importance of scale, climate, forest type and hydrological regime. *Journal of Hydrology*, 546, 44–59.
<https://doi.org/10.1016/j.jhydrol.2016.12.040>
- Zhao, B., Li, Z., Li, P., Xu, G., Gao, H., Cheng, Y., Chang, E., Yuan, S., Zhang, Y., Feng, Z. (2017). Spatial distribution of soil organic carbon and its influencing factors under the condition of ecological construction in a hilly-gully watershed of the Loess Plateau, China. *Geoderma*, 296, 10–17.
<https://doi.org/10.1016/j.geoderma.2017.02.010>
- Zhu, Z., Woodcock, C. E., and Olofsson, P. (2012). Continuous monitoring of forest disturbance using all available Landsat imagery. *Remote Sensing of Environment*, 122, 75–91. <https://doi.org/10.1016/J.RSE.2011.10.030>

APPENDICES

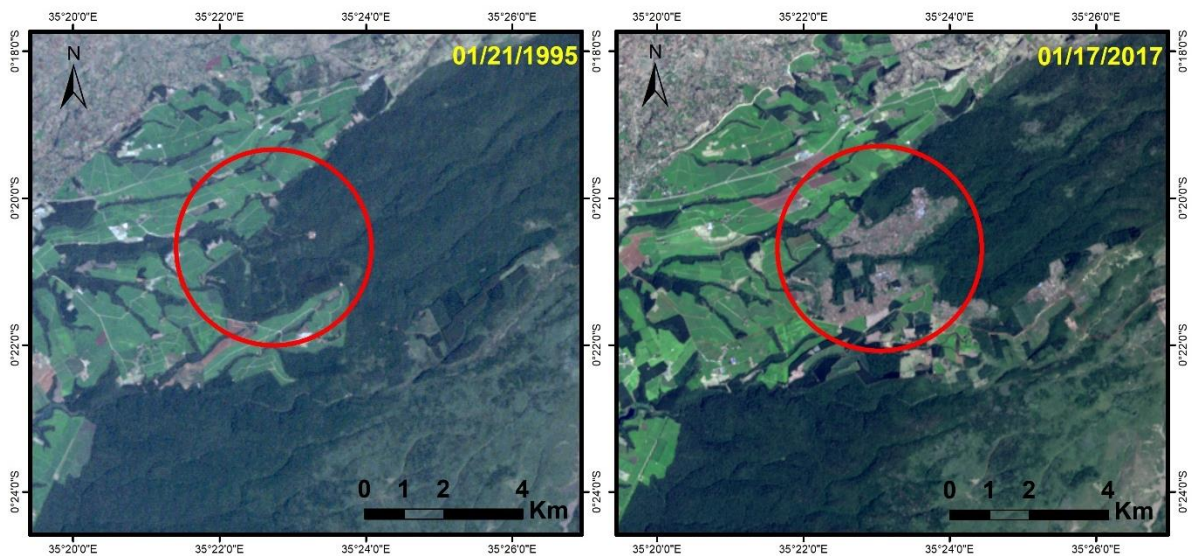
Appendix 1: Training and validation samples based on visual interpretation from High-resolution Google imagery and Multispectral Landsat images. The figure shows the Land cover class identification and sample from the high-resolution imagery (a) and Landsat TM, ETM+ (5-4-3 spectral band combination), and Landsat 8 OLI (6-5-4 spectral band combination) (b) for each land cover class used for the classification scheme.



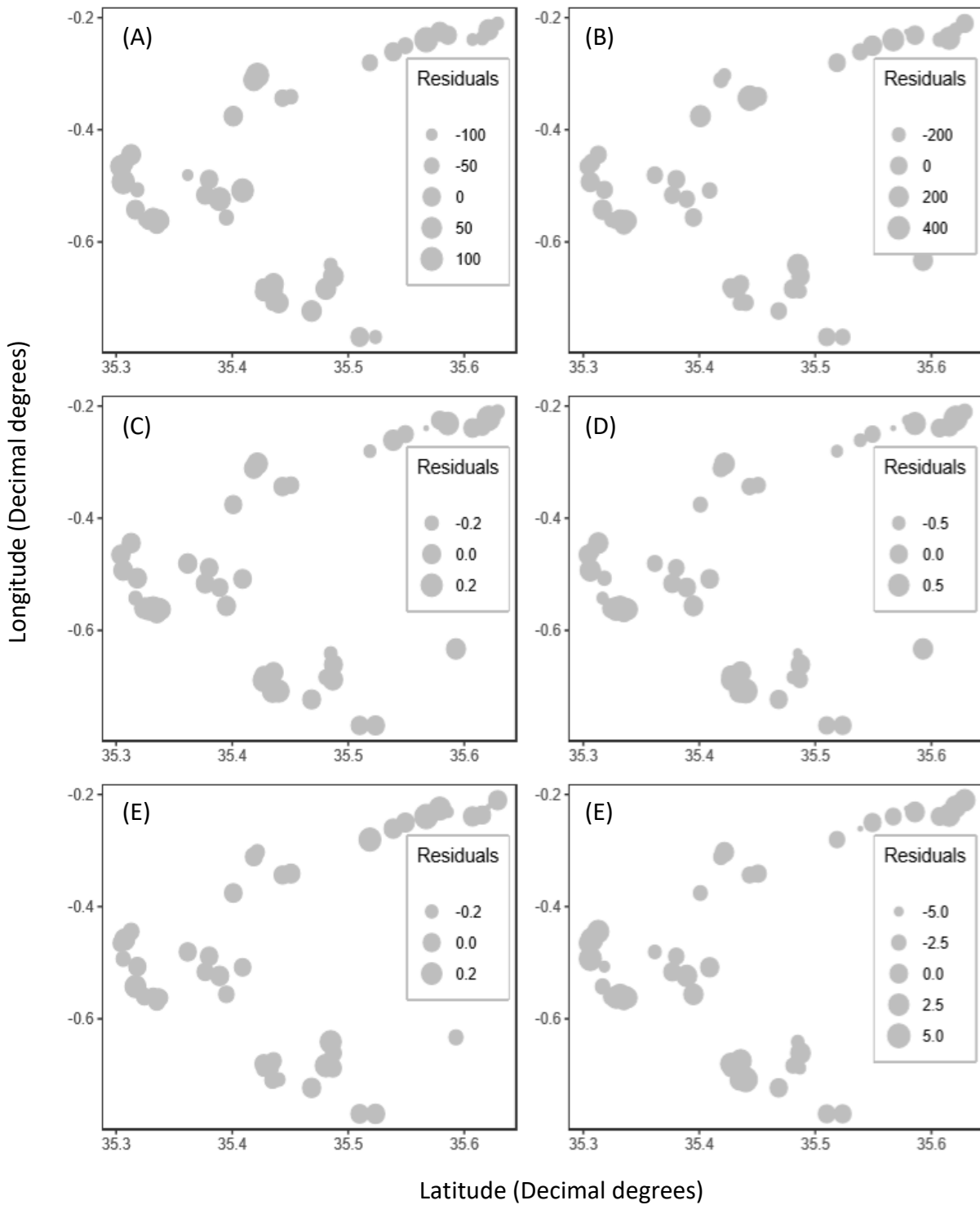
Appendix 2: Areas that were forest in 1986, 2000, and cleared in 2017 on the Landsat 5, 7, and 8 imagery respectively displayed as a true color composite in RGB (321 spectral) band combination for Landsat 5, 7, and 432 spectral band combination for Landsat 8 in the 1st row (A), and the processed Imagery displayed in three standard RGB color guns as Band 1: Bare substrate (S) in red, Band 2: Live and Photosynthetic Vegetation (PV) in Green and dead /Non Photosynthetic Vegetation (NPV) in Blue in the 2nd row (B)



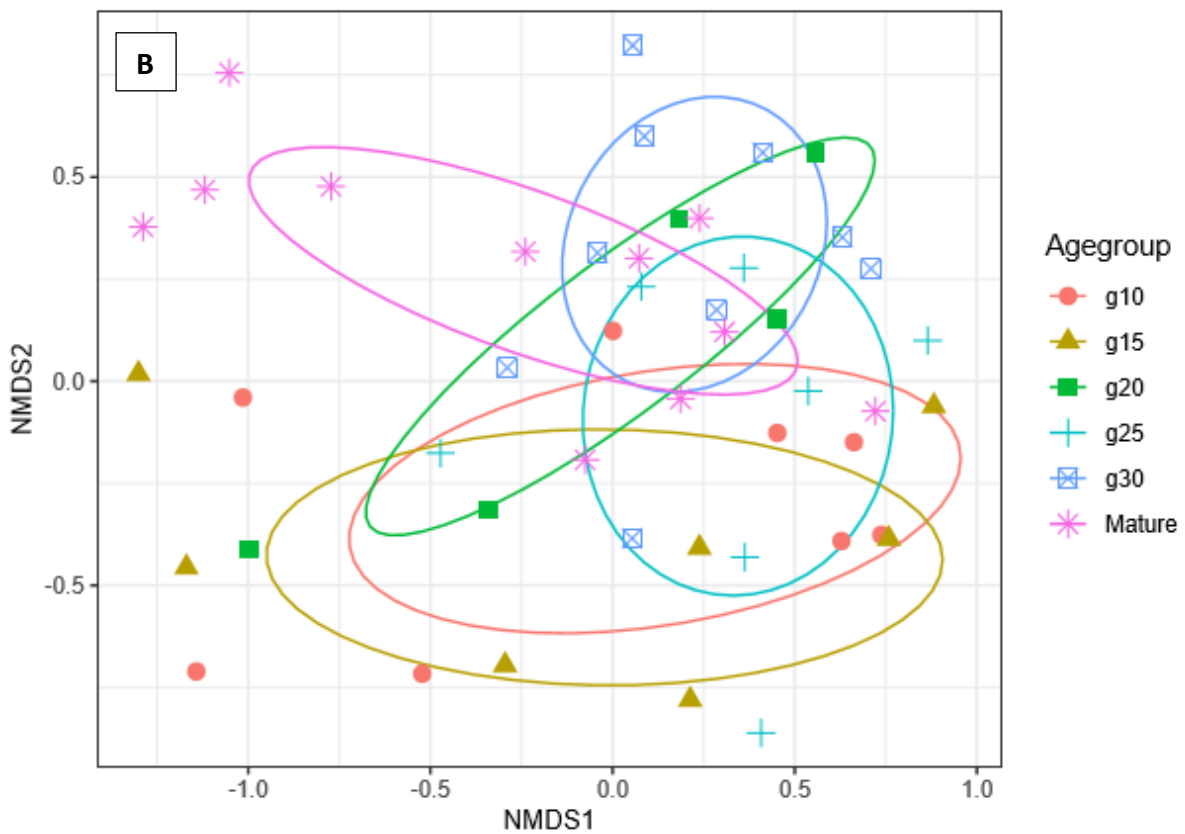
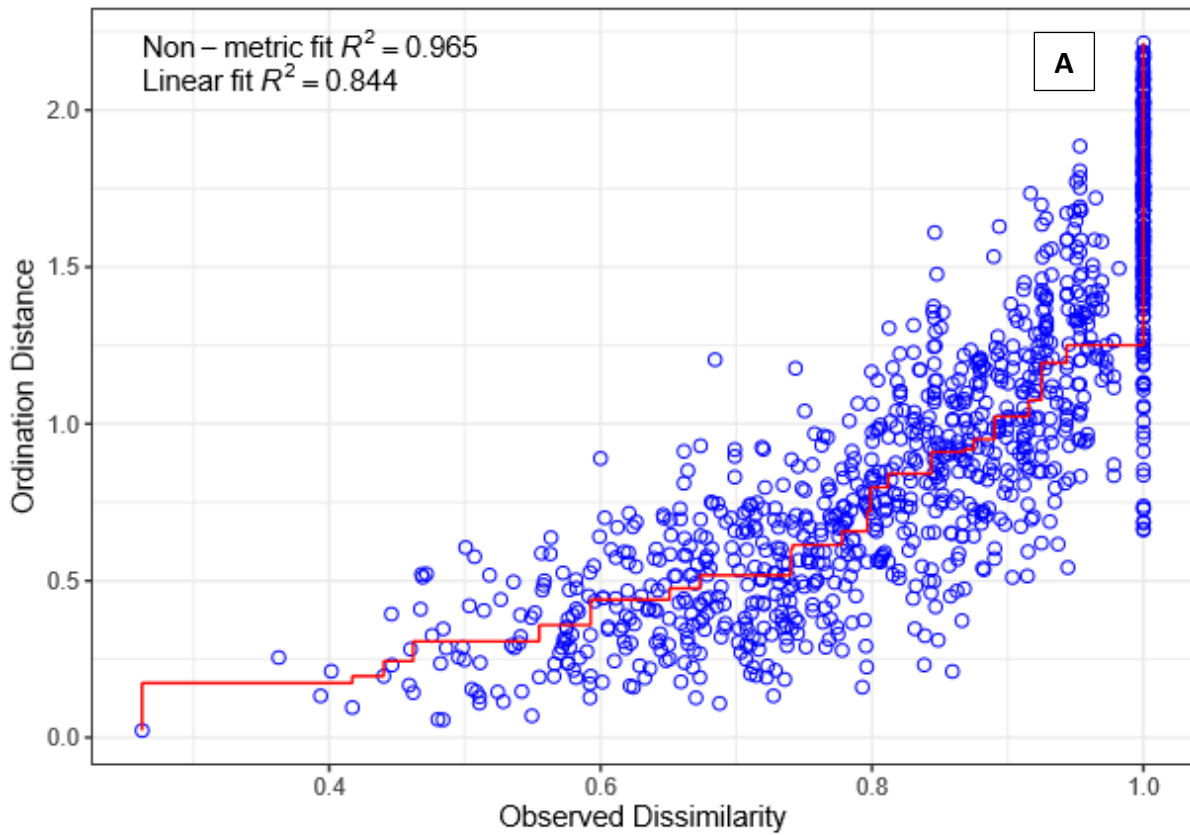
Appendix 3: Areas that were forest in 1995 on the Landsat 5 imagery (A) displayed as a true color composite in RGB (321 spectral band combination) currently seen converted into agriculture in 2017 Landsat 8 imagery/high-resolution Google imagery (B) displayed in RGB (432 spectral band combination).



Appendix 4: Spatial Autocorrelation plots for the residuals of the models for determining the recovery rates in the Mau forest complex.



Appendix 5: Stress plot for the NMDS for the species ordination (A) and the Elipses plot for the MDS analysis (B).



Appendix 6: Summary of the inventory data showing the forest structure and species and families in the sampled plots in Mau forest complex

Plot	X	Y	Block	BA (m ² ha ⁻¹)	DBH (cm)	Height (m)	Stem Density (tree ha ⁻¹)	Slope (%)	Elevation (m)	Logging	Grazing	Charcoal	Elephant damage	Fire wood	Under growth
1	35.57886	-0.22503	1	2.32	45.07	15.69	120	10.00	2347	Yes	Yes	Yes	No	Yes	No
2	35.58586	-0.23113	1	1.14	16.28	6.75	460	15.00	2306	Yes	Yes	Yes	No	Yes	Yes
3	35.60707	-0.23908	1	1.41	22.56	10.09	280	7.00	2415	Yes	Yes	Yes	No	Yes	Yes
4	35.61540	-0.23655	1	1.73	15.01	8.75	830	5.00	2352	Yes	Yes	No	No	Yes	No
5	35.62091	-0.22170	1	0.48	17.10	8.84	170	12.00	2283	Yes	Yes	No	No	Yes	Yes
6	35.56712	-0.23936	1	4.97	21.38	10.93	870	25.00	2358	Yes	No	Yes	No	Yes	No
7	35.42163	-0.30270	1	4.13	33.88	18.80	280	18.00	2242	Yes	Yes	Yes	No	Yes	Yes
8	35.54920	-0.25000	1	3.30	21.59	12.33	640	13.00	2336	Yes	Yes	Yes	No	Yes	No
9	35.53872	-0.26085	1	3.08	25.90	12.29	430	20.00	2309	Yes	Yes	Yes	No	Yes	No
10	35.51865	-0.28038	1	1.22	17.13	12.29	440	3.00	2519	Yes	Yes	Yes	No	Yes	Yes
11	35.43472	-0.70918	3	1.66	28.86	13.58	190	5.56	2170	No	Yes	Yes	Yes	No	Yes
12	35.44008	-0.70822	3	4.01	33.39	17.20	320	5.00	2124	No	Yes	No	Yes	No	Yes
13	35.48716	-0.66114	3	3.40	26.04	13.51	470	6.00	2261	No	Yes	No	Yes	No	Yes
14	35.42714	-0.68893	3	2.91	48.57	17.50	120	5.56	2225	Yes	Yes	Yes	No	Yes	Yes
15	35.43332	-0.68710	3	4.48	38.05	16.43	300	15.00	2225	Yes	Yes	No	No	Yes	Yes
16	35.42707	-0.68038	3	4.01	25.91	12.68	390	20.00	2218	Yes	Yes	No	No	No	Yes
17	35.43561	-0.67486	3	4.39	30.59	14.21	400	9.00	2239	Yes	Yes	No	No	No	Yes
18	35.46840	-0.72304	3	0.97	21.07	9.87	230	14.00	2173	Yes	No	No	Yes	No	Yes
19	35.48482	-0.64112	3	2.46	19.77	12.54	690	35.00	2290	No	No	No	No	No	No
20	35.59279	-0.63295	3	1.75	17.96	9.72	570	35.00	2394	No	Yes	No	Yes	Yes	No
21	35.52348	-0.76941	3	1.69	25.63	13.34	270	4.17	2240	No	Yes	No	No	Yes	Yes
22	35.50982	-0.76940	3	1.54	20.94	11.17	340	4.17	2180	No	No	No	Yes	No	Yes
23	35.48669	-0.68769	3	1.29	24.47	13.17	200	28.00	2169	No	Yes	No	Yes	No	Yes
24	35.48066	-0.68350	3	1.98	20.17	12.98	400	0.83	2224	No	Yes	No	No	Yes	Yes
25	35.32427	-0.56033	2	2.08	26.12	15.99	310	18.00	2087	No	Yes	No	No	Yes	Yes
26	35.32846	-0.56152	2	3.05	26.31	14.84	390	2.78	2081	No	Yes	No	No	Yes	Yes
27	35.33495	-0.56927	2	2.71	22.98	15.09	540	30.00	2015	Yes	Yes	No	No	Yes	Yes
28	35.33179	-0.55846	2	3.92	24.65	15.99	490	10.00	2081	No	Yes	No	No	No	Yes

29	35.33835	-0.56251	2	3.17	24.52	15.58	510	1.39	2070	No	Yes	No	No	Yes	Yes
30	35.31657	-0.54234	2	4.10	25.41	15.23	630	11.00	2050	No	Yes	No	No	No	Yes
31	35.33667	-0.56029	2	3.35	23.85	14.55	530	5.00	2070	No	Yes	No	No	Yes	No
32	35.37669	-0.51624	2	3.38	26.66	14.30	430	5.56	2138	No	Yes	No	No	Yes	No
33	35.38913	-0.52346	2	6.59	36.42	17.62	430	5.56	2196	No	Yes	No	No	Yes	No
34	35.31816	-0.50690	2	3.16	24.65	16.86	460	2.78	2267	No	Yes	No	No	No	Yes
35	35.40889	-0.50807	2	4.03	27.94	16.91	370	2.22	2227	No	Yes	No	No	Yes	Yes
36	35.39491	-0.55630	2	3.33	24.20	13.58	480	0.56	2176	Yes	Yes	No	No	Yes	Yes
37	35.36162	-0.48064	2	2.32	23.20	16.53	420	1.39	2210	No	No	No	Yes	No	Yes
38	35.30602	-0.49291	2	4.32	26.13	18.70	620	0.28	1999	No	No	No	Yes	No	Yes
39	35.30402	-0.46515	2	3.45	27.57	18.17	430	1.11	2020	No	No	No	Yes	No	Yes
40	35.31286	-0.44426	2	3.58	25.60	16.18	470	1.94	2106	No	No	No	Yes	No	No
41	35.30730	-0.45865	2	0.87	16.72	13.42	340	5.00	2020	No	No	No	Yes	No	Yes
42	35.38010	-0.48849	2	1.16	17.35	12.57	400	10.00	2253	No	No	No	Yes	No	Yes
43	35.40088	-0.37558	2	3.04	21.51	13.56	690	20.00	2315	No	Yes	No	No	No	No
44	35.41858	-0.31107	1	1.05	20.92	12.58	230	8.00	2257	No	Yes	Yes	Yes	No	Yes
45	35.62873	-0.21022	1	1.25	14.77	11.46	500	20.00	2368	Yes	Yes	Yes	No	Yes	Yes
46	35.45064	-0.34096	1	2.72	21.56	13.19	540	5.00	2365	No	Yes	No	No	Yes	No
47	35.44332	-0.34350	1	2.98	17.76	14.32	1040	16.00	2341	No	Yes	No	No	No	No

Note: Block 1 = Western Mau, 2 = Transmara and 3 = South western Mau

Appendix 7: Summary of forest structure and composition i.e. Diameter at Breast height (DBH), tree height (H), Stem Density, Basal area (BA), aboveground biomass (AGB), and aboveground Carbon (AGC); Forest species richness and diversity indices i.e. Shannon's diversity index (H), Evenness (J) and the Simpson's Diversity Index (D) for the 47 plots in the three blocks of the Mau forest complex distributed in the 6 different recovery stages.

Recovery stage (years)	DBH (cm)	Height (m)	Stem density (tree ha ⁻¹)	BA (m ² ha ⁻¹)	AGB (Mg ha ⁻¹)	AGC (Mg C ha ⁻¹)	Shannon's (H)	Evenness (J)	Simpson's (D)
<10	18.82 ± 2.13	11.02 ± 2.35	321.25 ± 101.34	11.48 ± 4.50	60.20 ± 40.32	28.30 ± 18.95	1.25 ± 0.45	0.66 ± 0.18	0.47 ± 0.19
10 - 15	18.83 ± 3.86	11.67 ± 1.82	570.00 ± 186.28	18.76 ± 6.57	91.14 ± 34.07	42.84 ± 16.02	1.27 ± 0.41	0.62 ± 0.13	0.46 ± 0.16
15 - 20	24.91 ± 2.64	13.63 ± 2.06	386.00 ± 153.40	24.36 ± 8.57	173.26 ± 70.02	81.43 ± 32.91	1.82 ± 0.36	0.81 ± 0.09	0.27 ± 0.11
20 - 25	27.21 ± 9.95	15.06 ± 2.08	472.86 ± 296.74	28.46 ± 7.33	198.32 ± 78.11	93.21 ± 36.71	1.63 ± 0.26	0.79 ± 0.10	0.28 ± 0.07
25 - 30	27.59 ± 4.98	16.17 ± 1.76	440.00 ± 130.00	35.63 ± 8.65	282.35 ± 82.88	132.70 ± 38.95	1.80 ± 0.36	0.80 ± 0.10	0.27 ± 0.12
Mature	28.95 ± 7.06	14.81 ± 2.39	445.46 ± 187.58	39.51 ± 11.32	282.86 ± 71.64	132.94 ± 33.67	1.63 ± 0.51	0.75 ± 0.13	0.36 ± 0.16

Appendix 8: Identified and recorded species and the percentage composition in the 3 Blocks of Mau forest complex

Family	Species	No. of species recorded in each forest class						Composition in each forest class (%)					
		10	15	20	25	30	Old-growth	10	15	20	25	30	Old-growth
<i>Fabaceae</i>	<i>Acacia lahai</i>	2	-	-	-	-	-	0.66	-	-	-	-	-
<i>Mimosaceae</i>	<i>Acacia melanoxylon</i>	35	-	-	-	-	-	11.55	-	-	-	-	-
<i>Ericaceae</i>	<i>Agauria salicifolia</i>	1	1	-	-	-	-	0.33	0.30	-	-	-	-
<i>Mimosaceae</i>	<i>Albizia gummifera</i>	1	-	2	6	6	6	0.33	-	1.03	1.80	1.52	1.25
<i>Sapindaceae</i>	<i>Allophylus abyssinicus</i>	-	2	3	1	11	-	-	0.60	1.54	0.30	2.78	-
<i>Sapotaceae</i>	<i>Aningeria adolfi-friederici</i>	-	-	-	-	-	2	-	-	-	-	-	0.42
<i>Melanthaceae</i>	<i>Bersama abyssinica</i>	1	-	-	2	1	-	0.33	-	-	0.60	0.25	-
<i>Flacourtiaceae</i>	<i>Casearia battiscombei</i>	6	2	2	5	45	8	1.98	0.60	1.03	1.50	11.36	1.66
<i>Rhisophoraceae</i>	<i>Cassipourea malosana</i>	3	-	-	22	18	20	0.99	-	-	6.61	4.55	4.16
<i>Ulmaceae</i>	<i>Celtis africana</i>	4	8	1	7	4	29	1.32	2.39	0.51	2.10	1.01	6.03
<i>Rubiaceae</i>	<i>Coffea eugenoides</i>	-	4	-	-	-	-	-	1.19	-	-	-	-
<i>Euphorbiaceae</i>	<i>Croton macrostachyus</i>	16	10	3	11	5	6	5.28	2.99	1.54	3.30	1.26	1.25
<i>Araliaceae</i>	<i>Cussonia holstii</i>	1	-	-	-	-	-	0.33	-	-	-	-	-
<i>Ebenaceae</i>	<i>Diospyros abyssinica</i>	-	-	1	-	5	43	-	-	0.51	-	1.26	8.94
<i>Sterculiaceae</i>	<i>Dombeya torrida</i>	16	6	22	4	1	2	5.28	1.79	11.28	1.20	0.25	0.42
<i>Salicaceae</i>	<i>Dovyalis abyssinica</i>	-	-	-	-	-	1	-	-	-	-	-	0.21
<i>Dracaenaceae</i>	<i>Dracaena steudneri</i>	-	-	-	-	7	1	-	-	-	-	1.77	0.21
<i>Boraginaceae</i>	<i>Ehretia cymosa</i>	21	-	7	-	4	8	6.93	-	3.59	-	1.01	1.66
<i>Meliaceae</i>	<i>Ekerbergia capensis</i>	-	-	2	-	2	2	-	-	1.03	-	0.51	0.42
<i>Ebenaceae</i>	<i>Euclea divinorum</i>	12	48	1	-	-	7	3.96	14.33	0.51	-	-	1.46
<i>Euphorbiaceae</i>	<i>Euphorbia obovata</i>	-	1	-	-	-	-	-	0.30	-	-	-	-
<i>Moraceae</i>	<i>Ficus natalensis</i>	-	-	-	-	-	2	-	-	-	-	-	0.42
<i>Moraceae</i>	<i>Ficus thonningii</i>	-	1	-	-	2	4	-	0.30	-	-	0.51	0.83
<i>Oleaceae</i>	<i>Fraxinus berlandieriana</i>	-	-	-	7	-	-	-	-	-	2.10	-	-
<i>Saxifragaceae</i>	<i>Galineria saxifraga</i>	-	-	5	1	16	4	-	-	2.56	0.30	4.04	0.83
<i>Stilbaceae</i>	<i>Halleria lucida</i>	-	1	-	-	-	-	-	0.30	-	-	-	-
<i>Aquifoliaceae</i>	<i>Ilex mitis</i>	-	-	-	-	2	3	-	-	-	-	0.51	0.62

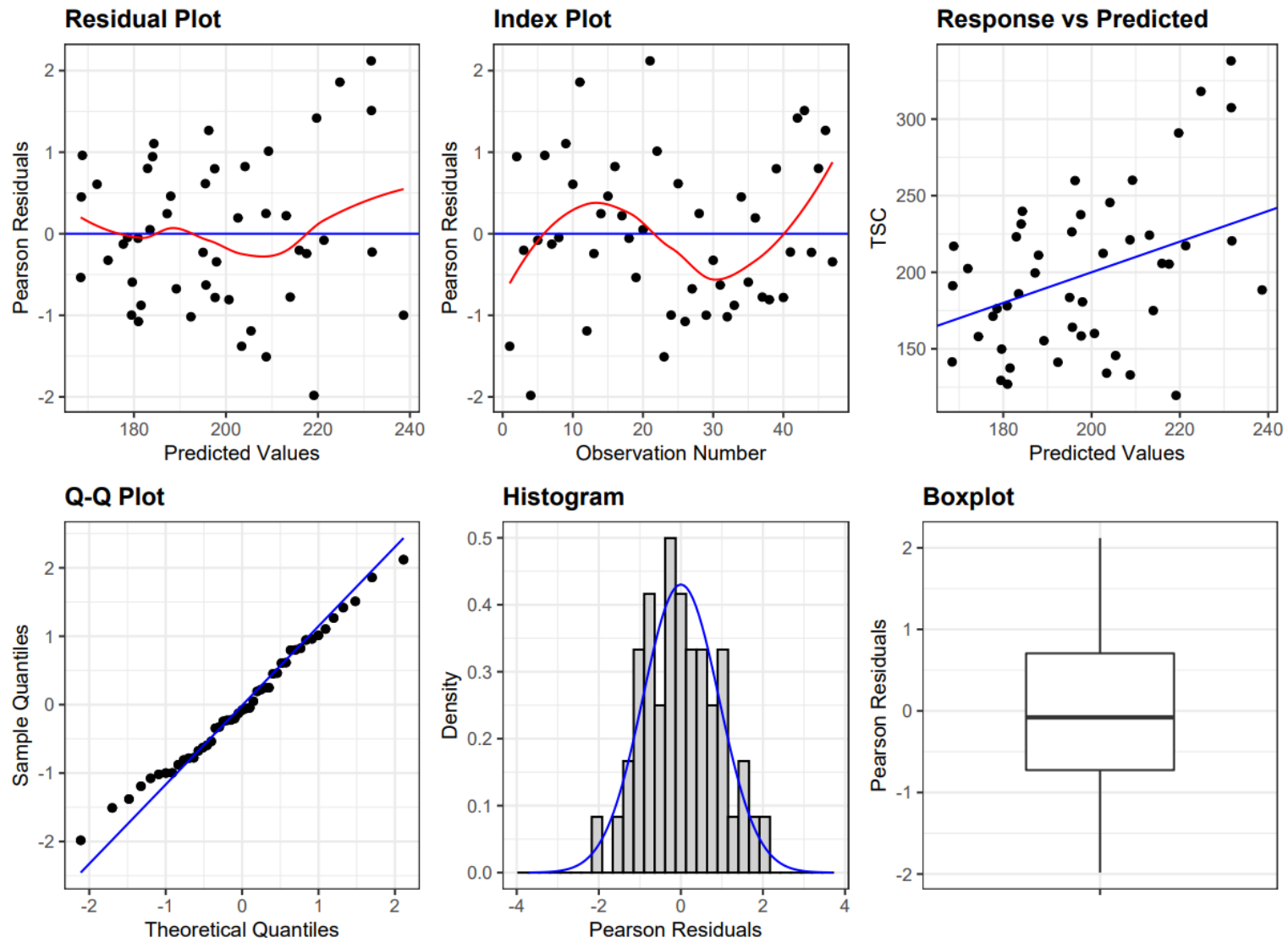
<i>Cupressaceae</i>	<i>Juniperus procera</i>	1	3	-	-	-	-	0.33	0.90	-	-	-	-
<i>Euphorbiaceae</i>	<i>Macaranga kilimandscharica</i>	-	2	3	12	1	25	-	0.60	1.54	3.60	0.25	5.20
<i>Euphorbiaceae</i>	<i>Makaranga cabensis</i>	2	35	5	12	7	25	0.66	10.45	2.56	3.60	1.77	5.20
<i>Celastraceae</i>	<i>Maytenus heterophylla</i>	2	7	-	-	-	-	0.66	2.09	-	-	-	-
<i>Celastraceae</i>	<i>Mystroxyton aethiopicum</i>	15	-	5	10	-	-	4.95	-	2.56	3.00	-	-
<i>Euphorbiaceae</i>	<i>Neoboutonia macrocalyx</i>	110	67	23	73	30	33	36.30	20.00	11.79	21.92	7.58	6.86
<i>Stilbaceae</i>	<i>Nuxia congesta</i>	-	2	-	-	-	-	-	0.60	-	-	-	-
<i>Oleaceae</i>	<i>Olea africana</i>	7	32	-	5	-	16	2.31	9.55	-	1.50	-	3.33
<i>Oleaceae</i>	<i>Olea capensis</i>	-	-	-	4	-	2	-	-	-	1.20	-	0.42
<i>Rubiaceae</i>	<i>Pavetta gardeniifolia</i>	2	5	1	14	1	-	0.66	1.49	0.51	4.20	0.25	-
<i>Pittosporaceae</i>	<i>Pittosporum viridiflorum</i>	1	3	-	-	-	-	0.33	0.90	-	-	-	-
<i>Podocarpaceae</i>	<i>Podocarpus latifolius</i>	-	-	-	1	-	-	-	-	-	0.30	-	-
<i>Araliaceae</i>	<i>Polyscias fulva</i>	-	-	1	-	2	1	-	-	0.51	-	0.51	0.21
<i>Araliaceae</i>	<i>Polyscias kikuyensis</i>	-	-	1	1	-	3	-	-	0.51	0.30	-	0.62
<i>Rosaceae</i>	<i>Prunus africana</i>	1	1	2	2	2	2	0.33	0.30	1.03	0.60	0.51	0.42
<i>Rubiaceae</i>	<i>Psydrax parviflora</i>	-	-	-	1	-	-	-	-	-	0.30	-	-
<i>Rubiaceae</i>	<i>Psydrax schimperiana</i>	1	26	23	64	30	20	0.33	7.76	11.79	19.22	7.58	4.16
<i>Rhamnaceae</i>	<i>Rhamnus prinoides</i>	-	-	-	-	5	-	-	-	-	-	1.26	-
<i>Anacardiaceae</i>	<i>Rhus natalensis</i>	1	4	1	-	-	-	0.33	1.19	0.51	-	-	-
<i>Araliaceae</i>	<i>Schefflera abyssinica</i>	5	2	1	-	1	-	1.65	0.60	0.51	-	0.25	-
<i>Araliaceae</i>	<i>Schefflera volkensii</i>	-	-	-	-	1	-	-	-	-	-	0.25	-
<i>Oleaceae</i>	<i>Schrebera alata</i>	2	-	-	-	-	-	0.66	-	-	-	-	-
<i>Bignoniaceae</i>	<i>Spathodea campanulata</i>	-	-	-	1	-	-	-	-	-	0.30	-	-
<i>Euphorbiaceae</i>	<i>Suregada procera</i>	-	-	20	9	33	17	-	-	10.26	2.70	8.33	3.53
<i>Myrtaceae</i>	<i>Syzygium guineense</i>	4	8	3	30	22	9	1.32	2.39	1.54	9.01	5.56	1.87
<i>Apocynaceae</i>	<i>Tabernaemontana stapfiana</i>	15	39	46	23	110	64	4.95	11.64	23.59	6.91	27.78	13.31
<i>Asteraceae</i>	<i>Tarconanthus camphoratus</i>	5	-	-	-	-	-	1.65	-	-	-	-	-
<i>Rutaceae</i>	<i>Teclea nobilis</i>	1	12	3	2	6	20	0.33	3.58	1.54	0.60	1.52	4.16
<i>Hamamelidaceae</i>	<i>Trichocladus ellipticus</i>	7	-	-	-	-	91	2.31	-	-	-	-	18.92
<i>Rutaceae</i>	<i>Vangueria madagascariensis</i>	1	2	3	-	1	-	0.33	0.60	1.54	-	0.25	-
<i>Rubiaceae</i>	<i>Warburgia ugandensis</i>	-	1	-	-	-	1	-	0.30	-	-	-	0.21

<i>Canellaceae</i>	<i>Xymalos monospora</i>	-	-	-	-	4	-	-	-	-	-	1.01	-
<i>Monimiaceae</i>	<i>Zanthoxylum gillettii</i>	1	-	5	3	11	4	0.33	-	2.56	0.90	2.78	0.83
<i>Unknown</i>	<i>Unknown</i>	1	22	-	2	-	9	0.33	6.57	-	0.60	-	1.87
Total		303	335	195	333	396	481	100	100	100	100	100	100

Appendix 9: Soil physical and chemical properties for plots sampled at different recovery periods of the Mau Forest Complex. The values indicate the mean, standard deviation (SD) of the data for the 6 recovery periods for Bulk Density (BD), Soil organic matter (SOM), Carbon concentration (C), Nitrogen concentration (N), C:N Ratio, Soil organic carbon (SOC), Total soil Nitrogen (TSN) and Aboveground Carbon (AGC) at plot level with combined soil profile (0-60 cm).

Recovery (years)	BD (g/cm ³)	SOM (%)	pH	C (%)	N (%)	C:N Ratio	TSN (Mg ha ⁻¹)	SOC (Mg ha ⁻¹)	AGC (Mg ha ⁻¹)
<10	0.9 ± 0.2a	15.3 ± 4.4a	5.5 ± 0.7a	3.9 ± 0.7a	0.4 ± 0.1a	12.2 ± 2.9a	16.4 ± 4.8a	184.1 ± 41.0a	28.3 ± 18.9a
10 - 15	0.9 ± 0.1a	15.7 ± 2.7a	5.6 ± 1.0a	4.8 ± 1.3a	0.4 ± 0.1a	12.3 ± 2.6a	18.1 ± 4.1a	217.4 ± 52.5a	42.8 ± 16.0ab
15 - 20	0.8 ± 0.2a	16.1 ± 2.9a	5.4 ± 0.9a	4.7 ± 0.6a	0.4 ± 0.0a	11.1 ± 0.8a	18.2 ± 4.3a	195.0 ± 40.7a	81.4 ± 32.9bc
20 - 25	0.9 ± 0.1a	17.2 ± 2.5a	5.1 ± 0.3a	3.9 ± 1.0a	0.4 ± 0.1a	11.9 ± 3.7a	17.3 ± 5.1a	195.6 ± 81.7a	93.2 ± 36.7cd
25 - 30	0.8 ± 0.2a	17.9 ± 1.3a	4.9 ± 0.5a	3.9 ± 0.4a	0.4 ± 0.1a	11.5 ± 2.0a	16.5 ± 3.9a	173.8 ± 30.7a	132.7 ± 38.9cd
Old-growth	0.8 ± 0.1a	15.9 ± 2.2a	5.1 ± 0.8a	4.6 ± 0.7a	0.4 ± 0.1a	11.1 ± 1.8a	20.1 ± 3.9a	217.9 ± 51.8a	132.9 ± 33.7d

Appendix 10: Model diagnostic plots for the selected Total Soil Carbon (TSC) prediction (Soil C stocks).



Appendix 11: Model diagnostic plots for the selected model for Total Soil Nitrogen (TSN) prediction (Soil N stocks).

